2013

Examining the Regulation of Cell Division by the Spindle Assembly Checkpoint

Maria Maldonado

EXAMINING THE REGULATION OF CELL DIVISION BY THE SPINDLE ASSEMBLY CHECKPOINT

A Thesis Presented to the Faculty of

The Rockefeller University

in Partial Fulfillment of the Requirements for

the degree of Doctor Of Philosophy

by

María Maldonado

June 2013

EXAMINING THE REGULATION OF CELL DIVISION BY

THE SPINDLE ASSEMBLY CHECKPOINT

María Maldonado, Ph.D.

The Rockefeller University 2013

Accurate chromosome segregation during cell division is essential for the maintenance of a cell's genomic stability. The molecular surveillance mechanism called the spindle assembly checkpoint (SAC) inhibits chromosome segregation before all chromosomes are correctly attached (bi-oriented) on the microtubule spindle to prevent segregation errors that may lead to chromosomal instability and cell death. In this thesis, I have developed and used tools to examine the roles of different checkpoint proteins in the mechanism of SAC signaling. In the first part of the thesis, I manipulate the localization of the checkpoint protein Mad1 and show that its constitutive presence at the kinetochore is sufficient to induce checkpoint arrest. Being able to uncouple checkpoint signaling from chromosome biorientation, I use the system as a tool to examine the roles of checkpoint kinases in SAC signaling downstream of kinetochore recruitment of Mad1. I show that the kinases Mps1 and Aurora B are necessary for the maintenance of checkpoint arrest, independently of their other "upstream" checkpoint functions. I also show that localization of Mad1 at other chromosomal locations is not *per se* sufficient to induce checkpoint arrest. In the second part of the thesis, I collaborate in the development of a tool for the study of the protein dynein, a microtubule-associated motor with mitotic regulatory roles in spindle assembly, kinetochore-microtubule

interactions and SAC silencing, as well as a variety of cargo-translocation roles in interphase. I examine the effects of the small molecule “ciliobrevin” in mitotic cells and help validate it as the first specific dynein inhibitor. Although I determine that its effects on the microtubule spindle will preclude its use in checkpoint silencing studies, ciliobrevin will still be a powerful tool for other biochemical, structural and cellular investigations of dynein function.

“Le rêve de toute cellule: devenir deux cellules.”

François Jacob

ACKNOWLEDGEMENTS

My thanks to everyone who made this work possible. Thanks to all the members of the Kapoor lab, particularly Emily Arias Foley and Lei Tan, for all their help, time and inspiration. Thanks to the members of the Funabiki, de Lange and Muir labs, who never hesitated to share reagents, protocols or equipment. Thanks to the Rockefeller Imaging Facility, particularly Shawn Galdeen, for their training and help. Thanks to the members of the Dean's Office for promptly solving all those little problems.

Many thanks to my thesis committee members, Titia de Lange and Fred Cross, for their teachings, suggestions and encouragement ever since my summer- and rotation-student days. I have fond memories of the time spent in their labs and on their courses.

Big thanks to my thesis advisor, Tarun Kapoor, for inculcating the importance of thinking critically about the question to be investigated, of going after big questions and of being precise with one's statements. Thanks for showing me how to be a better scientist and a better writer.

Thanks to my family for their transoceanic support for almost the last 10 years—who knows where I would have ended up had they not encouraged me to apply for the Cambridge scholarship in the first place? Thanks to my Rockefeller friends, particularly Josefina del Mármol, Taeryn Kim, Jeff Liesch and Frej Tulin, as well as those from Argentina and beyond, without whom these years would have been much duller and bleaker.

Lastly, infinite thanks to my husband, James Letts, for encouraging, supporting and challenging me throughout my PhD and, hopefully, many years to come.

Table of Contents

List of Figures

Chapter 1: Introduction to the Spindle Assembly Checkpoint

Overview of the cell cycle and mitosis

Mitosis, the biological process by which a cell divides into two "daughter" cells, is essential for the maintenance of organisms' lives. In multicellular organisms, mitosis is necessary for growth, development, organ homeostasis and wound-healing. The maintenance of genetic fidelity in (most) somatic cells is essential for the well-being of the organism, given that genetic instability can give rise to a variety of diseases and death (Pfau and Amon, 2012; Holland and Cleveland, 2012).

Before being able to divide, cells must pass through an orderly, unidirectional and irreversible series of phases of the cell cycle. Progression through the cell cycle is driven by complex, interlocking molecular circuits, powered by the activity of conserved cyclin-dependent kinases (CDKs; Morgan, 2008a, b). The first phase of a newly formed cell is G1 (gap) phase, in which the cell can grow and carry out its functions. Most somatic cells exist in this phase or a similar, quiescent phase called G0 (for cells that do not divide). For a cell to be able to divide into two genetically identical daughter cells, i.e. to undergo mitosis, it must first duplicate its genetic material (DNA, wrapped around nucleosomes to form chromosomes). Upon certain proliferative stimuli, cells progress

from G1 to S (DNA synthesis) phase, in which chromosomes and (other cellular structures such as the centrosomes) are replicated. At this point, the replicated chromosome is held together (i.e., its two sister chromatids are under cohesion). Further growth and housekeeping processes are carried out during the ensuing phase, G2, before the cell is ready to start mitosis (M phase). During the prophase stage of mitosis, the chromosomes condense, the nuclear envelope breaks down and the microtubule cytoskeleton is rearranged into a bipolar structure called the spindle. Chromosomes are then bound by microtubule polymer bundles (kinetochore fibers) at a specialized proteinaceous structure called the kinetochore and are then aligned in the middle of the cell at the metaphase plate. When kinetochores of both sister chromatids of all kinetochores are bioriented, i.e. when each sister kinetochore of the pair is attached to microtubules emanating from a different spindle pole, the cell breaks the cohesion between the chromosomes to allow metaphase to progress into anaphase (Fig. 1.1). During anaphase, the separated chromatids are physically transported to opposite sides of the cytoplasm (driven by kinetochore fiber depolymerization), after which nuclear envelopes re-form (telophase) and the membrane in the middle of the cell ingresses into a furrow that will eventually completely separate both sides of the cytoplasm (cytokinesis), giving rise to two independent cells. These newly formed cells then enter G1 phase if they are to remain proliferative, or G0 phase if they are to become quiescent.

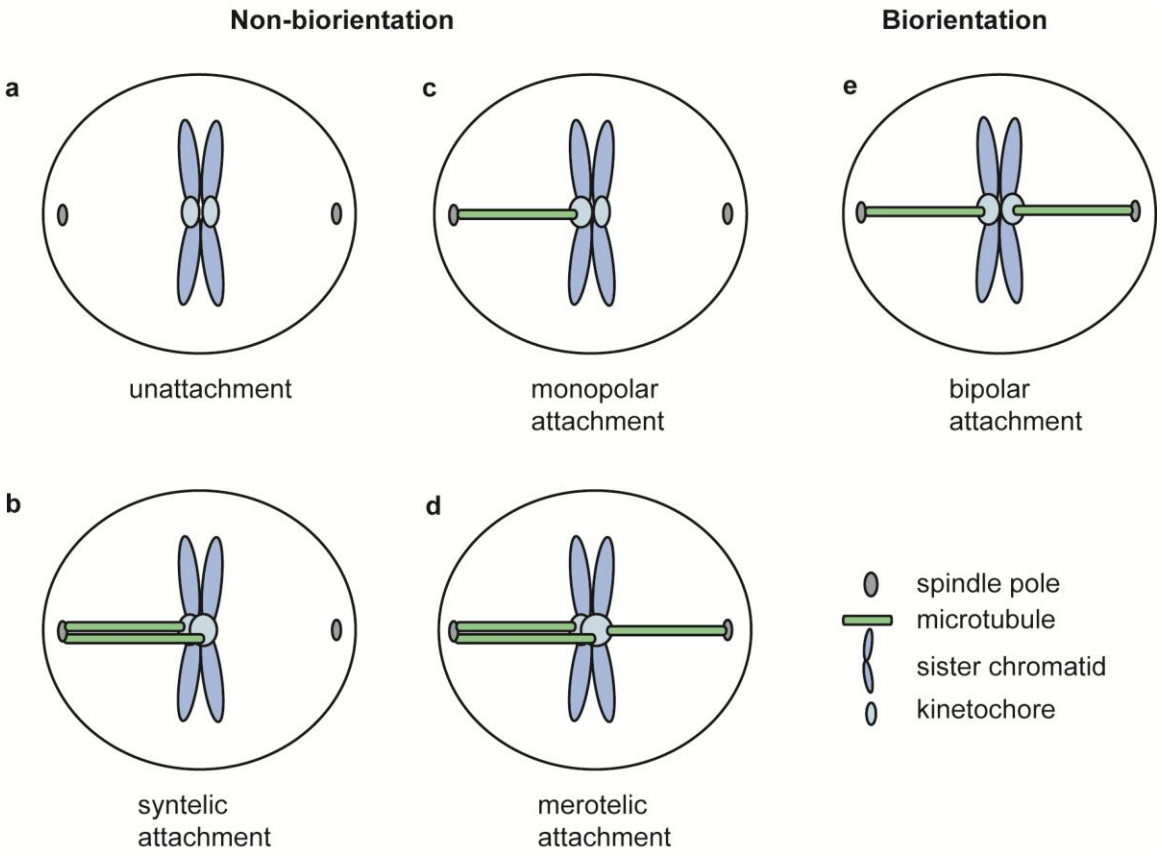

Figure 1.1 Types of chromosome-microtubule attachment and orientation on the spindle. Non-bioriented chromosomes can be: **(a)** unattached, **(b)** monopolarly attached (only one kinetochore of the pair contacts microtubules), **(c)** syntelically attached (both kinetochores are attached by microtubules emanating from a single pole), **(d)** merotelically attached (both kinetochores are attached, but one of them contacts microtubules emanating from two different poles), or **(e)** bipolarly attached (both kinetochores are attached, each to microtubules emanating from a single and distinct pole). Biorientation only occurs when the chromosome is bipolarly attached.

Molecular checkpoints ensure the fidelity of cell cycle progression

Errors in the sequence or timing of mitotic events can lead to genetic instability and cell death. Because of the importance of fidelity of cell division in the maintenance of genomic stability, cell cycle events must be tightly coordinated. Coordination of the cell cycle of eukaryotic cells is achieved by "checkpoints": molecular surveillance mechanisms (dependent relationships) that do not allow late events to occur before the successful completion of early ones (Hartwell and Weinert, 1989). A number of checkpoints exist at different stages of the cell cycle (G1/S, S, G2/M, etc).

For the work described here, I have focused on the spindle assembly checkpoint (SAC): the mechanism that arrests mitotic cells in metaphase, preventing the progression into anaphase until all chromosomes are bioriented and providing time for orientation errors to be corrected (Musacchio and Salmon, 2007). Because depolymerization of the kinetochore-attached microtubule fibers powers chromatid translocation during anaphase, proper kinetochore-microtubule interactions are essential to ensure faithful segregation (Mitchison et al., 1986; Gorbsky et al., 1987; Koshland et al., 1988). By only allowing chromosomal segregation in cells with a full complement of correctly attached (bioriented) chromosomes, the spindle assembly checkpoint prevents mis-segregation events that would lead to genetic aberrations, instability and death in the daughter cells.

The Spindle Assembly Checkpoint

A short history of spindle assembly checkpoint origins

The concept of a cell cycle checkpoint was originally formally proposed by Hartwell and Weinert in 1989 (Hartwell and Weinert, 1989). They recognized that the order of events of the cell cycle is regulated in wild type cells such that late events do not occur until the successful completion of previous events has been finished and that these pathways of dependent relationships are key for the fidelity of cell division. In their seminal article, they review existing data and propose that a variety of such checkpoints are true feedback control mechanisms, as opposed to mere "substrate-product" intrinsic structural requirements (Hartwell and Weinert, 1989). The initial criterion for the identification of these pathways as control mechanisms was the existence of "relief of dependence conditions" such as mutations or chemical inhibition that allowed a late event to occur in the absence of the completion of an earlier event. Hartwell and Weinert argued that these relief-of-dependence observations were very unlikely to arise from structural changes in the proteins and thus established the concept of checkpoint control mechanisms.

In fact, Hartwell and Weinert themselves established the role of the protein RAD9 in the DNA damage checkpoint of budding yeast (Weinert and Hartwell, 1988). They showed that, at the restrictive temperature, *rad9* temperature-sensitive mutants in which DNA damage has been induced by x-ray irradiation fail to arrest in G2 and instead proceed into cell division regardless of the DNA damage present (which, on the

contrary, causes G2 arrest in wild type cells or in *rad9* mutants at the permissive temperatures). Furthermore, irradiated rad9 cells can efficiently repair damaged DNA if cells are blocked in G2 is using microtubule poisons. Thus, they established that RAD9 forms part of a feedback mechanism (a checkpoint) that delays entry into mitosis in the presence of DNA damage.

The initial discovery of the spindle assembly checkpoint genes came a couple of years later from the laboratories of Andrew Hoyt and Andrew Murray (Hoyt et al., 1991; Li and Murray, 1991). They hypothesized that the mitotic arrest seen when microtubules are disrupted is also due to a checkpoint mechanism. To test this, Rong Li and Andrew Murray devised a screen that would differentiate "structural" mutants (e.g. with a deficiency in tubulin polymerization) from mutants arising from a true checkpoint mechanism (Li and Murray, 1991). They incubated the mutagenized budding yeast cells in sub-lethal concentrations of the microtubule depolymerizing agent benomyl. Under these conditions, three distinct responses would be seen from the different populations. In wild type cells, completion of mitosis would be delayed (not blocked) until a proper spindle could be assembled and proper biorientation, achieved. Structural mutants would be unable to assemble a spindle and progress through mitosis at all. On the other hand, mutants in the putative feedback checkpoint mechanism would fail to delay mitosis in response to the improperly assembled spindle and would progress through mitosis un-delayed, which would lead to chromosome mis-segregation and cell death. Moreover, this benomyl hypersensitivity should be rescued by a delay in S-phase, which would allow a longer time for the yeast spindle to form. From this carefully designed

screen, Li and Murray were able to isolate three checkpoint mutants: Mad1, Mad2 and Mad3 (Li and Murray, 1991).

Similarly, Andrew Hoyt and Tibor Roberts carried out an independent screen to identify relief-of-dependence mutants that would fail to arrest in mitosis with a disrupted spindle (Hoyt et al., 1991). They initially identified mutants that failed to efficiently recover from a transient, complete block of microtubule polymerization (by exposure to high concentrations of benomyl), presumably due to their inability to pause the cell cycle while the spindle recovered. Under closer inspection, a number of these mutants also underwent several rounds of budding in the presence of benomyl. Moreover, this new group of mutants was also hypersensitive to sub-lethal concentrations of benomyl. This screen thus identified the second group of checkpoint genes: Bub1, Bub2, Bub3 (Hoyt et al., 1991).

These two seminal screens established the existence of a feedback mechanism that arrests the cell cycle in mitosis in response to microtubule disruption and laid the foundation for the field of study of the spindle assembly checkpoint. Following the initial discovery of the first SAC genes, the loci were cloned and the proteins, biochemically and cell-biologically characterized.

We now know that more proteins are required for or involved in checkpoint arrest and silencing, including the motor proteins CENP-E, CENP-F and dynein, the dynein-interacting proteins Spindly and RZZ complex (Rod, Zwilch, ZW10), the Mad2-inhibitor p31/Comet, the phosphatase PP1-gamma, as well as the mitotic kinases Mps1 and Aurora B (Musacchio and Salmon, 2007; Musacchio, 2012).

Following initial discovery of checkpoint genes, researchers focused on examining what the primary signal for the feedback mechanism is and how the signal is transduced in the cytoplasm. Early studies showed that cells progress into anaphase after the last chromosome has been properly attached, suggesting that non-bioriented chromosomes produce a diffusible, "stop-anaphase" signal that prevents cell cycle progression, and that even a single unattached kinetochore is sufficient to induce metaphase arrest (Rieder et al., 1994; Rieder et al., 1995). We now understand that the presence of unattached or improperly attached (i.e. non-bioriented) kinetochores acts as a primary signal that is detected, transduced and amplified by checkpoint proteins into the cytoplasmic "stop-anaphase" signal. Upon biorientation of all chromosomes, the checkpoint is satisfied and the diffusible signal is disassembled, allowing the cell to progress onto chromosome segregation (Musacchio and Salmon, 2007).

In the following sections, I shall explain how the checkpoint proteins interact with non-bioriented chromosomes to detect, transduce, amplify and finally silence the spindle assembly mechanism that inhibits APC/C-cdc20.

Molecular basis of checkpoint arrest

In order to progress into anaphase, the cell must degrade two key mitotic proteins: cyclin B and securin. Cyclin B is the binding partner and activator of cyclin-dependent kinase 1 (CDK1), the master regulator of mitotic entry and early mitosis. Securin is a protein that inhibits the protease (separase) that cleaves the cohesion between the sister chromatids. Once all chromosomes are bioriented, cyclin B and securin are

ubiquitylated by the E3 ubiquitin ligase APC/C (anaphase promoting complex/cyclosome) and thus targeted for degradation by the proteosome, allowing progression into anaphase (Barford, 2012). Accordingly, the SAC prevents anaphase progression until all chromosomes are bioriented by inhibiting the interaction of the APC/C with its co-activator cdc20. By preventing the activation of the APC/C, the SAC prevents the degradation of cyclin B and securin and thus keeps the cells in a state of high CDK activity and cohesed chromosomes (Fig. 1.2).

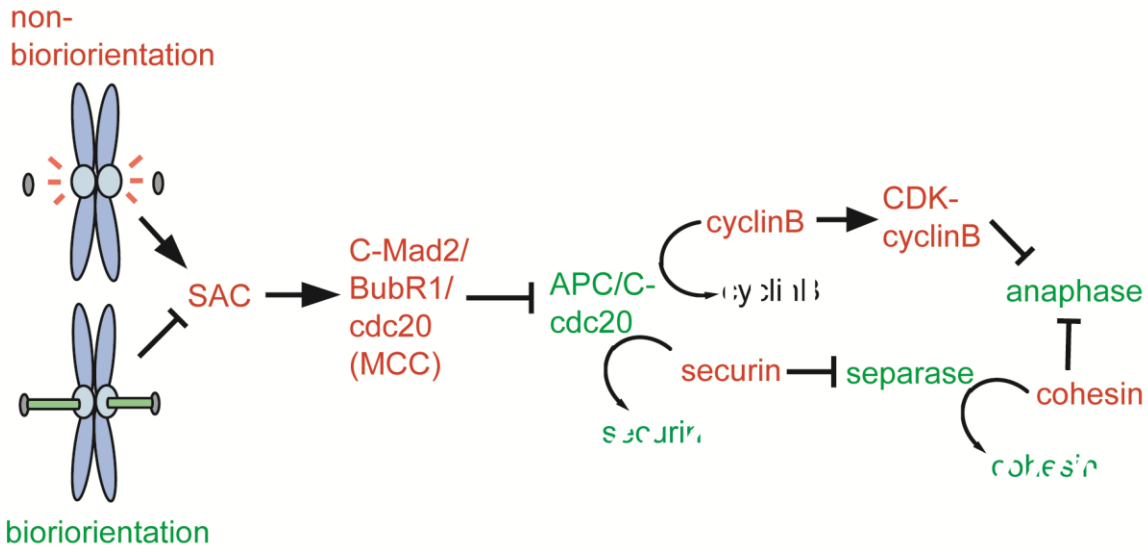

Figure 1.2 Spindle assembly checkpoint (SAC) simplified circuitry. The lack of chromosome biorientation signals through the SAC to prevent progression into anaphase. The mitotic checkpoint complex (MCC, composed of C-Mad2, BubR1 and cdc20) inhibits cdc20 from co-activating the E3 ubiquitin ligase APC/C, preventing the ubiquitylation and subsequent degradation of cyclin B and securin and maintaining the cell in a metaphase state. Biorientation silences checkpoint signaling, allowing the progression into anaphase. Green font indicates anaphase-promoting activities; red font, anaphase-inhibiting ones.

Detection of the primary signal

As mentioned above, the primary signal for spindle assembly checkpoint arrest is the presence of non-bioriented chromosomes, i.e. those whose kinetochores are either unattached by microtubules or improperly interacting with them. In fact, the kinetochore—the complex multi-protein structures that assemble on centromeric DNA at the start of mitosis and whose assembly is hierarchical and highly regulated, for instance by the kinases Aurora B and Mps1—is not only the site of microtubule attachment, but also the site of detection of the checkpoint primary signal (Cheeseman and Desai, 2008; Santaguida and Musacchio, 2009; DeLuca and Musacchio, 2012). Checkpoint protein Mad1-Mad2 tetramers are recruited to non-bioriented kinetochores, after which they can start the primary signal transduction and amplification that will lead to metaphase arrest (Hardwick and Murray, 1995; Chen et al., 1996; Hardwick et al., 1996; Li and Benezra, 1996; Chen et al., 1998; Waters et al., 1998). Mad1 and Mad2 are the main detectors of the primary signal, and their kinetochore localization is sufficient to induce checkpoint arrest (this work, second Chapter). Importantly, because Mad1-Mad2 recruitment to unattached kinetochores occurs 'by default' (owing to kinetochore-localization sequences and mitotic kinase phosphorylation), and because this recruitment occurs early in prometaphase when most kinetochores are still unattached, the SAC is a constitutively active surveillance mechanism that requires active silencing for cells to progress through mitosis.

Transduction and amplification of the SAC primary signal.

Given that a single kinetochore can achieve the same outcome as every unattached kinetochore and that the APC/C inhibitory signal must be detected throughout the metaphase plate to prevent an unsynchronized anaphase onset, the SAC primary signal must not only be transduced into a cytoplasmic signal, but also amplified.

In most signal transduction pathways, signal amplification is achieved by enzymatic catalysis. In the SAC, amplification and maintenance of the anaphase-inhibitory signal is achieved by the combined action of checkpoint proteins such as Mad1 and Mad2, together with mitotic kinases such as Aurora B and Mps1. Although not a canonical enzyme, Mad1-bound Mad2 can indeed act as a *de facto* enzymatic-like catalyst (Lad et al., 2009; Simonetta et al., 2009). Thanks to a wealth of cellular, biochemical, biophysical and structural work, we now have a very detailed model (the "Mad2 conformational activation" or "template model") for how Mad1 and Mad2 act at unattached kinetochores to transduce and amplify the primary signal of non-biorientation into the diffusible anaphase-inhibitory signal (Luo and Yu, 2008).

Mad1 and Mad2 can interact all throughout the cell cycle, forming a tightly bound tetramer consisting of a Mad1 dimer and two Mad2 molecules (Chen et al., 1999; Sironi et al., 2002). During interphase, the Mad1-Mad2 tetramer rests in the nucleoplasmic side of the nuclear membrane (Iouk et al., 2002; Lee et al., 2008). Upon nuclear envelope breakdown, the Mad1-Mad2 tetramer is recruited to unattached kinetochores, *via* Mad1's kinetochore binding domain and its interactions with kinetochore proteins such as Ndc80, aided by phosphorylation by Mps1 (Abrieu et al.,

2001; Martin-Lluesma et al., 2002; DeLuca et al., 2003). Cells have an excess of Mad2 relative to Mad1, and the ratio between the two is crucial to a robust checkpoint arrest (Chung and Chen, 2002; Barnhart et al., 2011).

Remarkably, Mad2 exists in two topologically distinct, stable conformational states: an open (O-Mad2) and a closed (C-Mad2) configuration, differing in the position of the N- and C-terminal strands of its beta-sheet (Luo et al., 2004). In the open-to-closed conversion, the N-terminal strand detaches from the beta sheet to form an extra turn on the first alpha-helix. More notably, the two C-terminal beta strands detach from the sheet, cross over and re-bind the beta sheet on the other side. This causes a loop to traverse the body of the beta sheet, forming a structure reminiscent of a seat belt. Open-Mad2 and C-Mad2 are at equilibrium with very slow inter-conversion rates; in HeLa cells, open Mad2 is the predominant form (Luo et al., 2004). Only C-Mad2 can bind cdc20 and hence ultimately lead to APC/C inhibition (Mapelli et al., 2007; Yang et al., 2008; Luo and Yu, 2008). Therefore, C-Mad2 is the active conformer.

Interaction of O-Mad2 with Mad1 lowers the energetic barrier of the transition between O-Mad2 and C-Mad2 (De Antoni et al., 2005; Yang et al., 2008). Therefore, the Mad1-dimer-bound Mad2 species are two C-Mad2 molecules (i.e., the core tetramer consists of a Mad1 dimer and two C-Mad2 protomers). These C-Mad2 molecules are capable of recruiting O-Mad2 molecules from the cytoplasm and promoting their conversion to C-Mad2 (active) molecules (Luo et al., 2004; De Antoni et al., 2005; Luo and Yu, 2008). These processes are entirely catalytic and reversible, i.e. the rates of inter-conversion are accelerated, but the equilibria are not altered. Since the Mad1-

bound closed-Mad2 remains stably associated with the Mad1 dimer, kinetochore-localized C-Mad2 acts as a catalyst for the conversion of a large number of cytoplasmic O-Mad2 (Simonetta et al., 2009). These newly formed C-Mad2 molecules can bind and inhibit cdc20. Although it is speculated that cdc20 binds to a high energy intermediate (I-Mad2) that forms during the O-to-C-Mad2 conversion (as opposed to cdc20 binding to a C-Mad2 that has been fully converted and released to the cytoplasm), this is still unclear (Luo and Yu, 2008). Another point of debate is whether C-Mad2 in the cytoplasm can also carry out an auto-amplification loop (converting more O-Mad2 molecules to the closed form), to further amplify the signal (De Antoni et al., 2005). Although this is feasible in principle (and is supported by computational modeling studies; Simonetta et al., 2009), there is no biological evidence for it. On the contrary, recent studies in budding yeast indirectly suggest that there is no auto-amplification Mad2 loop in the cytoplasm (Lau and Murray, 2012). This issue remains to be more directly tested in yeast and in higher organisms. These uncertainties notwithstanding, it is clear that the primary signal of non-biorientation is detected, transduced and amplified by the kinetochore-bound Mad1-Mad2 core tetramer to lead to the inhibition of cdc20-APC/C.

As described, this model relies entirely on Mad1 and Mad2 for the amplification of the stop signal; there is no mention or need for the involvement of any of the checkpoint kinases which are known to be essential for regulating checkpoint activity. This simplification partially rests on the fact that *in vitro* studies with purified Mad1 and Mad2 (and even purified chromosomes, without associated kinases) can catalyze the

production of the inhibitory signal by acting directly on Mad2 (Vink et al., 2006; Kulukian et al., 2009). Moreover, given that checkpoint kinases such as Aurora B and Mps1 have upstream roles in kinetochore and spindle assembly, it has been very difficult to determine whether these kinases also have direct roles in checkpoint signaling, downstream of checkpoint protein recruitment to the kinetochores (Meraldi et al., 2004b; Lan and Cleveland; Ditchfield et al., 2003; Kallio et al., 2002; Hauf et al., 2003; Petersen and Hagan, 2003; Pinsky et al., 2006; Emanuele et al., 2008; Vanoosthuyse and Hardwick, 2009; Saurin et al. 2011). In Chapter 2, I shall describe and discuss the method I designed to address this difficulty. My results, together with mounting evidence from yeast, Xenopus and other human studies, make it now clear that Aurora B and Mps1 do in fact have essential roles in the maintenance of checkpoint arrest (Kallio et al., 2002; Petersen and Hagan, 2003; Emanuele et al., 2008; Vanoosthuyse and Hardwick, 2009; Maldonado and Kapoor, 2011; Santaguida et al., 2011), indicating that checkpoint signaling may not be as different from other signaling pathways as once thought (Figure 1.3).

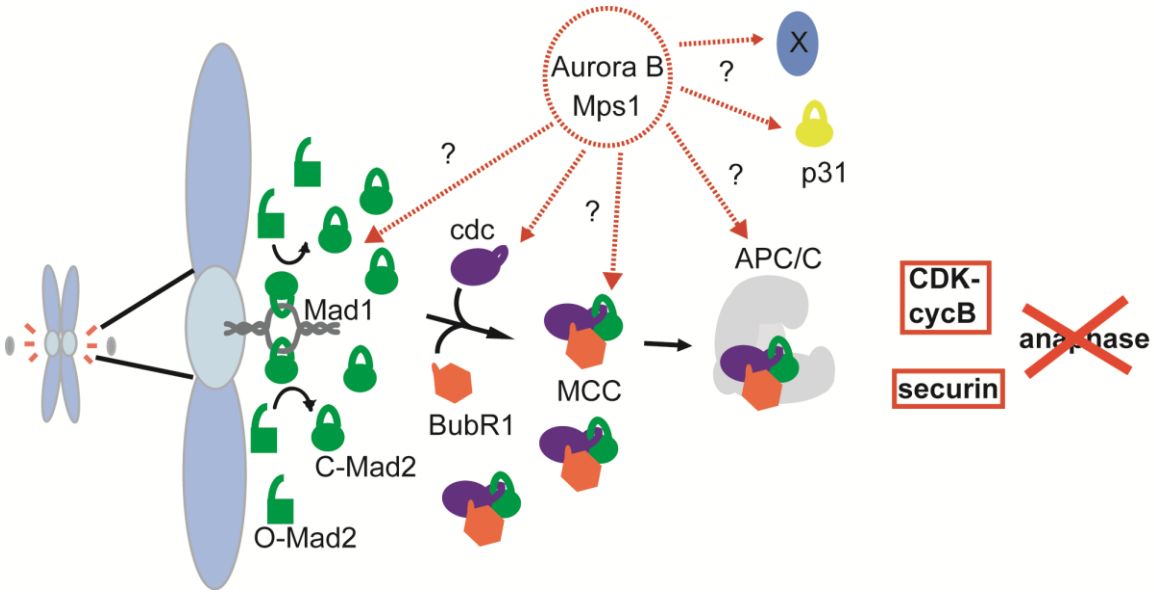

Figure 1.3 Schematic representation of spindle assembly checkpoint establishment and maintenance. Mad1-C-Mad2 tetramers are recruited to unattached kinetochores. Mad1-bound C-Mad2 catalyses the conversion of cytoplasmic O-Mad2 to C-Mad2. C-Mad2 binds cdc20 and, together with BubR1, forms the inhibitory MCC, which blocks APC/C activation and, consequently, cyclin B and securin degradation. Catalytic activity of checkpoint kinases such as Aurora B and Mps1 is also needed to maintain checkpoint signaling. The full complement of their checkpoint substrates is unknown, but it includes MCC components, likely, APC/C subunits and, speculatively, p31.

APC/C inhibition by the checkpoint

How do checkpoint components inhibit cdc20 to prevent APC/C activation? Although C-Mad2 can bind and inhibit cdc20 by itself *in vitro*, in cells C-Mad2 forms a cdc20-inhibitory mitotic checkpoint complex (MCC; Sudakin et al., 2001; Fig. 1.3). The MCC is composed of cdc20 and C-Mad2, together with BubR1 and the accessory protein Bub3 (Sudakin et al., 2001; Chao et al. 2012). Importantly, both C-Mad2 and BubR1 can bind and inhibit cdc20, and it has been shown *in vitro* and in yeast that these proteins act synergistically to inhibit cdc20 and prevent anaphase progression (Fang, 2002; Tang et al., 2001; Lau and Murray, 2012). The C-Mad2-BubR1-cdc20 trimer is indeed the most downstream effector of the SAC (Lau and Murray, 2012). A recent structure of this trimer confirmed and augmented previous biochemical studies and showed how the inhibition of the APC/C co-activator takes place (Chao et al., 2012). BubR1 directly inhibits cdc20-APC/C by using its pseudo-KEN box (one of the APC/C's substrate recognition sequences) to obstruct the degron recognition patch on cdc20. C-Mad2 aids this interaction by optimally positioning BubR1's pseudo-KEN box for cdc20 inhibition. Moreover, C-Mad2's interactions with cdc20 (which is, effectively, trapped by C-Mad2's "seat belt") partially sequester cdc20's APC/C interaction and activation motifs, further contributing to cdc20 inhibition.

Recent studies have also shown that, although purified C-Mad2 and BubR1 can inhibit APC/C-cdc20 *in vitro*, checkpoint kinase activity is needed to sustain these interactions—and checkpoint arrest— in cells. For instance, Mps1-mediated phosphorylation of C-Mad2 have recently been found necessary for checkpoint arrest

maintenance, and a number of phosphorylation sites for Mps1 and other checkpoint kinases have been found on other MCC and APC/C-cdc20 components (Tang et al., 2004; King et al., 2007; Kang et al., 2008; Zich et al., 2012). This is, of course, consistent with the fact that Aurora B and Mps1 activities are directly needed for checkpoint signaling and strongly suggests that the MCC and APC/C-cdc20 may be the kinases' cytoplasmic substrates whose phosphorylation prevents cell cycle progression. Identifying the full set of checkpoint kinase substrates is an important task for the full elucidation of the mechanism of checkpoint arrest.

These remaining issues notwithstanding, the consensus is emerging that checkpoint signal amplification and mitotic arrest is not only mediated by Mad2's catalytic template mechanism: enzyme catalysis by checkpoint kinases is also needed for the cytoplasmic C-Mad2 molecules to associate with BubR1 and APC/C-cdc20 in a robust manner. Given the importance of phosphorylation in the regulation of most other events in the cell cycle, and the usefulness of enzymatic activity for signal amplification, this is not too surprising.

Silencing of the checkpoint signal

Once all chromosomes have achieved bipolar attachment, the checkpoint must be silenced. This allows the degradation of cyclin B and securin such that chromatids can be segregated and anaphase, irreversibly initiated. In contrast to the numerous cell-biological, biochemical, and structural advances in our understanding of the establishment of checkpoint arrest, the elucidation of checkpoint silencing pathways has

lagged behind. In human cells, at least three different processes for SAC silencing have been suggested. These include: motor-protein-based processes, such as the dynein-dependent removal of checkpoint proteins from microtubule-attached kinetochores (Howell et al., 2001) and the CENP-E-mediated silencing of BubR1 signaling (Mao et al., 2005); mechanisms that involve inhibition of active SAC signaling proteins, such as the p31/Comet-mediated, structural mimicry-based inhibition of “active” Mad2 (Xia et al., 2004); pathways that mediate the chemical modification of checkpoint proteins, such as the ubiquitylation (and ensuing degradation) of cdc20 (Reddy et al., 2007; Nilsson et al., 2008), or the dephosphorylation of “key” substrates of mitotic kinases by phosphatases. These processes contribute to SAC silencing both on the kinetochore and in the cytoplasm, but their relative importance and interdependence are still not well understood (Fig. 1.4).

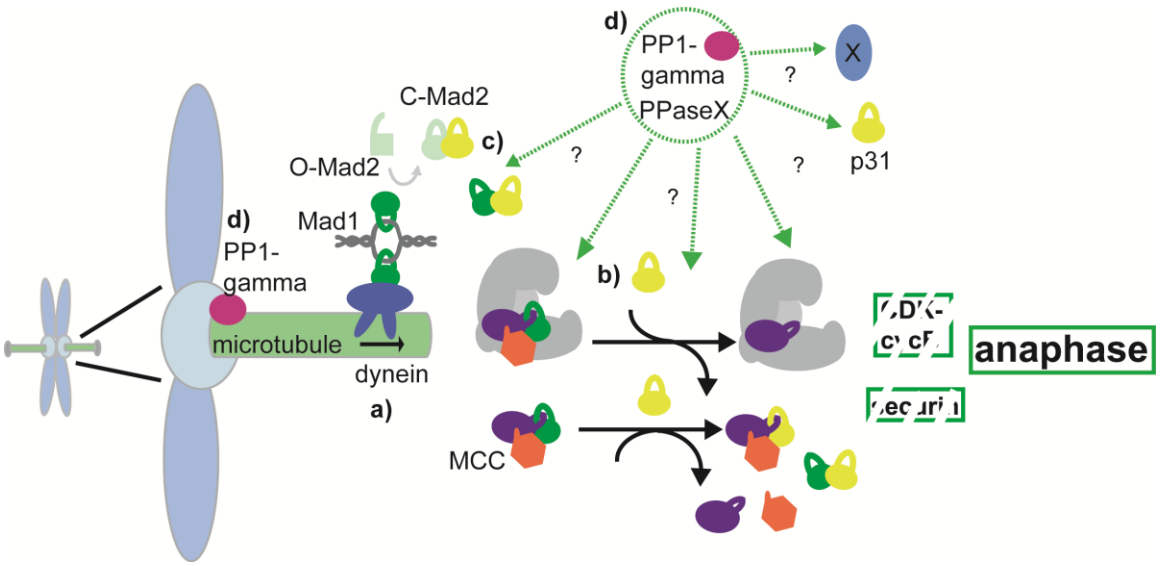

Figure 1.4 Schematic representation of spindle assembly checkpoint silencing pathways. Upon biorientation, **(a)** dynein removes Mad1-C-Mad2 tetramers from kinetochores, **(b)** p31 disassembles MCC and may also block O-Mad1-to-C-Mad2 catalysis at kinetochores **(c)**, **(d)** phosphatase activity (PP1-gamma and perhaps others) dephosphorylate checkpoint kinase substrates, both at the kinetochore and in the cytoplasm, all of which relieves the inhibition on APC/C, allowing cyclin B and securin degradation and, consequently, anaphase onset. For simplicity, other pathways such as cdc20 ubiquitylation and CENPE-mediated BubR1 inhibition are not shown.

Dynein stripping

At the kinetochore, the main checkpoint silencing mechanism is "dynein stripping": the motor-protein dynein mediates the removal of Mad1-Mad2 tetramers and other checkpoint proteins towards spindle poles. Early in mitosis, dynein is recruited to unattached kinetochores by the protein Spindly and the RZZ complex (Starr et al., 1998; Griffis et al., 2007; Inoue et al., 2008). Upon chromosome biorientation, dynein is activated by phospho-regulated mechanism and the "stripping" process begins. Because dynein depletion or reduced recruitment to kinetochores causes a delay in mitotic progression, it was proposed that dynein contributes to SAC silencing (Faulkner et al., 2000; Howell et al., 2001; Stehman et al., 2007). However, it has been shown that detectable levels of Mad2 remain at attached kinetochores and that depletion of Mad2 from kinetochores is not required for anaphase onset (Canman et al., 2002). Similarly, in Chapter 2, I show that checkpoint arrest can be overcome by kinase inhibition in the cytoplasm, regardless of the continued localization of Mad1-Mad2 tetramers at kinetochores. Hence, the extent to which, and the kinetics with which, dynein stripping contributes to SAC silencing are still an unresolved question. To try to examine these matters, I joined an ongoing collaboration with Dr James Chen's laboratory (Stanford), who was in the process of validating and characterizing the first specific small molecule dynein inhibitor (Firestone et al., 2012). This work is discussed in Chapter 3.

Ubiquitylation, degradation and p31/Comet

In the cytoplasm, a variety of inter-related mechanisms have been proposed to play roles in checkpoint silencing. For instance, APC/C-mediated proteolysis of cyclin B,

securin, and Mps1 is thought to contribute to the maintenance of SAC silencing during anaphase, once tension is lost (Palframan et al., 2006). Similarly, auto-ubiquitylation of cdc20 is thought to promote its dissociation from Mad2 and the MCC to overcome the arrest. Interestingly, cdc20 auto-ubiquitylation-mediated turnover is also thought to be active throughout SAC arrest, and this is thought to allow rapid disengagement from MCC and checkpoint silencing once biorientation is achieved (Mansfeld et al., 2011; Reddy et al., 2007; Nilsson et al., 2008).

Another protein that is thought to be involved in MCC disassembly and the release of cdc20 inhibition is the "C-Mad2 inhibitor" p31/Comet. This protein is structurally similar to C-Mad2 and can bind both Mad1- and cdc20-bound C-Mad2; however, it does not support further Mad2 O-to-C conversion (Yang et al., 2007). Therefore, p31/Comet is thought to provide a "brake" to the Mad2 template amplification at the kinetochore. Furthermore, by binding to cdc20-bound C-Mad2, p31/Comet not only thwarts C-Mad2's APC/C inhibitory activity, but also facilitates the disassembly of C-Mad2-cdc20 complexes (in part because C-Mad2 and p31/Comet share a common binding site on cdc20; Yang et al., 2007). P31/Comet also promotes the autoubiquitylation and degradation of cdc20 during prometaphase, a homeostatic mechanism to maintain steady states of MCC-cdc20 that is thought to promote timely exit from mitosis, even if not needed for SAC silencing *per se* (Varetti et al., 2011). The full details of p31/Comet activity and its regulation, the process of cdc20 autoubiquitylation during metaphase and anaphase and the interactions and relative contributions between these two processes remain to be fully elucidated.

PP1-gamma-mediated dephosphorylation

Finally, another mechanism involved in SAC silencing is the dephosphorylation of checkpoint effectors. Although intuitively obvious that the kinase phosphorylations necessary for SAC arrest must be reversed for progression into anaphase, it has only been recently that the process began to be clarified. Dissection of this mechanism has greatly benefited from studies in yeast, organisms in which, notably, most of the other silencing pathways are currently thought to be non-essential or non-existent. Studies in budding and fission yeast have shown that the phosphatase PP1-gamma is essential for checkpoint silencing (Pinsky et al., 2009; Vanoosthuyse and Hardwick, 2009). Further studies in yeast and vertebrate cells showed that PP1-gamma acts not only in the cytoplasm, but also at the kinetochore, and revealed that a bi-stable PP1/AuroraB mechanism operates to recruit PP1-gamma when kinetochores have been attached by microtubules (Liu et al., 2010; Meadows et al., 2011; Rosenberg et al., 2011). These results began to uncover how checkpoint silencing is coupled to chromosomal biorientation, a crucial question that remains unanswered. Determining the identity of all checkpoint PP1 substrates, as well as the interplay between PP1-gamma-mediated silencing and the other mechanisms described above will also be important questions for future research.

Unresolved questions and motivation for thesis research

Although we know a lot of the molecular details of the checkpoint mechanism, there are still many basic questions that have not been studied in detail. For instance: we know

that Mad1-Mad2's dynamic localization (at unattached kinetochores and removed upon biorientation) strongly correlates with spindle checkpoint activity, but it is unknown whether this kinetochore localization is necessary and/or sufficient for checkpoint arrest. Would the sustained presence of Mad1-Mad2 at kinetochores be sufficient to maintain checkpoint arrest, even if all chromosomes were bioriented? If so, would removal of Mad1-Mad2 from kinetochores be sufficient to silence the checkpoint? Some evidence that suggests this removal is not necessary (Canman et al., 2002). Otherwise, what is the major checkpoint silencing mechanism?

With respect to necessity of kinetochore localization of Mad1-Mad2, what are the roles of kinetochores in checkpoint arrest? In other words, could Mad1-Mad2 induce robust checkpoint arrest from ectopic locations, such as other chromosomal sites, or even the cytoplasm? We know that kinetochores are necessary for checkpoint signaling: kinetochore-null cells cannot establish the SAC and only kinetochore-bound Mad1-Mad2 can sustain a robust O-to-C-Mad2 catalytic amplification (Janke et al., 2001; Kline et al., 2006; Salmon and Mussachio, 2007). On the other hand, some evidence indicates that, if Mad1-Mad2 cannot be recruited to kinetochores (for instance, due to Bub3 depletion in budding yeast), checkpoint arrest can nevertheless be established from the cytoplasm, albeit transiently and weakly (Windecker et al., 2009). Moreover, overexpression overexpression of Mad2 induces metaphase arrest in a variety of systems, including human cells (Chen et al., 1998; Sironi et al., 2001; Howell et al., 2004; De Antoni et al, 2005). This suggests that the role of kinetochores may mainly be to act as recruitment platforms that induce Mad1-Mad2 clustering to establish a robust

checkpoint arrest. Could we activate checkpoint by artificially or ectopically clustering Mad1-Mad2?

If dynamic localization of Mad1-Mad2 is necessary for function, if their kinetochore localization is sufficient to induce checkpoint arrest and if, therefore, perturbing localization has downstream effects on checkpoint signaling, then we should be able to bypass the requirement of a primary signal for the recruitment of Mad1-Mad2 and ensuing checkpoint arrest by artificially tethering the proteins to kinetochores. If we could develop a system that, by controlling Mad1 localization, controls checkpoint signaling regardless of detection of the primary signal, then this uncoupling of checkpoint activity from chromosome biorientation would enable us to study details of checkpoint signaling and silencing that are not possible to study with other methods. For instance, we could examine the roles of "checkpoint" kinases in checkpoint signaling. Because kinases such as Aurora B and Mps1 have a variety of functions in processes that are necessary to be in place for checkpoint signaling to occur (e.g. assembling the spindle and kinetochores, recruiting checkpoint proteins, controlling kinetochore-microtubule interactions), it has been very difficult to dissect whether these kinases also had bona fide roles in checkpoint establishment and maintenance, or if the checkpoint-abrogating effects seen upon their inhibition was merely due to the disruption of their necessary "upstream" functions.

In this thesis work, I have tackled some of these questions. In Chapter 2, I present an approach that, by constitutively localizing Mad1 at kinetochores *via* a fusion to the kinetochore protein Mis12, allows us to uncouple checkpoint signaling from

chromosome biorientation. I used this system to examine the roles of different checkpoint kinases in the maintenance of the arrest downstream of Mad1-Mad2 kinetochore recruitment. I also used similar approaches of fusing Mad1 to non-kinetochore chromosomal proteins to examine whether checkpoint arrest can be established ectopically. In Chapter 3, I describe my characterization of the mitotic effects of the small molecule ciliobrevin D, the first specific inhibitor of the motor protein dynein. This work, which was part of a collaboration with James Chen's laboratory (Stanford University), sought to establish this small molecule as a tool for the study of checkpoint silencing. In Chapter 4, I conclude with a discussion of possible future directions of my findings, as well as of the spindle assembly checkpoint field in general. I have also included an appendix with preliminary results for follow-up studies to the Mis12-Mad1 project.

Chapter 2: Constitutive Mad1 targeting to kinetochores uncouples checkpoint signaling from chromosome biorientation

Summary

Accurate chromosome segregation depends on biorientation, whereby sister chromatids attach to microtubules emanating from opposite spindle poles. The spindle assembly checkpoint is a conserved surveillance mechanism in eukaryotes that inhibits anaphase onset until all chromosomes are bioriented (Hartwell and Weinert, 1989; Rieder et al., 1994; Musacchio and Salmon, 2007). In current models, the recruitment of Mad2, *via* Mad1, to improperly attached kinetochores is a key step needed to stop cell cycle progression (Musacchio and Salmon, 2007; Chen et al., 1996; Li and Benezra, 1996; Chen et al., 1998). However, it is not known if the localization of Mad1-Mad2 to kinetochores is sufficient to block anaphase. Furthermore, it is unclear if other signaling proteins (e.g. Aurora B kinase; Meraldi et al., 2004b) that regulate chromosome biorientation have checkpoint functions downstream of Mad1-Mad2 recruitment to kinetochores or if they act upstream to merely quench the primary error signal (Pinsky

and Biggins, 2005; Pinsky et al., 2006). To address both these issues, I engineered a Mad1 construct which, unlike endogenous Mad1, localizes to kinetochores that are bioriented. In this Chapter, I show that Mad1's constitutive localization at kinetochores is sufficient for a metaphase arrest that depends on Mad1-Mad2 binding. By uncoupling the checkpoint from its primary error signal, I show that Aurora kinase, Mps1 and BubR1, but not Polo-like kinase, are needed to maintain the checkpoint arrest even when Mad1 is present on bi-oriented kinetochores. Together, my data suggest a model in which the biorientation errors, which recruit Mad1-Mad2 to kinetochores, may be signaled not only through Mad2's templated activation dynamics, but also through the activity of widely conserved kinases, to ensure the fidelity of cell division.

Rationale

The spindle assembly checkpoint, which can block anaphase when even a single chromosome is improperly attached to spindle microtubules, depends on Mad1 and Mad2 (Musacchio and Salmon, 2007). In current models of checkpoint signaling, a key step is the recruitment of Mad1 and Mad2 to kinetochores that lack proper microtubule attachments. Mad1 forms a homodimer that binds two Mad2 molecules, forming a "core tetramer", which "templates" the conversion of cytosolic Mad2 from an inactive "open" conformation to a "closed" form (Fig. 2.1; Sironi et al., 2002; Luo and Yu, 2008;). A diffusible cytosolic complex, which includes closed-Mad2, blocks anaphase progression by inhibiting the activation of APC/C, the E3 ubiquitin ligase required for anaphase (Musacchio and Salmon, 2007; Hardwick et al., 2000; Sudakin et al., 2001).

The binding of microtubules to the kinetochore removes Mad1-Mad2 and thereby suppresses the generation of closed-Mad2 (Fig. 2.1; Musacchio and Salmon, 2007). As Mad1, unlike Mad2, is not expected to undergo conformational dynamics at kinetochore sites (Sironi et al., 2002; Luo and Yu, 2008) and is not a component of the soluble complex that inhibits APC/C activation (Hardwick et al., 2000; Sudakin et al., 2001), we envisioned that engineering the constitutive localization of Mad1 to kinetochores may dissociate checkpoint signaling from the status of biorientation, the primary error signal.

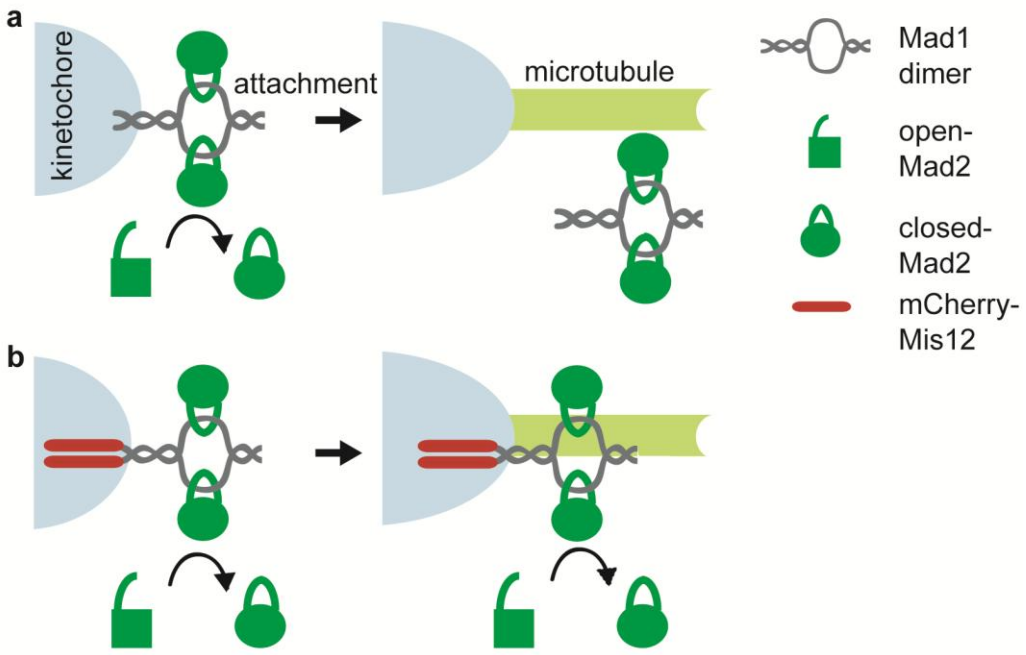

Figure 2.1 Experimental design to recruit Mad2 to kinetochores independently of microtubule attachment. (a) Endogenous Mad1 (grey) localizes to kinetochores that are not attached to microtubules and recruits Mad2 (dark green), forming a Mad1-Mad2 core tetramer. The Mad1-bound Mad2 catalytically converts open-Mad2 molecules (dark green square) into closed-Mad2 molecules (dark green circle). Microtubule (light green) binding displaces Mad1, and therefore Mad2, from kinetochores. **(b)** We fused Mad1 to Mis12 (red), a protein whose kinetochore localization is microtubule-binding independent. This construct could retain Mad1 (and Mad2) on microtubule-attached kinetochores.

Constitutive kinetochore localization of Mad1 induces Mad2-dependent checkpoint arrest

To localize Mad1 at all kinetochores, I considered fusing it to Mis12, a kinetochore resident protein and member of the KMN complex, a core component of the outer kinetochore (Cheeseman et al., 2004). Since KMN proteins are implicated in recruiting endogenous Mad1 to kinetochores (Santaguida and Musacchio, 2009), I reasoned that engineered fusion constructs could be designed to achieve a kinetochore localization of Mad1 similar to the endogenous one, but independent of kinetochore-microtubule attachment. A fusion construct with an N-terminal mCherry tag, followed by a flexible linker, Mis12, a second flexible linker and Mad1 at the C-terminus— such that interactions with Mad2 would likely remain unaffected— was found to express at levels that were similar to endogenous Mad1 (Fig. 2.2a). In live cells, I found that mCherry-Mis12-Mad1 localized to puncta on the chromosomes, as would be expected for a kinetochore-targeted protein, in mitotic and interphase cells (Fig. 2.2b). Unlike endogenous Mad1, this signal was observed on chromosomes at the metaphase plate, suggesting that the fusion construct localized at properly bioriented chromosomes. In addition, immunofluorescence analysis of CREST and tubulin signals in fixed cells revealed the robust localization of mCherry-Mis12-Mad1 at outer kinetochores that were aligned at the metaphase plate and had microtubule bundles with intensities similar to that of control mitotic cells (Fig. 2.2c-e). To visualize interactions between mCherry-Mis12-Mad1 and Mad2 in live cells, I generated a HeLa cell line that stably expresses GFP-Mad2 and transiently transfected it with mCherry-Mis12-Mad1. I

incubated these cells in the proteosome inhibitor MG132, such that metaphase spindles would accumulate and the endogenous Mad1 would be removed from the kinetochores. Live imaging revealed that GFP and mCherry signals co-localized on all chromosomes of the mCherry-positive cells, even if they had tight metaphase plates that persisted for hours (Fig. 2.2f-g). These results show that fusion of Mad1 to Mis12 achieves constitutive kinetochore localization of Mad1 and Mad2, regardless of microtubule attachment.

Figure 2.2 A mCherry-Mis12-Mad1 fusion can recruit Mad2 to kinetochores independently of microtubule attachment. (a) The expression levels of mCherry-Mis12-Mad1, mCherry-Mis12-Mad1 K541A L543A (AA) and mCherry-Mad1 (upper bands) are similar to the levels of endogenous Mad1 (lower bands), by immunoblotting. **(b)** Analysis of mCherry-Mis12-Mad1 localization in live cells. Differential interference contrast (DIC) and mCherry-fluorescence images of a mCherry-Mis12-Mad1-transfected cell at metaphase. **(c-e)** mCherry-Mis12-Mad1 localizes at kinetochores, even when they are attached to microtubules. Immunofluorescence images of HeLa (control) **(c)** and mCherry-Mis12-Mad1-transfected **(d)** cells, stained for DNA, tubulin, CREST and mCherry. Overlay shows tubulin (green), CREST (blue) and mCherry (red). Insets (selected optical sections) **(e)** show individual microtubule-attached kinetochores from (d), 5-fold magnification. **(f)** Analysis of Mad2 recruitment by mCherry-Mis12-Mad1. DIC, mCherry- and GFP-fluorescence images of a HeLa cell stably-expressing GFP-Mad2, transfected with mCherry-Mis12-Mad1 are shown. MG132 (10 μM, 1 h) was used to accumulate live cells at metaphase with many microtubule-attached chromosomes. (g) The metaphase arrest induced by mCherry-Mis12-Mad1 is persistent. Live mCherry-fluorescence images of a mCherry-Mis12-Mad1-transfected HeLa cell at metaphase are shown. The indicated times (h: min) are relative to time of transfection. Scale bar, 5 μm.

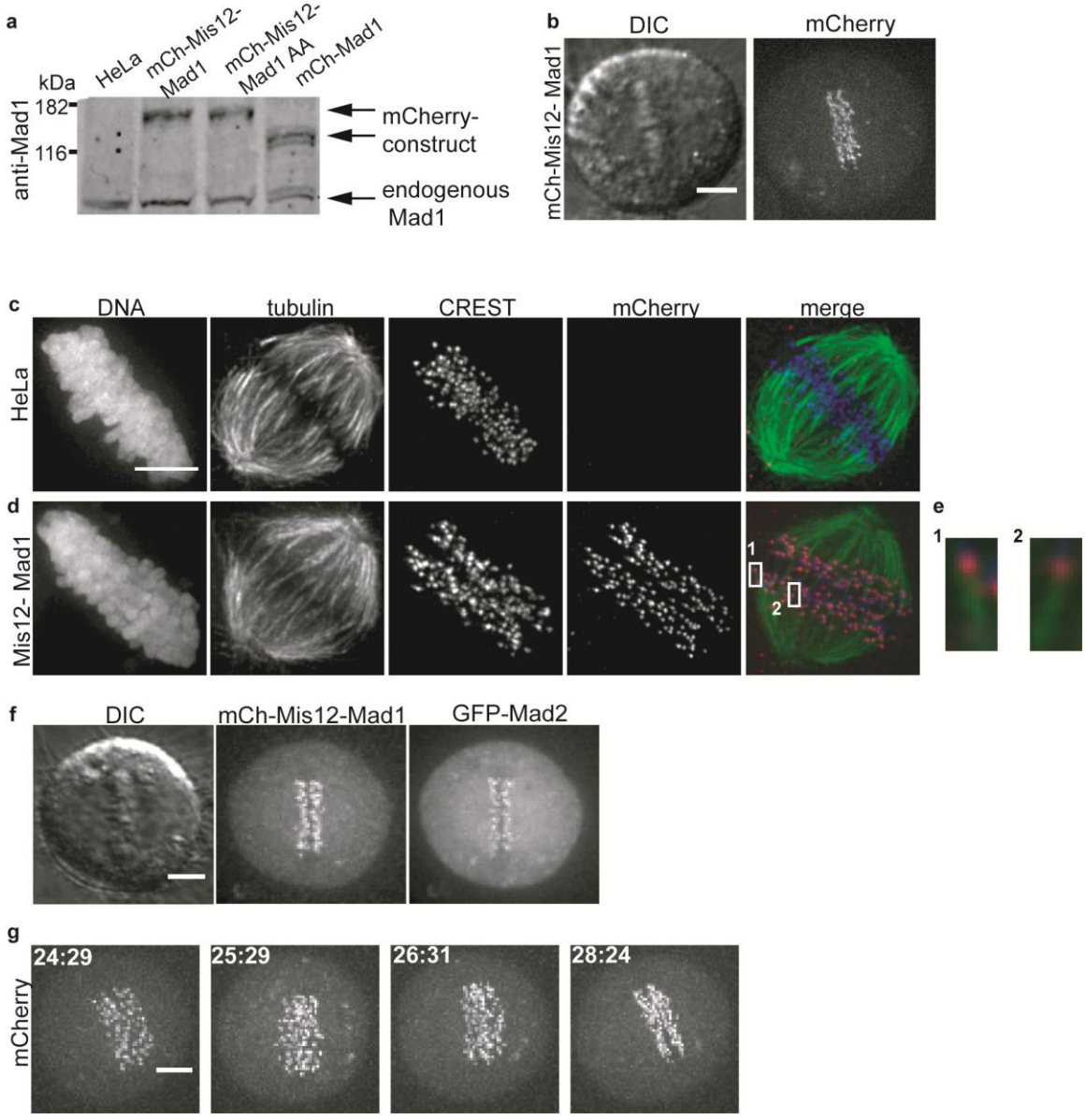
a
HeLa
mCh-Mis12-Mad1
mCh-Mis12-Mad1 AA
mCh-Mad1
kDa
182
116
anti-Mad1
mCherry-construct
endogenous Mad1
b
DIC
mCherry
mCh-Mis12- Mad1
c
DNA
tubulin
CREST
mCherry
merge
HeLa
d
Mis12- Mad1
1
2
e
1
2
f
DIC
mCh-Mis12-Mad1
GFP-Mad2
g
mCherry
24:29
25:29
26:31
28:24

I then investigated the effects of the constitutively kinetochore-localized Mad1-Mad2 on cell cycle progression. Compared to untransfected control cells, I observed a ~5-fold increase (27.6% ± 2%) in the mitotic index of the mCherry-positive cells, 24 h post-transfection. Of these mitotic cells, 95.6% (± 1.7%) were at metaphase (Fig. 2.3a). Thirty hours after transfection, the mitotic index of the mCherry-Mis12-Mad1-transfected population increased to 43% (± 6.2%), indicating that this metaphase arrest was persistent. Similar results were found with live imaging experiments (Fig. 2.2g). In addition, mCherry-Mis12-Mad1 transfected into immortalized RPE-1 cells also resulted in a persistent metaphase arrest (Fig. 2.3b). To confirm that the increased mitotic index seen in mCherry-Mis12-Mad1-transfected cells was not caused by overexpression of Mad1 alone, I transfected cells with mCherry-Mad1. This construct was expressed at levels similar to that of mCherry-Mis12-Mad1 (Fig. 2.2a), and the transfected population did not show an increase in the mitotic index (Fig. 2.3c). This suggests that it is the kinetochore targeting of the forced-localized Mad1, and hence Mad2, that is responsible and sufficient for inducing a persistent metaphase arrest.

Figure 2.3 Constitutive kinetochore localization of Mad1 causes a persistent, Mad2-dependent metaphase arrest. (a) Analysis of mitotic index and phenotypes in HeLa, mCherry-Mis12-Mad1- and mCherry-Mis12-Mad1 AA- transfected cells. Cells were fixed 24 h and 30 h after transfection. **(b)** Analysis of mitotic index of mCherry-Mis12-Mad1- and mCherry-Mis12-Mad1 AA- transfected, or untransfected RPE-1 cells. Cells were fixed 48 h after transfection. **(c)** Analysis of mitotic index in mCherry-Mad1-transfected and untransfected HeLa cells. Cells were fixed 24 h after transfection. For **(a-c)**, mCherry, tubulin and DNA staining (not shown) was used to determine mitotic index and fraction of cells in metaphase, anaphase and all other mitotic states (*n*= 3 independent experiments, > 400 cells counted per condition per time). **(d)** The increase in mitotic index induced by mCherry-Mis12-Mad1 is Mad2-dependent. HeLa cells were transfected with small-interfering RNA against Mad2 or GFP, 24 h before transient transfection with mCherry-Mis12-Mad2 or mCherry-Mis12-Mad1-AA, or no transfection. Mitotic indices were determined after another 24 h (n= 3 independent experiments, > 250 cells counted per condition per time). **(e-g)** mCherry-Mis12-Mad1 AA localizes at kinetochores in interphase **(e)**, metaphase **(f)** and anaphase **(g)**. Staining for DNA, tubulin, CREST and mCherry is shown. **(h)** mCherry-Mis12-Mad1 AA does not prevent the completion of mitosis. mCherry fluorescence images of a live cell are shown. The indicated times (min) are relative to the first frame (prometaphase). **(i-k)** Expression of mCherry-Mis12-Mad1 and mCherry-Mis12-Mad1 AA are similar, by quantification of normalized, corrected fluorescence levels of mCherry by immunoblotting (*n*= 3 independent experiments) **(i)**, of mCherry in whole cells by live imaging (*n*= 2 independent experiments, > 14 cells counted per condition per time) **(j)** and of mCherry at individual kinetochores by immunofluorescence (*n*= 2 independent experiments, > 3 kinetochores counted per cell, 69 kinetochores per condition in total) **(k)**. **(l-m)** mCherry-Mis12-Mad1-AA localizes at kinetochores, but does not recruit GFP-Mad2. mCherry- **(l)** and GFP- **(m)** fluorescence images of a mCherry-Mis12-Mad1-AA transfected cell at metaphase. MG132 (10 µM, 1 h) was used to accumulate live cells at metaphase with many microtubule-attached chromosomes. Scale bar, 5 µm. Average ± s.e.m. shown.

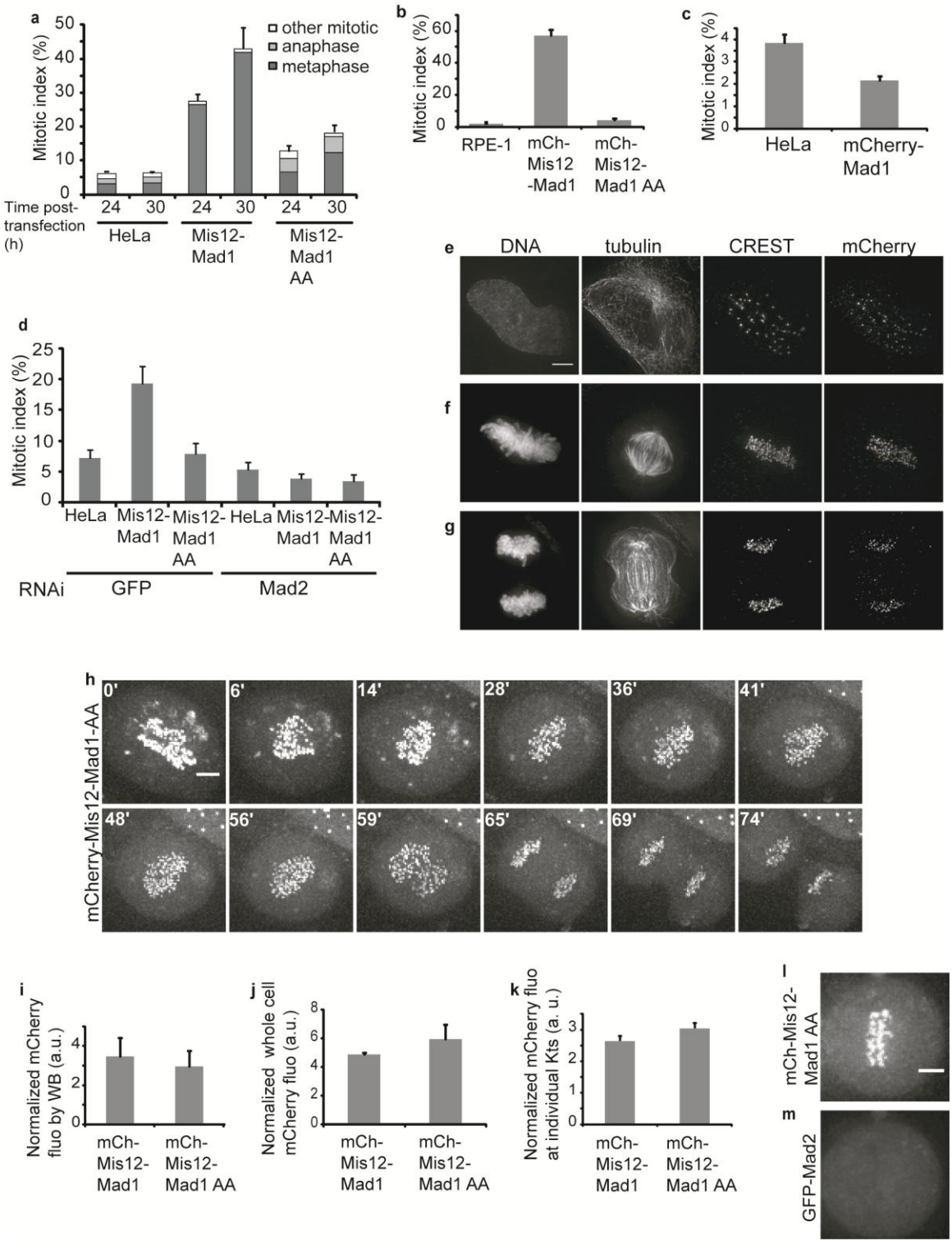
a
Mitotic index (%)
other mitotic
anaphase
metaphase
Time post-transfection (h)
24 30 24 30 24 30
HeLa
Mis12-Mad1
Mis12-Mad1 AA
b
Mitotic index (%)
RPE-1
mCh-Mis12-Mad1
mCh-Mis12-Mad1 AA
c
Mitotic index (%)
HeLa
mCherry-Mad1
d
Mitotic index (%)
HeLa Mis12-Mad1 Mis12-Mad1 AA HeLa Mis12-Mad1 Mis12-Mad1 AA
RNAi
GFP
Mad2
e
DNA
tubulin
CREST
mCherry
f
g
h
mCherry-Mis12-Mad1-AA
0' 6' 14' 28' 36' 41'
48' 56' 59' 65' 69' 74'
i
Normalized mCherry fluo by WB (a.u.)
mCh-Mis12-Mad1
mCh-Mis12-Mad1 AA
j
Normalized whole cell mCherry fluo (a.u.)
mCh-Mis12-Mad1
mCh-Mis12-Mad1 AA
k
Normalized mCherry fluo at individual Kts (a. u.)
mCh-Mis12-Mad1
mCh-Mis12-Mad1 AA
l
mCh-Mis12-Mad1 AA
m
GFP-Mad2

Next, I analyzed whether this mitotic index increase was a *bona fide*, Mad2-dependent checkpoint arrest in two ways. First, I used RNA interference (RNAi) to deplete Mad2. I observed a significant decrease in the mitotic index of the mCherry-Mis12-Mad1 population upon transfection with Mad2 siRNA (two-tailed T-test, p=0.026; Fig 2.3d). Second, I used a Mad1 K541A L543A mutant construct (hereafter, mCherry-Mis12-Mad1 AA), which does not interact with Mad2 owing to mutations in the Mad2-binding motif (Sironi et al., 2002). I found that the mCherry-Mis12-Mad1 AA fusion localized at kinetochores both in mitotic and interphase cells (Fig. 2.3e-h) and expressed at similar levels to those of mCherry-Mis12-Mad1 (Fig. 2.2a, 2.3i-k). As expected, I did not detect co-localization of mCherry-Mis12-Mad1 AA and GFP-Mad2 (Fig. 2.3l-m). The mitotic index of cells transfected with this "mutant" construct was 12.7% (± 1.7%; Fig. 2.3a), which was significantly different from mCherry-Mis12-Mad1-transfected cells (two-tailed T-test, p=0.005). Moreover, mCherry-Mis12-Mad1 AA-positive cells divided without appreciable chromosome segregation defects (Fig. 2.3g-h). Together, these results indicate that the increase in the mitotic index resulting from mCherry-Mis12-Mad1 expression is dependent on Mad2-binding.

Mis12-Mad1 does not induce overt alterations in kinetochore structure or function

I then examined if the prolonged mitotic arrest was due to indirect effects on kinetochore structure and kinetochore-microtubule binding. First, I used cold treatment to analyze the stability of kinetochore-microtubule attachments in mCherry-Mis12-

Mad1 and -Mad1-AA- expressing cells. Immunofluorescence showed the presence of cold-stable kinetochore-microtubule bundles, with co-localizing mCherry and CREST signals at the kinetochore ends (Fig. 2.4c-f). These cold-stable microtubules had organizations that were indistinguishable from those in control cells (Fig. 2.4a-b).

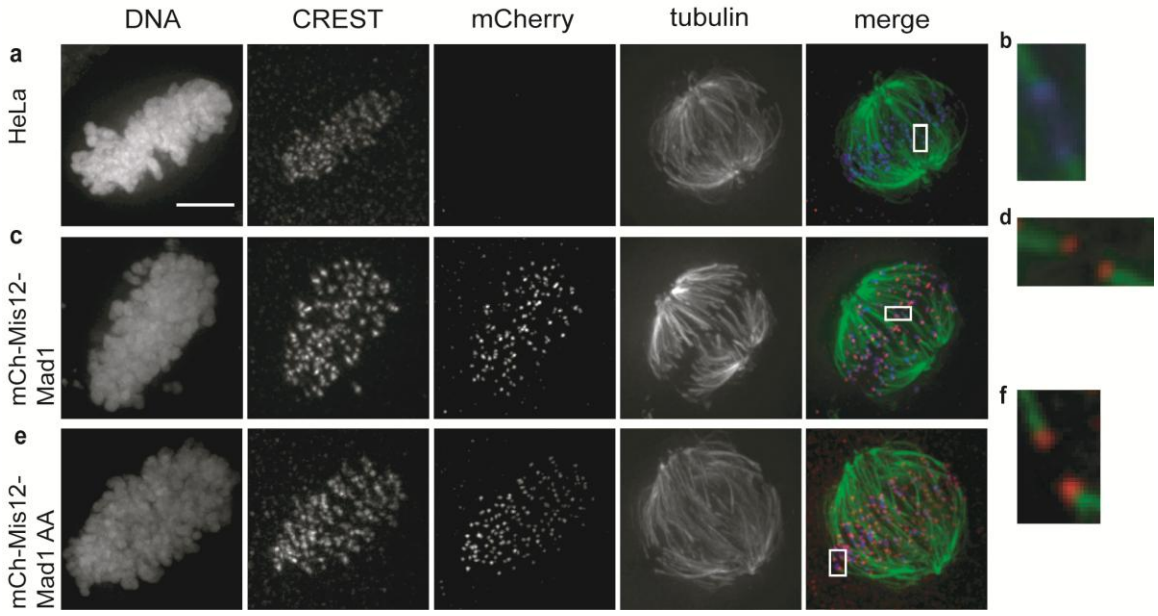

Figure 2.4 Analysis of cold-stable microtubules shows that forced kinetochore localization of Mad1 does not disrupt microtubule attachment. HeLa **(a)**, mCherry-Mis12-Mad1- **(c)** or mCherry-Mis12-Mad1-AA-transfected **(e)** cells were incubated in MG132 (10 µM, 1 h) to accumulate cells at metaphase and were then placed on ice (10 min) before fixation. Cells were stained for DNA, CREST (blue), mCherry (red) and tubulin (green). Individual channels and an overlay are shown. Insets (selected optical sections) **(b, d, f)** show individual cold-stable microtubule-attached kinetochores (4-fold magnification). Scale bar, 5 µm.

Next, I analyzed the localization of $p150^{Glued}$, CENP-E, Bub1, ROD and ZW10—checkpoint proteins that reside at the kinetochore corona. Since kinetochore assembly is hierarchical, correct recruitment of corona components suggests proper kinetochore assembly (Cheeseman et al., 2004; Cheeseman and Desai, 2008). These checkpoint proteins are recruited to kinetochores that have not yet bioriented and are completely or partially removed from those sites upon biorientation, in unperturbed mitotic cells (Musacchio and Salmon, 2007; Hoffman et al., 2001; Karess, 2005). I first exposed the cells to the microtubule depolymerizing drug nocodazole to suppress biorientation. $P150^{Glued}$, CENP-E, Bub1, Rod and ZW10 were all seen on unattached kinetochores, both in mCherry-Mis12-Mad1-expressing and control cells (Fig. 2.5a-e, first to third columns). Additionally, $p150^{Glued}$ and CENP-E recruitment was also undisrupted in nocodazole-treated mCherry-Mis12-Mad1 AA-transfected cells (Fig. 2.5f-g). I then examined the localization of these proteins on otherwise unperturbed, bioriented mCherry-Mis12-Mad1-positive kinetochores. Immunofluorescence revealed that the removal (or reduction) of each of these proteins was consistent with published data on their localization on bioriented chromosomes (Fig. 2.5a-e, fourth and fifth columns). Together, these data suggest that there are no overt dominant-negative effects on kinetochore structure or microtubule attachments caused by mCherry-Mis12-Mad1.

Figure 2.5 Analysis of localization of checkpoint proteins in cells with mCherry-Mis12-Mad1 shows that forced kinetochore localization of Mad1 does not disrupt kinetochore structure. (a-g) HeLa, mCherry-Mis12-Mad1- **(a-e)** and mCherry-Mis12-Mad1-AA- **(f, g)** transfected cells were incubated in nocodazole (1 µg ml-1, 45 min; **a-e** first to third columns; **f, g**) or left unperturbed (**a-e** fourth and fifth columns). Cells were stained for DNA, CREST, mCherry and the relevant checkpoint protein. Immunofluorescence images show staining for mCherry and $p150^{Glued}$ **(a, f)**, CENP-E **(b, g)**, Bub1 **(c)**, ROD **(d)** or ZW10 **(e)**. Scale bar, 5 µm.

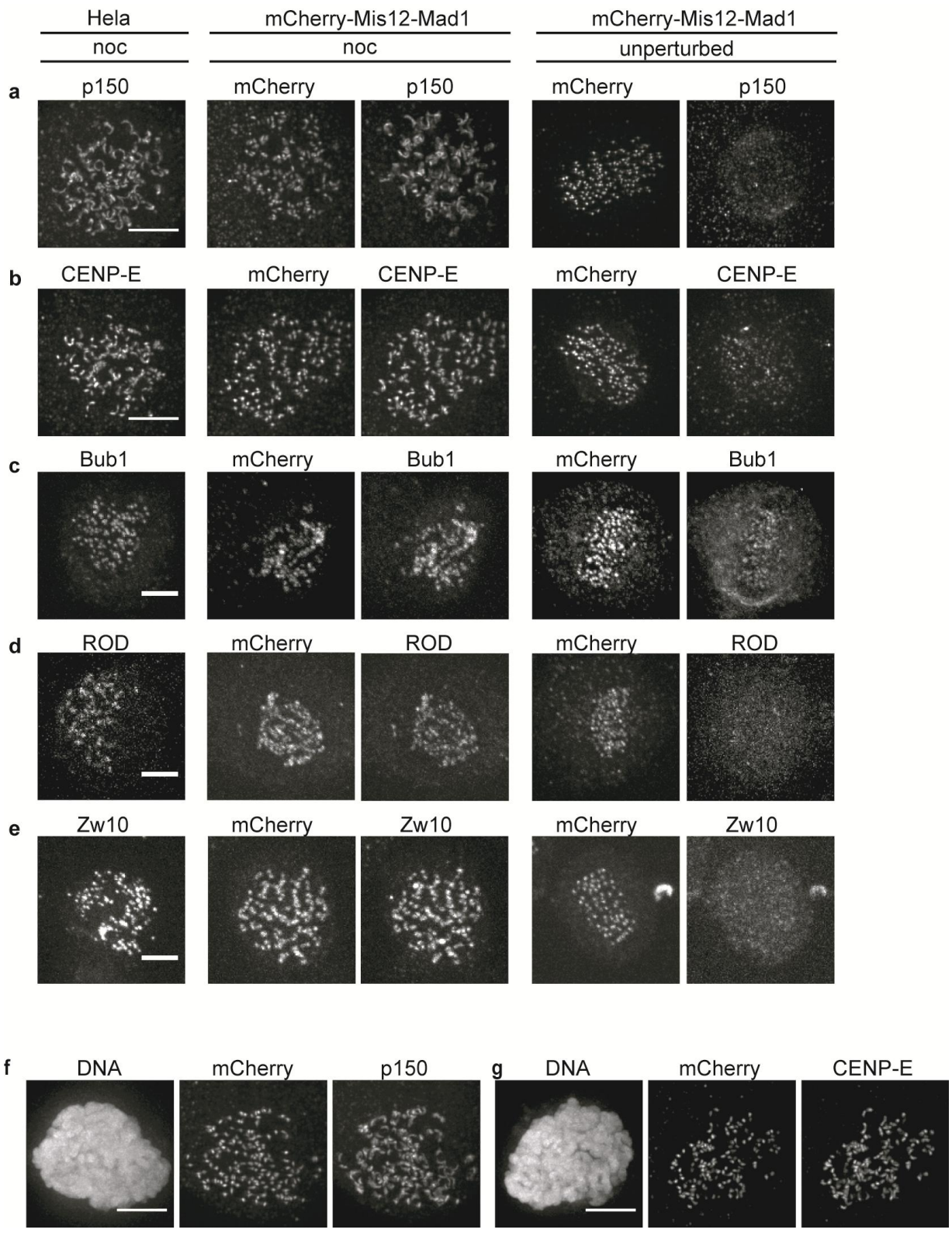
Hela
noc
mCherry-Mis12-Mad1
noc
mCherry-Mis12-Mad1
unperturbed
a
p150
mCherry
p150
mCherry
p150
b
CENP-E
mCherry
CENP-E
mCherry
CENP-E
c
Bub1
mCherry
Bub1
mCherry
Bub1
d
ROD
mCherry
ROD
mCherry
ROD
e
Zw10
mCherry
Zw10
mCherry
Zw10
f
DNA
mCherry
p150
g
DNA
mCherry
CENP-E

Constitutive localization of Mad1 to non-kinetochore locations does not induce checkpoint arrest

Next, I examined whether it was the kinetochore location of Mad1 that was necessary for such an arrest, by force-localizing Mad1 to two different chromosomal locations. First, I mis-localized Mad1 all along chromosomes by fusing it to histone H2B. The mCherry-H2B-Mad1 fusion showed the expected localization (Fig. 2.6a-i) and did not have dominant-negative effects (Fig. 2.6d-e). mCherry-H2B-Mad1-expressing cells were able to undergo anaphase normally (Fig. 2.6h-i) and the mitotic index of this population was indistinguishable from that of the control (Fig. 2.6j; two-tailed T-test, $p=0.20$). To confirm that, despite not having apparent mitotic effects, mCherry-H2B-Mad1 indeed interacted with Mad2, I transfected the construct into the GFP-Mad2 line. I found that mCherry-H2B-Mad1 and GFP-Mad2 co-localized throughout all chromosomes in interphase and mitosis, including anaphase (Fig. 2.6k-p). This suggests that chromosomal recruitment of Mad2 is not sufficient for establishing checkpoint arrest.

Figure 2.6 Forced localization of Mad1 to chromosome arms by fusion to H2B recruits Mad2, but does not affect mitosis. HeLa cells **(a-e)** or HeLa cells stably expressing GFP-Mad2 **(f-p)** were transfected with mCherry-H2B-Mad1 and processed 48 h later. **(a)** GFP-Mad2 co-localizes with mCherry-H2B-Mad1 throughout chromosome arms. Immunofluorescence images of a chromosome spread show staining for DNA, mCherry and GFP. **(b)** mCherry-H2B-Mad1-transfected cells were incubated in nocodazole (1 μg/ml, 45 min) and stained for DNA, mCherry, CREST and CENP-E. Insets (selected optical sections) **(c)** show various kinetochores where CENP-E crescents are observed (4-fold magnification). **(d)** Analysis of cold-stable microtubules. mCherry-H2B-Mad1-transfected cells were incubated in MG132 (10 μM, 1 h) to accumulate cells at metaphase and were then placed on ice (10 min) before fixation. Cells were stained for DNA, CREST, mCherry and tubulin Insets (selected optical sections) **(e)** show individual cold-stable microtubule-attached kinetochores (4-fold magnification). **(f-p)** Expression of mCherry-H2B-Mad1 does not affect mitotic progression. DIC **(f, h, k, n)**, mCherry- **(g, i, l, o)** and GFP-fluorescence **(m, p)** images of an interphase cell (**f, g)**, a prometaphase cell **(k-m)** and a cell undergoing anaphase **(h, i, n-p)** are shown. **(j)** Mitotic indices were calculated by analyzing mCherry, tubulin and DNA staining (*n*= 3 independent experiments, > 350 cells counted per condition per time). Scale bar, 5 μm. Average ± s.e.m. shown.

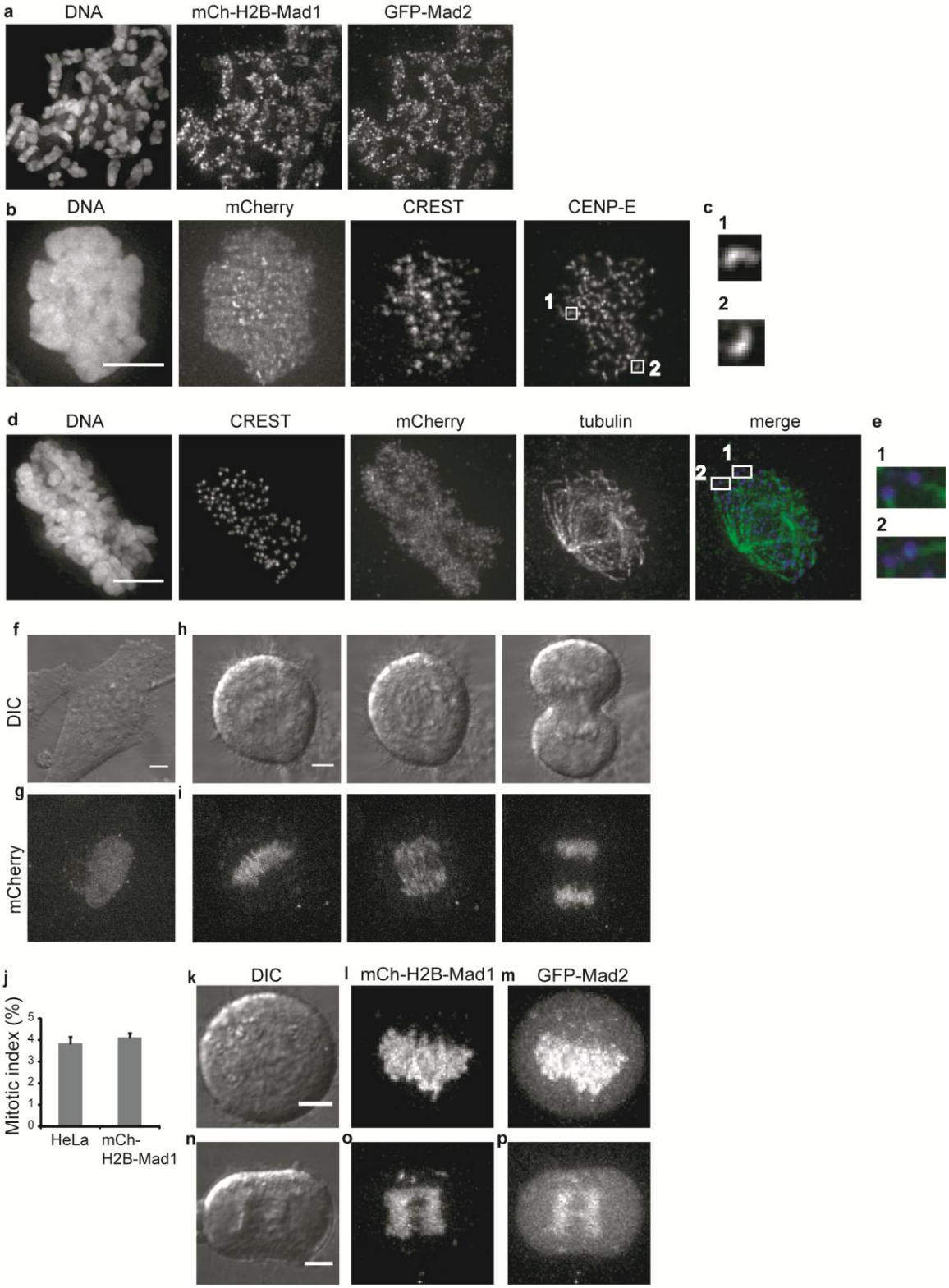
a
DNA
mCh-H2B-Mad1
GFP-Mad2
b
DNA
mCherry
CREST
CENP-E
1
2
c
1
2
d
DNA
CREST
mCherry
tubulin
merge
1
2
e
1
2
f
DIC
h
g
mCherry
i
j
Mitotic index (%)
0
1
2
3
4
5
HeLa
mCh-H2B-Mad1
k
DIC
l
mCh-H2B-Mad1
m
GFP-Mad2
n
o
p

Second, I mis-localized Mad1 at centromeres, *via* fusion with CENP-B's centromere-targeting domain. Unexpectedly, this fusion protein had deleterious effects on kinetochore-microtubule attachments (Fig. 2.7a-g). Although some cells achieved apparent biorientation, live-cell imaging revealed that the majority of these metaphase plates subsequently became mis-aligned, or transitioned into anaphase with numerous lagging chromosomes (Fig. 2.7h-i). Therefore, the use of this construct to dissect checkpoint signaling from chromosome biorientation was unfeasible. Together, these data suggest that the kinetochore represents a specialized chromosomal location for proper Mad1-Mad2 signaling.

Figure 2.7 Fusion of Mad1 to CENP-B's centromere targeting domain has deleterious effects on microtubule attachment. (a-c) mCherry-CENP-B(aminoacids 1-158)-Mad1 localizes at centromeres in interphase **(a)** and mitotic **(b, c)** transfected HeLa cells. Mitotic cells with aligned **(b)** and misaligned chromosomes **(c)** are shown. Immunofluorescence images show staining for DNA, tubulin, CREST and mCherry. **(d)** Mitotic index of HeLa and mCherry-CENP-B-Mad1-transfected cells. **(e)** Comparison of abnormal mitotic phenotypes in HeLa, mCherry-Mis12-Mad1-, mCherry-Mis12-Mad1 AA- and mCherry-CENP-B-Mad1-transfected cells. mCherry, tubulin and DNA staining was used to calculate mitotic index and fraction of cells with multipolar spindles and misaligned chromosomes (*n*= 4 independent experiments, > 100 mitotic cells counted per condition per time). **(f-g)** Analysis of cold-stable microtubules. mCherry-CENP-B-Mad1 transfected cells were incubated in MG132 (10 µM, 1 h) to accumulate cells at metaphase and were then placed on ice (10 min) before fixation. Immunofluorescence images show staining for DNA, CREST, mCherry and tubulin, for two example cells. **(h-i)** Mitotic time-lapses of cells expressing mCherry-CENP-B-Mad1. Two example cells are shown where chromosomal alignment is transiently achieved before gross mis-alignment **(h)** or mis-segregation in anaphase **(i)**. DIC and mCherry channels are shown. Time (in minutes) is relative to the first frame. Scale bar, 5 µm. Average ± s.e.m. shown.

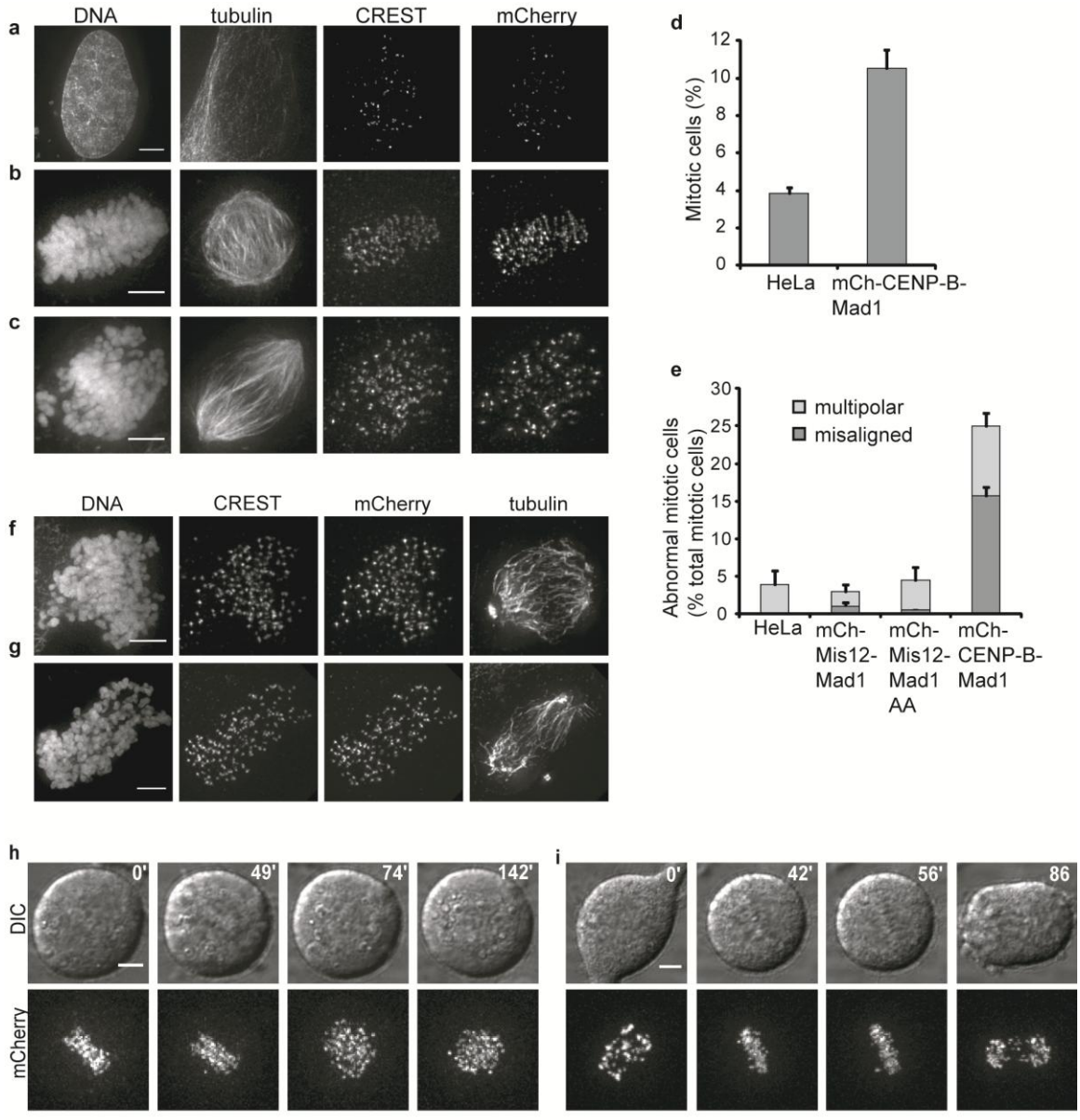
a
DNA
tubulin
CREST
mCherry
b
c
d
Mitotic cells (%)
12
10
8
6
4
2
0
HeLa
mCh-CENP-B-Mad1
e
Abnormal mitotic cells (% total mitotic cells)
30
25
20
15
10
5
0
multipolar
misaligned
HeLa
mCh-Mis12-Mad1
mCh-Mis12-Mad1 AA
mCh-CENP-B-Mad1
f
DNA
CREST
mCherry
tubulin
g
h
DIC
mCherry
0'
49'
74'
142'
i
0'
42'
56'
86

Using Mis12-Mad1 as a tool to examine kinase contributions to checkpoint signaling

Positive and negative "control" kinases

Next, I used the kinetochore-localized Mad1 constructs to dissect the roles of checkpoint kinases in maintaining checkpoint arrest. Forced kinetochore-localization of Mad1 allows us to bypass the need for Mad1 and Mad2 recruitment to the kinetochore to establish checkpoint arrest and hence to dissect the requirements of checkpoint signaling upstream and downstream of Mad1/Mad2 recruitment. If activity of a checkpoint kinase were needed upstream Mad1/Mad2 recruitment, forced localization of Mad1 should bypass the need for such activity, and inhibition of the kinase should not alter the checkpoint arrest caused by Mis12-Mad1. On the other hand, if kinase activity were needed downstream of Mad1/Mad2 recruitment in order to maintain the checkpoint arrest, then inhibition of kinase activity should abrogate the arrest and cause a reduction in the mitotic index, regardless of the forced localization of Mad1.

I first examined the contributions of BubR1, a conserved cell cycle kinase that regulates kinetochore-microtubule attachment (Musacchio and Salmon, 2007), that has roles as a kinetochore-independent "timer" that sets the length of mitosis (Meraldi et al., 2004a) and that is also a component of the soluble complex that inhibits APC/C-cdc20 (Sudakin et al., 2001). Because of these functions, I predicted that BubR1 inhibition would override the arrest induced by mCherry-Mis12-Mad1. Owing to the lack of available BubR1 chemical inhibitors, I depleted the kinase with RNAi. Knockdown led

to a significant reduction in the mitotic index (two-tailed T-test, p=0.013) and an increase in the percentage of anaphase cells of the mCherry-Mis12-Mad1 population (Fig. 2.8a). Together with previous studies (Musacchio and Salmon, 2007; Sudakin et al., 2001; Meraldi et al., 2004a), our findings are consistent with BubR1 being necessary for checkpoint signaling downstream of Mad1-Mad2.

I then used this assay to examine the contributions of Polo-like kinase (Plk1) to checkpoint signaling. Plk1 is another widely conserved, cell cycle kinase involved in a variety of cell-cycle processes, including the regulation of kinetochore-microtubule attachments (Petronczki et al., 2008). Inhibition of Plk1 activity with its selective inhibitor BI2536 did not result in a reduction of the mitotic index of the mCherry-Mis12-Mad1 population, or in the appearance of anaphase cells (Fig. 2.8b). These findings are consistent with other studies of Polo-like kinases (Petronczki et al., 2008) and show that, although Plk1 is required for the regulation of chromosome biorientation, it is not directly involved in maintaining the checkpoint signals required for a prolonged mitotic arrest.

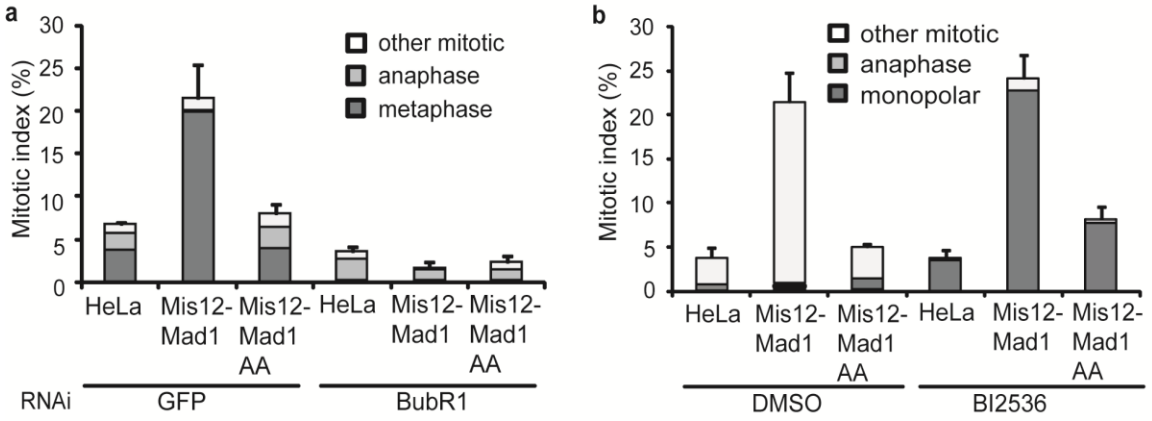

Figure 2.8 Inhibition of BubR1, but not of Plk1, is sufficient for entry into anaphase in cells expressing mCherry-Mis12-Mad1.(a-b) Analysis of mitotic index and phenotypes in HeLa (control), mCherry-Mis12-Mad1- and mCherry-Mis12-Mad1 AA- transfected cells upon BubR1 depletion **(a)** or Polo-like kinase **(b)**. Cells were transfected with siRNA against GFP (control) or BubR1 **(a)**, or incubated in DMSO, BI2536 (80 nM, 90 min before fixation) **(b)**. mCherry, tubulin and DNA staining was used to calculate mitotic index and fraction of cells in metaphase, anaphase and all other mitotic states **(a)** or with monopolar spindles, in anaphase or all other mitotic states **(b)** (*n*= 3 independent experiments, > 350 cells counted per condition per time). Average ± s.e.m. shown.

Kinases potentially directly involved in checkpoint signaling

Next, I used our assay to dissect the requirement for Mps1 and Aurora B in the maintenance of the checkpoint arrest. Both of these conserved kinases are involved in the recruitment of key checkpoint components to unattached kinetochores and in the regulation of the correction of erroneous microtubule attachments for the attainment of biorientation, in a variety of organisms (Meraldi et al., 2004b; Lan and Cleveland, 2010). Although some discrepancies exist, current models agree that Aurora B and Mps1 act in a common network of mitotic signaling (Lan and Cleveland, 2010; Saurin et al., 2011). Mps1 accumulates at unattached kinetochores, and biorientation depletes the kinase from kinetochores (Jelluma et al., 2010). Recent findings suggest that Mps1 has cytosolic as well as kinetochore-specific functions (Maciejowski et al. 2010; Lan and Cleveland, 2010). I reasoned that our assay would allow us to examine the requirement for cytosolic Mps1 in maintaining the checkpoint arrest when chromosomes are bioriented, and therefore independently of its kinetochore functions. To do this, I used two unrelated Mps1 inhibitors—Mps1-IN-1 (Kwiatkowski et al. 2010) and reversine (Santaguida et al. 2010)—in parallel experiments, to reduce the likelihood of overlapping off-target effects of either inhibitor. After a two-hour incubation with Mps1-IN-1, the mCherry-Mis12-Mad1 population showed a significant reduction in mitotic index (Fig. 2.9a; two-tailed T-test, $p=0.0069$) and a corresponding increase in anaphase cells (two-tailed T-test, $p=0.0081$). Similar results were obtained using reversine (Fig. 2.9b). I confirmed these results at a single-cell level, by following mCherry-Mis12-Mad1 metaphase cells after inhibitor addition, using live imaging (Fig.

2.9c-p). By 70 minutes after the Mps1-IN-1 wash-in, ~50% of the mCherry-Mis12-Mad1 cells that were initially at metaphase entered anaphase (Fig. 2.9o). Similarly, ~50% of the metaphase mCherry-Mis12-Mad1 cells entered anaphase ~75 minutes after reversine wash-in (Fig. 2.9p). Importantly, no lagging chromosomes were seen in the anaphase cells, either in the live- or fixed-cell experiments with either Mps1 inhibitor, supporting our observations that chromosomes are properly bioriented in the presence of mCherry-Mis12-Mad1. These results indicate that cytosolic activities of Mps1 are essential for maintaining checkpoint arrest, even when bioriented chromosomes are present.

Figure 2.9 Inhibition of Mps1 is sufficient for entry into anaphase, even when Mad1 persists at kinetochores. (a-b) Analysis of mitotic index and phenotypes in HeLa (control), mCherry-Mis12-Mad1- and mCherry-Mis12-Mad1 AA- transfected cells upon Mps1 inhibition. Cells were incubated in DMSO, Mps1-IN-1 (10 μM, 80 min) **(a)** or reversine (500 nM, 120 min) before fixation **(b)**. mCherry, tubulin and DNA staining was used to calculate mitotic index and fraction of cells in metaphase, anaphase and all other mitotic states (*n*= 3 independent experiments, > 350 cells counted per condition per time). **(c-p)** Analysis of the effects of inhibition of Mps1 in live mCherry-Mis12-Mad1-transfected cells. Metaphase mCherry-positive cells were selected before the medium was changed to one containing DMSO, Mps1-IN-1 (10 μM) or reversine (500 nM; *n*= 3 independent experiments, > 10 cells per condition per experiment). Each of those cells was imaged by multi-point re-visiting using microscope software. DIC **(c, d, g, h, k, l)** and mCherry-fluorescence **(e, f, i, j, m, n)** images at the indicated times before and after Mps1-IN-1 or reversine wash-in are shown. **(o, p)** Cumulative frequency of the imaged cells entering anaphase after Mps-IN-1 **(o)** or reversine **(p)** wash-in. Scale bar, 5 μm. Average ± s.e.m. shown.

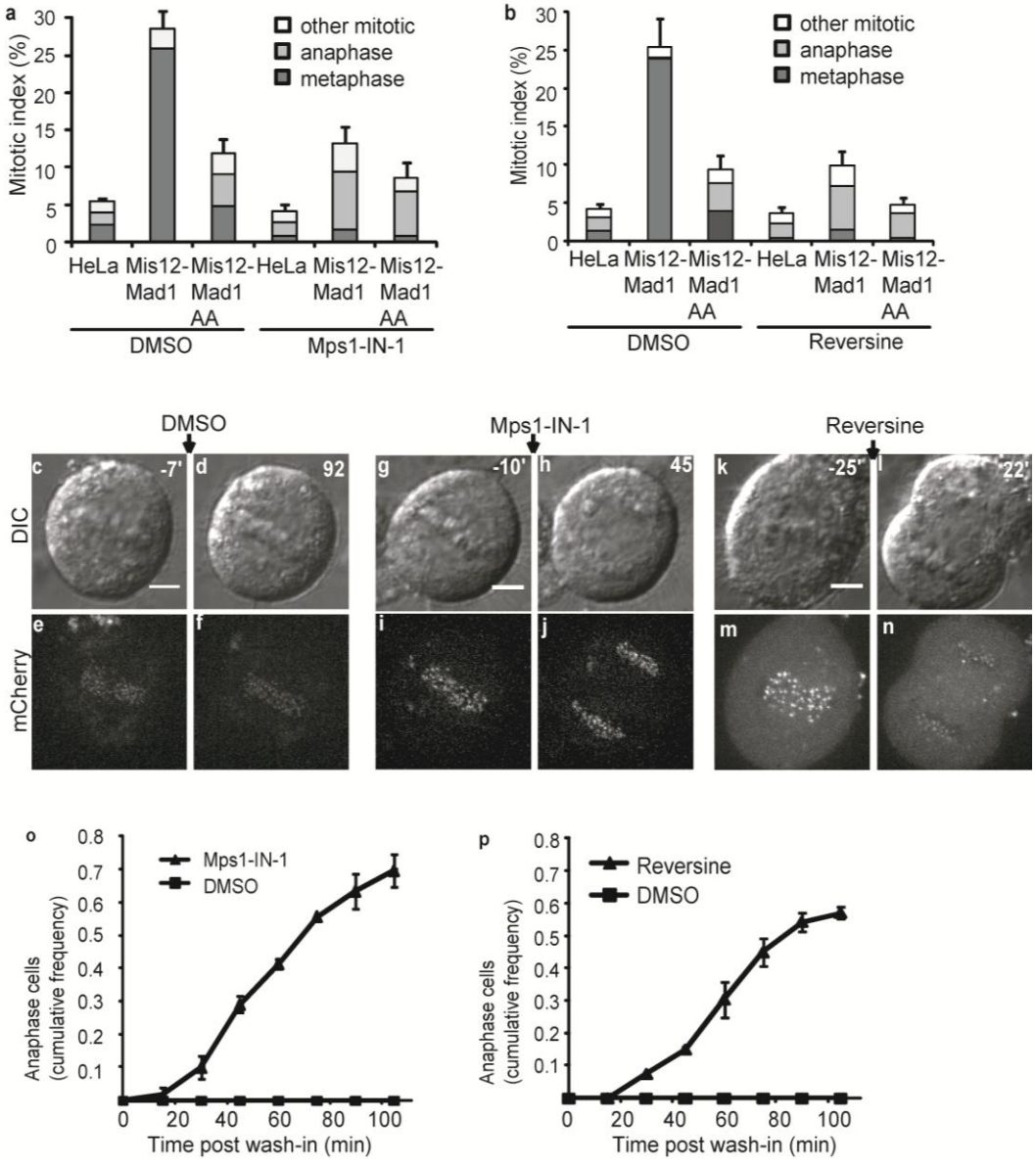
a
Mitotic index (%)
other mitotic
anaphase
metaphase
HeLa
Mis12-Mad1
Mis12-Mad1 AA
DMSO
Mps1-IN-1
b
Reversine
DMSO
Mps1-IN-1
Reversine
DIC
mCherry
-7'
92
-10"
45
-25"
22'
o
p
Anaphase cells (cumulative frequency)
Time post wash-in (min)

Next, I examined the role of Aurora B kinase in directly maintaining checkpoint arrest, independently of its upstream functions in kinetochore assembly and error correction (Meraldi et al., 2004b). I incubated mCherry-Mis12-Mad1-transfected cells in the Aurora B small-molecule inhibitor ZM447439 (Ditchfield et al., 2003). The mCherry-Mis12-Mad1 population showed a significant reduction in its mitotic index (Fig. 2.10a; two-tailed T-test, p=0.016) and in the percentage of metaphase cells (two-tailed T-test, p=0.0069) and, more importantly, a significant increase in the percentage of anaphase cells (two-tailed T-test, p=0.018). The intensity of the mCherry-Mis12-Mad1 signals was not reduced in the segregating chromosomes, ruling out the possibility that Aurora inhibition merely removed the construct from the bioriented kinetochores (data not shown). Similar results were obtained when I inhibited Aurora B with a different inhibitor (hesperadin; Hauf et al., 2003; Fig. 2.10b, g-j, l). I confirmed these results at a single-cell level with live imaging: 80 minutes after the addition of ZM447439 or hesperadin, ~50% of the mCherry-Mis12-Mad1 cells that were initially at metaphase transitioned to anaphase (Fig. 2.10c- l). Lagging chromosomes during anaphase were not observed in our experiments, with either of the two inhibitors. These results corroborate our fixed-cell analyses that inhibition of Aurora B activity is sufficient for overriding the checkpoint, despite retention of Mad1 on kinetochores (Fig. 2.10f, j). A recent study has shown that constitutive kinetochore localization of Mps1 also results in a persistent mitotic arrest, but that inhibition of Aurora activity does not induce anaphase entry in this case (Jelluma et al. 2010). This can be explained by the fact that Mps1 force-localized at bioriented kinetochores may access substrates that, under

normal conditions or in the presence of the Mis12-Mad1 fusion, it would not. Together with these data, our findings suggest that Mps1 must be released from kinetochores for Aurora inhibition to exert its anaphase-promoting effect. Further, our data indicate that Aurora B activity is needed for maintenance of checkpoint arrest in human cells, independently of its functions in kinetochore-protein recruitment and in biorientation.

Figure 2.10 Inhibition of Aurora B is sufficient for entry into anaphase, even when Mad1 persists at kinetochores. (a-b) Analysis of mitotic index and phenotypes in HeLa (control), mCherry-Mis12-Mad1- and mCherry-Mis12-Mad1 AA- transfected cells upon Aurora B inhibition. Cells were incubated in DMSO, ZM447439 (2 μM, 60 min) **(a)** or hesperadin (50 nM, 90 min) before fixation **(b)**. mCherry, tubulin and DNA staining was used to calculate mitotic index and fraction of cells in metaphase, anaphase and all other mitotic states (*n*= 3 independent experiments, > 350 cells counted per condition per time). **(c-l)** Analysis of the effects of inhibition of Aurora B in live mCherry-Mis12-Mad1-transfected cells. Metaphase mCherry-positive cells were selected before the medium was changed to one containing DMSO, ZM447439 (2 μM) or hesperadin (50 nM; *n*= 3 independent experiments, > 10 cells per condition per experiment). Each of those cells was imaged by multi-point re-visiting using microscope software. DIC **(c, d, g, h)** and mCherry-fluorescence **(e, f, i, j)** images at the indicated times before and after ZM447439 or hesperadin wash-in are shown. **(k, l)** Cumulative frequency of the imaged cells entering anaphase after ZM447439 **(k)** or hesperadin **(l)** wash-in. Scale bar, 5 μm. Average ± s.e.m. shown.

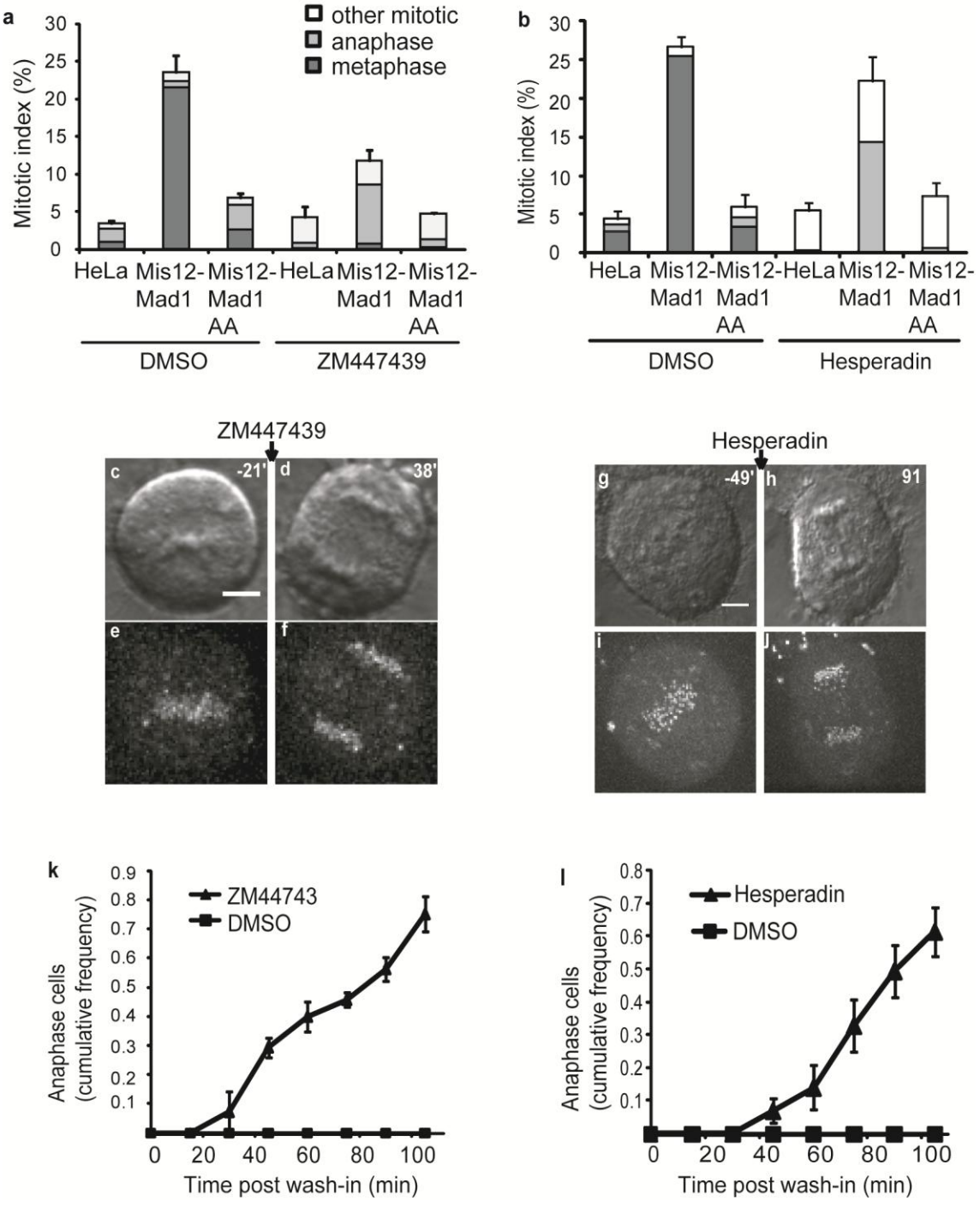
a
other mitotic
anaphase
metaphase
Mitotic index (%)
HeLa
Mis12-Mad1
Mis12-Mad1 AA
DMSO
ZM447439
b
Hesperadin
ZM447439
Hesperadin
-21'
-38'
-49'
91
k
l
ZM44743
DMSO
Anaphase cells (cumulative frequency)
Time post wash-in (min)

Conclusions and discussion

In this Chapter, I showed that the recruitment of Mad1 and Mad2 to kinetochores *via* the fusion of Mad1 to Mis12 is sufficient for the establishment of a checkpoint arrest, regardless of chromosome biorientation. On the contrary, recruitment of Mad1 to non-kinetochore chromosomal locations *via* the fusion to CENP-B or H2B did not elicit a checkpoint arrest independently of the status of microtubule attachment. In other words, the kinetochore recruitment of Mad1 and Mad2 is sufficient for checkpoint arrest, but whether this recruitment is also necessary is still unclear (further discussed in Chapter 4). Using the Mis12-Mad1 construct to uncouple checkpoint signaling from chromosome biorientation, I was able to assay the requirement for kinase activity in the maintenance of checkpoint arrest independently of their "upstream", indirectly necessary functions. I showed that Mps1 and Aurora B activities are *bona fide* checkpoint signaling components downstream of Mad1 and Mad2 kinetochore recruitment.

The spindle assembly checkpoint must maintain anaphase inhibition until biorientation of every chromosome is achieved. This requires the continuous generation of the "wait" signal at levels such that even one mal-oriented kinetochore can block progression (Rieder et al., 1994; Musacchio and Salmon, 2007). The Mad2-template model of checkpoint signaling provides an attractive framework for how Mad1 and Mad2 can detect the primary error and continuously produce the biochemical anaphase-inhibitory signal, even when those proteins do not have canonical enzymatic activities (Luo and Yu, 2008; Simonetta et al., 2009). Nevertheless, several kinases,

which as enzymes can phosphorylate multiple substrate molecules to generate a biochemically amplifiable signal, are believed to play a crucial role in the checkpoint (Burke and Stukenberg, 2008; Kang and Yu, 2009). However, examining their contribution to checkpoint establishment and maintenance had been difficult, especially because many of these kinases have essential functions in preceding steps needed for successful mitosis. This is particularly relevant for Aurora B kinase. It has been proposed that inhibition of Aurora leads to checkpoint silencing indirectly, due to the consequent stabilization of all improper attachments, which leads to the removal of Mad1-Mad2 from the kinetochores and hence to suppression of the primary error signal (Ditchfield et al., 2003; Hauf et al., 2003; Pinsky et al., 2006). Nevertheless, experiments involving Aurora inhibition together with the use of microtubule poisons suggest that Aurora is directly required for maintaining mitotic arrest (Ditchfield et al., 2003; Hauf et al., 2003; Emanuele et al., 2008; Kallio et al., 2002; Petersen and Hagan, 2003; Vanoosthuyse and Hardwick, 2009). The override of the arrest seen there has been difficult to interpret because prolonged arrest in high concentrations of Aurora inhibitors may disrupt kinetochore assembly (Emanuele et al., 2008) and may also accumulate chemical inhibitor's off-target effects in vertebrates. Therefore, dissecting the contributions of key cell cycle kinases (e.g. Aurora B) has remained challenging.

Using our constitutively-kinetochore-localized Mad1 assays, I was able to show in human cells that Aurora activity is directly required for the maintenance of checkpoint arrest. While it is difficult to rule out more complex models, I favor the hypothesis that Aurora kinase is acting downstream of Mad1-Mad2 recruitment. Together with findings

from others (Lan and Cleveland, 2010; Santaguida et al. 2011), our data suggest a model in which the APC/C-inhibitory signal is maintained not only by Mad2-templated dynamics, but also by Aurora kinase and cytosolic Mps1. Because in our assays cells arrest in mitosis with bioriented chromosomes, our results suggest that this signaling pathway is likely independent of mechanisms requiring the spatial separation of kinetochore substrates from centromeric Aurora (Liu et al., 2009). Finding the relevant molecular links between Aurora, Mps1 and the APC/C is an important next step. I speculate that the MCC, the APC/C, p31/Comet and other poorly characterized checkpoint silencing factors might be the relevant substrates. In fact, Mps1 phosphorylation sites on C-Mad2 necessary for checkpoint arrest maintenance have recently been found (Zich et al. 2012). However, based on how challenging it has been to find physiologically relevant mitotic kinase substrates, I anticipate that finding the complete set of substrates will be a substantial undertaking. It is likely that our constitutive kinetochore-localized Mad1 assay will be useful for these analyses.

It has recently been shown *in vitro* that chromosomes are not only required to generate the APC/C-inhibitory signal, but are also capable of catalyzing its production (Kulukian et al., 2009). Together with these data, our findings that recruitment of Mad1-Mad2 to the kinetochore– but not throughout chromosomes– is needed to induce mitotic arrest, suggest a model in which the local kinetochore environment is crucial for generating the signal that will block anaphase when even a single chromosome remains non-bioriented. Advances in high-resolution microscopy have built on a large body of genetic and biochemical data to reveal the kinetochore architecture at nanometer

resolution (Wan et al., 2009). Going forward, it will be important to dissect how the local protein chemistry at kinetochores contributes to generating the “wait-anaphase” signal.

Chapter 3: Characterizing the effects of ciliobrevin D— the first specific, small-molecule dynein inhibitor— in mitotic cells

Summary

Accurate chromosome segregation depends on proper spindle assembly, which allows for biorientation of kinetochores and progression into anaphase (Musacchio and Salmon, 2007). Proper spindle assembly and function depend on the activity of motor and non-motor microtubule-associated proteins that regulate microtubule polymerization and depolymerization dynamics, cross-linking of microtubules at the poles and chromosome-microtubule interactions at the kinetochores (Wadsworth et al., 2011). The minus-end-directed microtubule-based motor protein dynein, a member of the AAA+ protein family (ATPases associated with a variety of cellular activities), has activities both at the spindle poles and at the kinetochore-microtubule interface and plays important roles in proper spindle assembly (Vaisberg et al., 1993; Merdes et al., 1996; Erzberger and Berger, 2006). However, dynein's functions remain incompletely understood due to the paucity of robust molecular tools for its study. In particular, no

specific cell-permeable, acute, small molecule inhibitors—which would help further dissect the motor-protein's roles in spindle assembly and checkpoint silencing—had been described prior to the work by Firestone et al. (2012), to which I contributed as detailed below.

In this Chapter, I present work on "ciliobrevin D", the small molecule discovered by Dr James Chen and colleagues (Stanford University) that is the first specific dynein inhibitor. I characterize its effects on mitotic cells and I describe how, in agreement with known dynein functions, ciliobrevin D reversibly disrupts spindle bipolarity and the integrity of kinetochore-microtubule interactions. Using ciliobrevin D, I uncover a new role of dynein in spindle morphogenesis: dynein is involved not only in the establishment of bipolarity, but also in its maintenance. The ciliobrevin family of compounds will be valuable tools in the study of dynein roles in other mitotic and interphase investigations and may also guide the development of specific inhibitors of other AAA+ family members involved in a myriad of cellular and clinically relevant processes.

Introduction

Dynein structure, function and behaviour

Dynein is a molecular motor of the AAA+ ATPase family that couples ATP hydrolysis to movement towards the minus end of microtubules (Hughes et al., 1995). There are three main dynein subfamilies, whose members are involved in a variety of cellular

mechanisms (Hook and Vallee, 2006). At the axoneme, axonemal dynein is involved in coordinating the beating of flagella and cilia (King, 2012). Cytoplasmic dynein 2 carries out retrograde (minus-end-directed) intraflagellar transport and is necessary for axoneme biogenesis and Hedgehog signaling, among other roles (Blacque et al., 2008; Pazour et al., 1998). Cytoplasmic dynein 1, the most abundant of dyneins, is present in all microtubule-containing cells in the cytoplasm, cell cortex and kinetochores (Dujardin and Vallee, 2002; Bader and Vaughan, 2010). Cytoplasmic dynein 1 is responsible for the minus-end directed movement of a wide array of cargoes: proteins (e.g. the checkpoint proteins Mad1, Mad2; Howell et al., 2001), mRNA (e.g. the embryonic factors bicoid, gurken and oskar; Bullock et al., 2006) and vesicles (e.g. Golgi particles, endosomes, synaptic vesicles; Hunt and Stephens, 2011). As such, it is involved in diverse processes such as embryogenesis, cell migration, Golgi morphology, neural axon polarization, nerve regeneration and mitosis, among others.

Functional cytoplasmic dynein 1 is a ~1.5 mega-Dalton multi-complex of proteins, consisting of three homodimers of heavy, intermediate, intermediate light and light chains, associated with essential regulatory non-catalytic partners such as dynactin, LIS1 and Bicaudal D. These partners regulate dynein activity, processivity and cargo binding, and their inhibition or depletion can almost completely phenocopy loss of dynein itself (Kardon and Vale, 2009; Vallee et al., 2012).

The heavy chain is dynein's catalytic core. Each heavy chain polypeptide (> 500 kDa) contains a motor domain comprised of a hexameric repeat of AAA domains, a long ~15 nm antiparallel coiled-coil "stalk" that links the motor to the microtubule binding

domain, a short “buttress” antiparallel coiled-coil that supports the base of the stalk and contributes to force generation, a “linker” that acts as the main force transducer and moves position with the mechanochemical cycle and an unstructured N-terminal tail that interacts with the light/intermediate dynein chains, accessory non-catalytic partners and cargo (Fig. 3.1; Carter et al. 2011; Kon et al. 2012; Schmidt et al. 2012). Biochemical and structural studies have shown that the first AAA domain is the main ATP hydrolysis site, with domains AAA2-4 likely exerting regulatory and/or structural roles (Kon et al., 2004; Schmidt et al., 2012). It is obvious that substantial allosteric communication between the head and microtubule binding domain must occur in order to couple the ATP cycle to changes in microtubule affinity, but the details of this process are yet to be completely elucidated. Significant improvements in the characterization of dynein’s stepping behaviour have been recently described (DeWitt et al. 2012; Qiu et al. 2012). It was observed that, contrary to most motor proteins, dynein does not undergo a “hand-over-hand” movement but, instead, walks in a likely tension-dependent, partially-stochastic, partially-coordinated “inchworm” fashion.

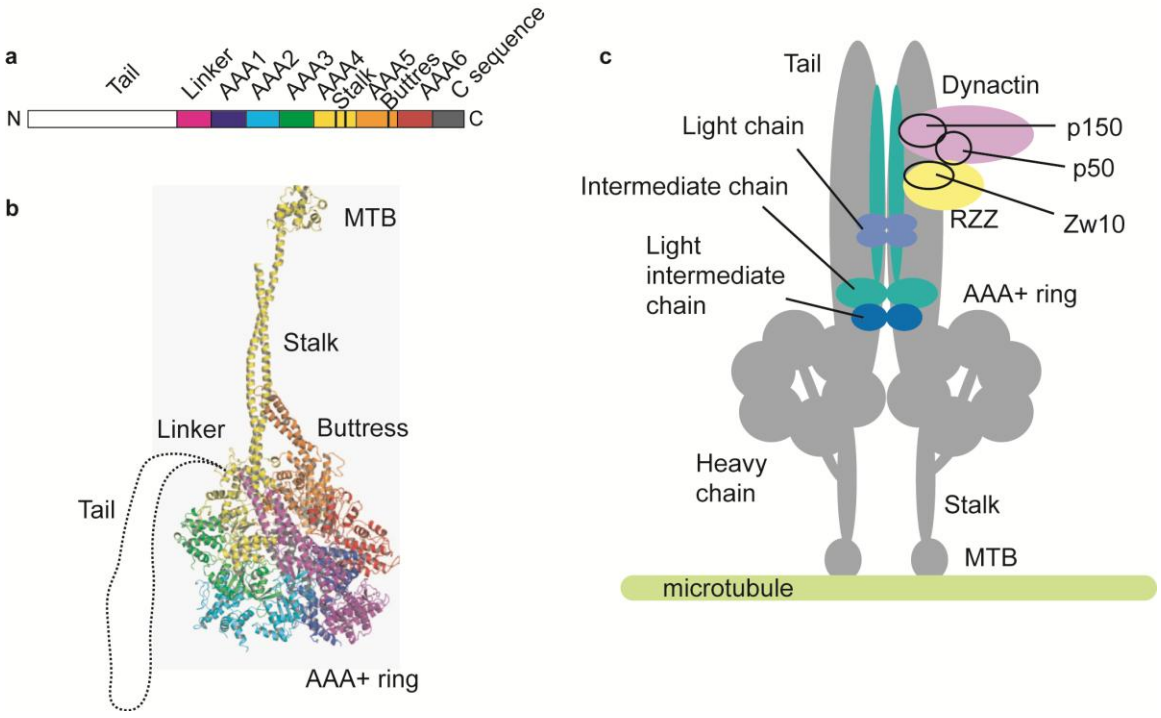

Figure 3.1 Dynein structure and binding partners. (a) Domain structure of dynein heavy chain. The color coding is retained in **(b)**. **(b)** X-ray crystal structure of *Dictyostelium discoideum* dynein heavy chain at 2.8 A resolution (Kon et al, 2012). Note that neither the N-terminal tail nor the C-terminal sequences are present. **(c)** Schematic representation of the dynein complex (heavy chains in grey, intermediate chains in green, light intermediate chains in darker blue, light chains in lighter blue) and some of its binding partners (dynactin in pink, RZZ in yellow).

Owing in part to the technical challenges posed by its large size, dynein has been a difficult protein to study. Despite recent advances in the structural and biophysical characterization of its motor domain and stepping behaviour, dynein remains much less well understood than other motor proteins such kinesins (the other main type of microtubule-based motor proteins), both *in vitro* and in cellular contexts. Another significant impediment to dynein studies has been the lack of a specific inhibitor that could be used acutely at the relevant time-scales needed. Although the ATP analogue erythro-9-[3-(2-hydroxynonyl)]adenine and the antioxidant nordihydroguaiaretic acid have been previously reported to abrogate dynein function (Bouchard et al., 1981; Arasaki et al., 2007), these compounds are non-specific, promiscuous enzyme antagonists. As such, their off-target effects cannot be overlooked. Moreover, only one specific inhibitor has been described for any other AAA+ family member (Chou et al. 2011). Therefore, the development of a specific small-molecule inhibitor of dynein would provide a significant tool for the advancement of the field and may also aid in the development of inhibitors for other types of AAA+ proteins.

History of the ciliobrevin project

Dr James Chen's laboratory at Stanford University uses chemical biology tools to study the Hedgehog pathway, a signaling cascade essential for embryogenesis and stem cell maintenance (Jiang and Hui, 2008). Hedgehog signaling is intimately related to cilia, where components of the pathway are regulated (Goetz and Anderson, 2010). As such, dynein activity is essential for proper Hedgehog signaling, as it is involved in the

necessary retrograde intraflagellar transport of the Hedgehog signaling complex. Accordingly, mouse embryos that are mutant for dynein heavy chain exhibit short and few cilia and have altered Hedgehog gene expression (Huangfu and Anderson, 2005).

One of the hits from a recent cell-based chemical screen for Hedgehog inhibitors in the Chen laboratory (Hyman et. Al., 2009), the benzoyl dihydroquinazolinone compound "HPI4", gave indications that it might be a dynein inhibitor: it not only blocked the Hedgehog pathway, but it also reduced the number and size of cilia and induced Gli2 plus-tip accumulation, as seen in the dynein mutants (Kim et al., 2009). Due to its effects on cilia, HPI4 was renamed "ciliobrevin". Dr Chen and Dr Kapoor initiated a collaboration to examine whether cilibrevin's target was in fact dynein and to characterize the effects of this small molecule on dynein activity *in vitro* and during mitosis.

After synthesizing and examining a series of benzoyl dihydroquinazolinone analogues with different chlorine substitution patterns and oxidation states, Chen-laboratory members observed that the derivative lacking a 3-chloro substituent on the benzoyl ring system (henceforth "compound 2") exhibited significantly diminished inhibitory activity in Hedgehog signaling and primary cilia formation assays. Compound 2 was thereafter used as a negative control for *in vitro* and cell biological assays. The analogue with a 7-chloro substitution (henceforth "ciliobrevin D") exhibited more potent inhibitory activity in Hedgehog signaling and cilia formation and was thus used as the potential dynein inhibitor in all subsequent experiments (Fig. 3.2; Firestone et al., 2012).

To examine the inhibitory activity of ciliobrevin D on dynein *in vitro*, colleagues in the Kapoor and Chen laboratories carried out microtubule gliding assays with purified bovine dynein and showed that ciliobrevin D, but not compound 2, reversibly and significantly reduced the average velocity of this motor (Fig. 3.2d, e). Moreover, they showed that ciliobrevin D is an ATP-competitive dynein inhibitor (Fig. 3.2f). Specificity was shown by the fact that ciliobrevin D has no inhibitory effects on other ATPase motor proteins such as kinesins, on other types of AAA+ ATPases such as p97 or Mcm2-7, on actin cytoskeleton dynamics or on other signaling pathways such as MAPK and PI3K kinase pathways (Fig. 3.2g; Firestone et al. 2012). To begin to examine ciliobrevin activity in a cellular context, our colleagues in the Gelfand laboratory (Northwestern University) examined the small molecule's effect on the dynein-dependent melanosome aggregation in Xenopus cells upon melatonin stimulation and showed that ciliobrevin D (but not compound 2) reversibly and selectively inhibited this process (Firestone et al. 2012).

Figure 3.2 Characterization of the effects of ciliobrevins *in vitro*. (a, b) Molecular structures of ciliobrevin D **(a)** and compound 2 **(b)**. **(c-g)** Figures have been adapted from figures 1 and 3 of Firestone et al. 2012. **(c)** Cilliary effects on NIH3T3 cells after a 24-hour incubation in a 30 μM dose of compound 2, ciliobrevin D or an equivalent amount of DMSO. Staining for DNA (DAPI; blue) and the cilium protein ARL13b (green) is shown. **(d-g)** Effects of ciliobrevins on recombinant or purified bovine dynein *in vitro*. **(d)** Kymographs of fluorescently labeled microtubules sliding on coverslip-adhered purified bovine dynein in the presence of 100 μM of ciliobrevin compounds are shown. **(e)** Quantification of data from **(d)**. Average from at least 56 microtubules ± s.e.m. shown. Asterisk indicates $P < 10\text{-}6$. **(f)** Hanes–Woolf plot of recombinant rat dynein motor in the presence of increasing concentrations of ciliobrevin D. **(g)** Effects of increasing concentrations of ciliobrevin D, compound 2 or DMSO on the ATPase activities of recombinant motor domains of rat cytoplasmic dynein, human kinesin-1 and human kinesin-5. Average for two independent experiments ± s.d. is shown. Scale bar, 10 μm.

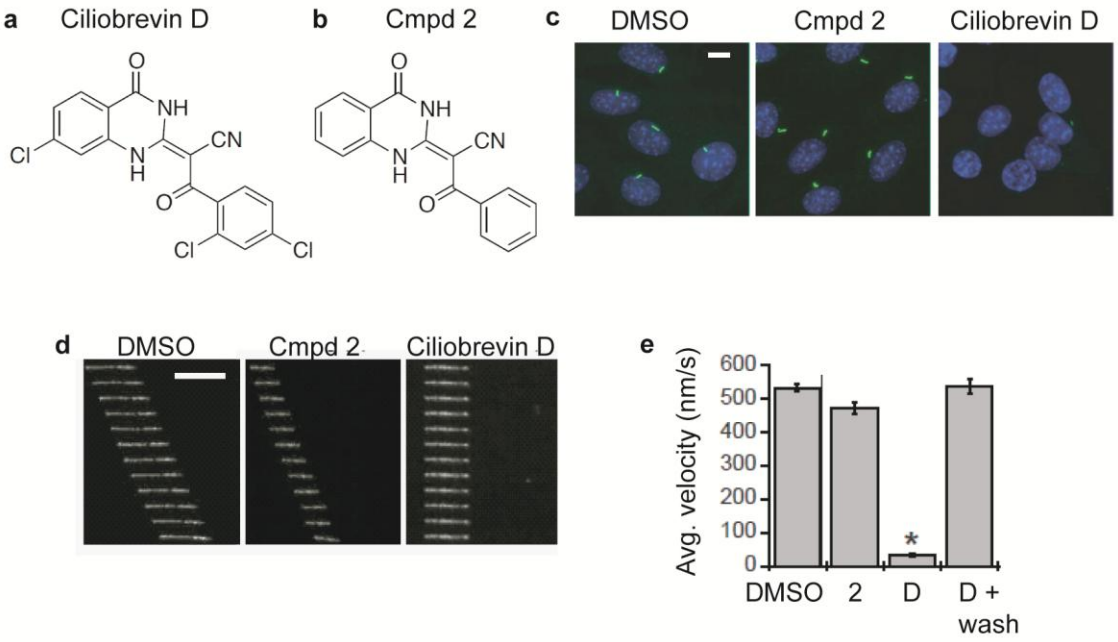
a
Ciliobrevin D
b
Cmpd 2
c
DMSO
Cmpd 2
Ciliobrevin D
d
DMSO
Cmpd 2
Ciliobrevin D
e
Avg. velocity (nm/s)
600
500
400
300
200
100
0
*
DMSO
2
D
D + wash
f
Recombinant dynein motor domain
DMSO
30 uM D
50 uM D
[ATP]/V (μM•s)
4000
3500
3000
2500
2000
1500
1000
500
-1500 -1000 -500 0 500 1000 1500
[ATP] (μM)
g
Recombinant dynein motor domain
Recombinant kinesin motor domain
Recombinant Eg5 motor domain
Relative ATPase activity
1.2
1
0.8
0.6
0.4
0.2
0
Ctrl
100
25
50
100
μM
2
D

With my colleagues having shown that ciliobrevin D is a specific and reversible inhibitor of dynein activity both *in vitro* and in interphase cells, my contribution to the project was to validate the small molecule's effects in mitotic cells by examining whether the phenotypes created agreed with phenotypes seen for other types of dynein mitotic inhibition. An expectation was that ciliobrevin might also be a useful tool for the study of the roles of dynein in checkpoint silencing and how dynein relates to other silencing-related proteins such as the Mad2-inhibitor p31/Comet. For instance, we could examine whether dynein inhibition enhances the Mis12-Mad1 checkpoint arrest or the requirement for p31/Comet in checkpoint silencing, or whether p31/Comet- and dynein-dependent silencing mechanisms are additive, synergistic, or redundant.

Dynein in mitosis

In mitosis, cytoplasmic dynein 1 (hereafter, dynein) localizes at kinetochores, at spindle poles and at the cell cortex and has functions in spindle assembly, spindle positioning, the regulation of kinetochore-microtubule interactions and the spindle assembly checkpoint.

Dynein interacts with and transports the cross-linking protein NuMA towards the microtubule minus ends. Hence, dynein has a crucial role in the spindle pole formation and organization, gamma-tubulin recruitment and thus in the establishment of spindle bipolarity (Merdes et al., 2000; Young et al., 2000). By acting on the cortical microtubules that emanate towards the cortex of the cell, dynein also plays a role in positioning the spindle within the cytoplasm (Moore et al., 2009; Grill and Hyman, 2005;

Kiyomitsu and Cheeseman, 2012). Dynein is also present at unattached kinetochores, to which it is recruited *via* the interaction of its non-catalytic partner p50 (a component of dynactin) with the RZZ complex component ZW10 (Starr et al., 1998). There, dynein has been proposed to participate in microtubule end-on attachment and to regulate the stability of kinetochore-microtubule interactions and kinetochore orientation (Varma et al., 2008). Dynein also removes checkpoint proteins such as Mad1 and Mad2 from bioriented kinetochores and transports them towards the spindle poles. This "dynein stripping" process is believed to contribute to checkpoint silencing and anaphase progression (Howell et al., 2001; see introduction for further details). Checkpoint silencing remains the least well understood step of checkpoint signaling; novel molecular tools for its study would therefore have a big impact on the field.

These and other presumed mitotic functions of dynein have been described and studied using cell-biological techniques such as the microinjection of antibodies, the overexpression of dominant-negative binding partners or heavy-chain truncations, or heavy chain RNA interference. These perturbations are crude, as their specificity, acuteness and reversibility are sub-optimal. In fact, significant inconsistency and controversy have arisen from the use of different techniques (Bader and Vaughan, 2010). It is thus that a specific, acute, reversible molecular tool such as a small-molecule inhibitor would be useful for the reliable characterization of dynein's functions during mitosis.

In the next section, I characterize the effects of ciliobrevin D in mitosis. I show that, in agreement with previously reported dynein functions, ciliobrevin D reversibly inhibits

spindle assembly, spindle pole organization and focusing, as well as stable kinetochore-microtubule interactions.

Results

Ciliobrevin disrupts spindle bipolarity in mammalian cells

As described above, dynein acts with the cross-linking protein NuMA to focus the minus ends of microtubules and help establish the spindle poles. Inhibition of dynein activity with anti-dynactin antibodies or the expression of dominant negative constructs thus results in unfocused poles (Merdes et al., 2000; Gaetz and Kapoor, 2004). To determine whether ciliobrevin D could recapitulate these phenotypes, I treated a metaphase-enriched population of NIH-3T3 cells with 50 µM of ciliobrevin D or the inactive analogue (compound 2) for one hour and examined their mitotic structures by immunofluorescence microscopy. Treated cells exhibited abnormal (unfocused, multipolar, or collapsed) mitotic spindles with disrupted gamma tubulin localization (Fig. 3.3a, d-f). Cells incubated with the non-cilia-disrupting analogue or vehicle alone (DMSO) exhibited normal spindle morphologies (Fig. 3.3b-c). Similar ciliobrevin-induced spindle defects were observed in HeLa and RPE-1 cells, although to a lesser extent (Fig. 3.3g-h).

Figure 3.3 Ciliobrevin D disrupts spindle bipolarity and spindle pole organization. (a-g) NIH3T3 **(a-f)** or HeLa **(g)** cells were incubated with 10 μM proteosome inhibitor MG132 for 90 min and subsequently cultured in a medium with both MG132 (10 μM) and either an inactive ciliobrevin analogue (compound 2) **(c)** or ciliobrevin D **(d-f)** at a 50 μM dose or an equivalent amount of DMSO **(a)**, for 1 hour. Cells were fixed and stained for DNA, α-tubulin, and γ-tubulin and the morphology of their spindles were scored as bipolar or abnormal (multipolar, collapsed or unfocused) **(a, g)** *n*= 3 independent experiments, > 150 spindles counted for each condition. **(b-f)** Representative images of NIH3T3 treated as above. **(h)** Dose-response curve for NIH-3T3, HeLa and RPE-1 cells exposed to increasing concentrations of ciliobrevin D. For each concentration, cells were treated, fixed and stained as above. Average ± s.e.m. shown. Scale bar, 5 μm.

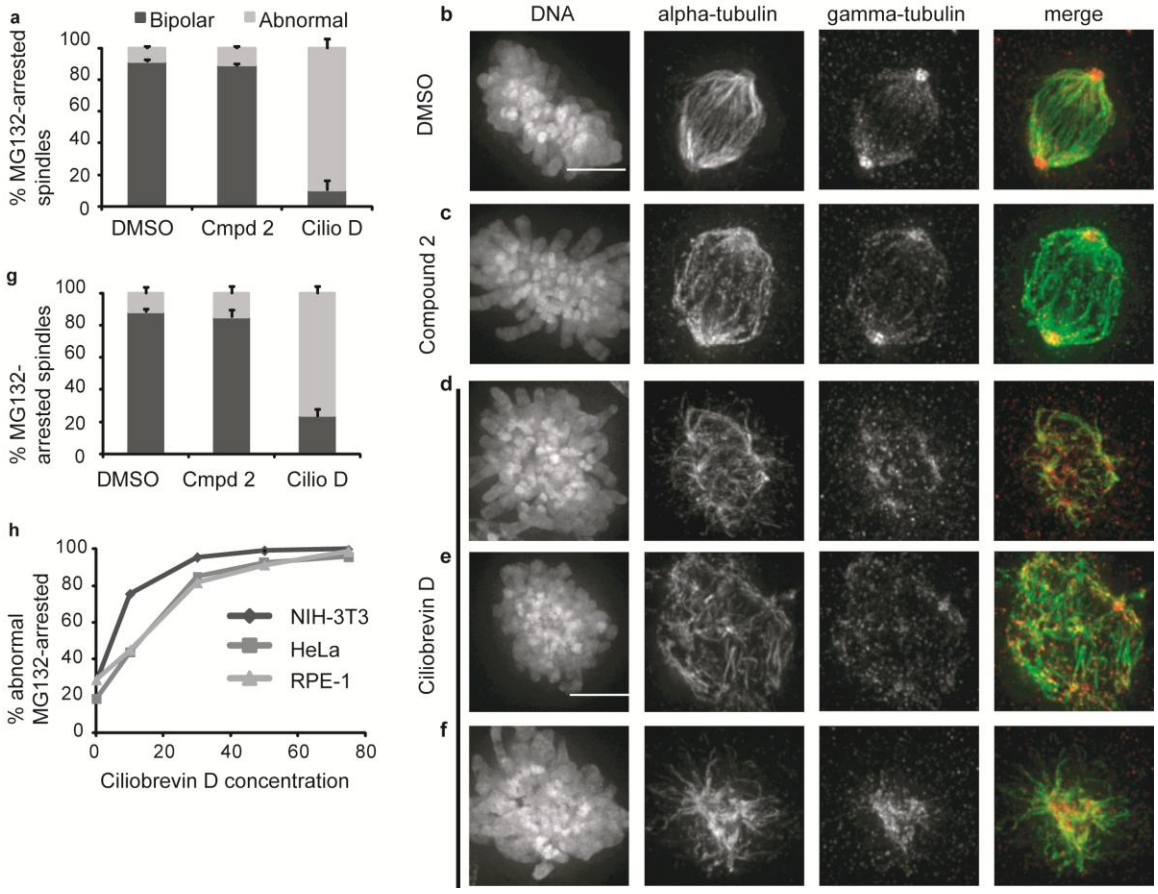
a
Bipolar
Abnormal
% MG132-arrested spindles
100
80
60
40
20
0
DMSO
Cmpd 2
Cilio D
g
% MG132-arrested spindles
100
80
60
40
20
0
DMSO
Cmpd 2
Cilio D
h
% abnormal MG132-arrested
100
80
60
40
20
0
0
20
40
60
80
Ciliobrevin D concentration
NIH-3T3
HeLa
RPE-1
b
DNA
alpha-tubulin
gamma-tubulin
merge
DMSO
c
Compound 2
d
e
Ciliobrevin D
f

Dynein is also required for establishing stable kinetochore-microtubule attachments (Varma et al., 2008). Accordingly, ciliobrevin D treatment disrupted the formation of cold-stable microtubules (as explained in the previous Chapter, an indicator of proper kinetochore-microtubule interactions) in both 3T3 and HeLa cells (Fig. 3.4).

Figure 3.4 Ciliobrevin D disrupts proper cold-stable kinetochore-microtubule interactions. (a-d) NIH-3T3 **(a-d)** or HeLa **(d)** cells were incubated with 10 μM proteosome inhibitor MG132 for 90 min and subsequently cultured in a medium with both MG132 (10 μM) and either an inactive ciliobrevin analogue (compound 2) **(b)** or ciliobrevin D **(c)** at a 50 μM dose or an equivalent amount of DMSO **(a)** for 1 hour before being incubated on ice for 10 min. Cells were then fixed and stained for DNA, α-tubulin, γ-tubulin and the kinetochore marker CREST. Individual channels and an overlay of CREST and α-tubulin are shown. Insets (selected optical sections) show individual cold-stable microtubule-attached **(a, b)** or unattached kinetochores **(c)** (4-fold magnification). **(d)** Quantification of the effects of DMSO, compound 2 or ciliobrevin D on NIH3T3 and HeLa cells treated as above. Average ± s.e.m. shown. Scale bar, 5 μm.

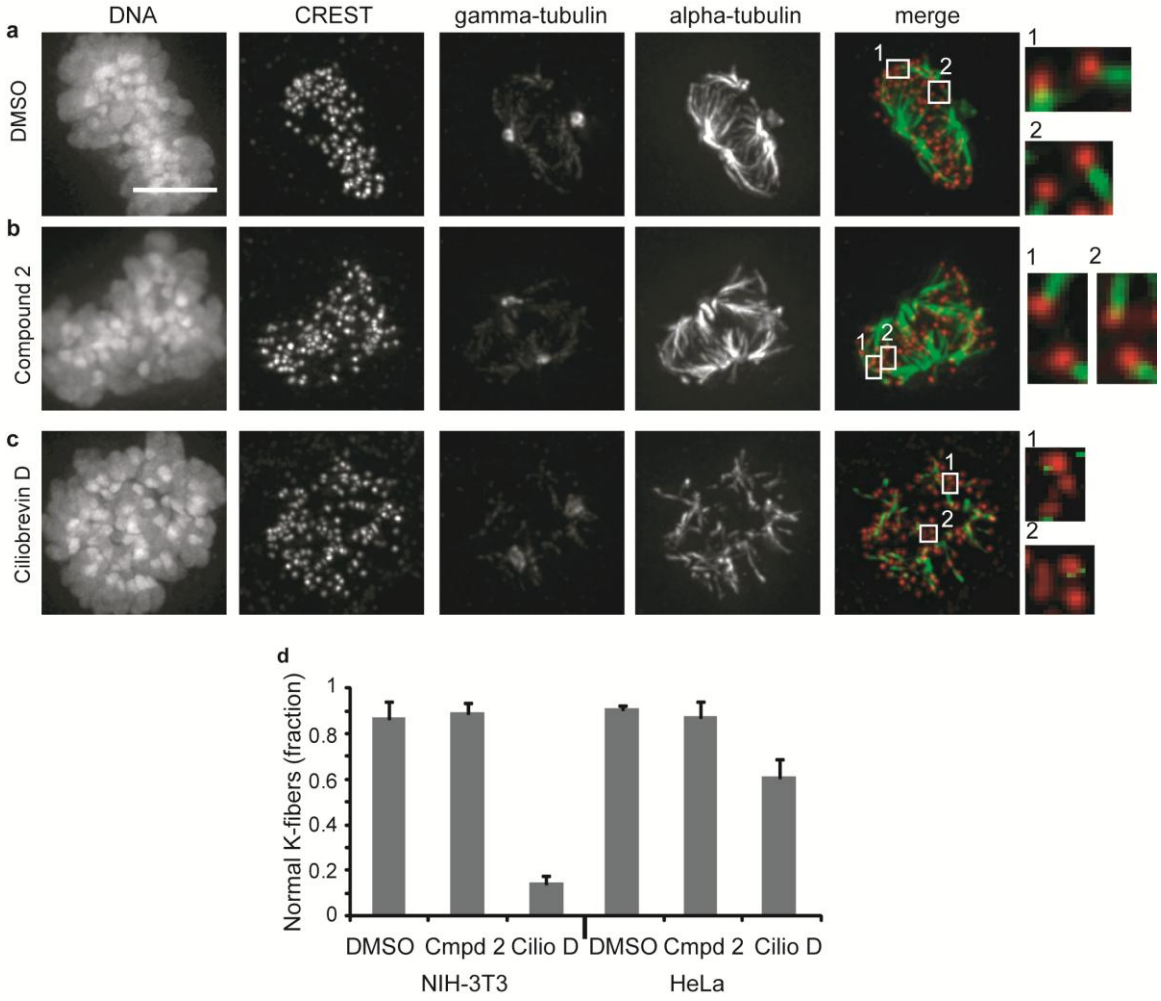
a
DNA
CREST
gamma-tubulin
alpha-tubulin
merge
DMSO
b
Compound 2
c
Ciliobrevin D
1
2
d
Normal K-fibers (fraction)
0
0.2
0.4
0.6
0.8
1
DMSO
Cmpd 2
Cilio D
DMSO
Cmpd 2
Cilio D
NIH-3T3
HeLa

Ciliobrevin does not affect dynein localization

To investigate if these spindle-disruptive effects were associated with altered localization of dynein, I examined the targeting of key binding partners that recruit or co-localize with this motor at different intracellular sites. $p150^{Glued}$ is the main component of the dynein essential non-catalytic partner dynactin, and it tightly interacts with dynein's intermediate chain throughout mitosis (Holzbaur et al., 1991; Kardon and Vale, 2009). Dynactin recruits dynein to kinetochores and spindle poles during mitosis; moreover, disruption of $p150^{Glued}$ function mimics loss of dynein activity (Starr et al., 1998; King et al., 2003; Schroer, 2004). Therefore, I analyzed the subcellular localization of $p150^{Glued}$ in the presence of ciliobrevin D. Immunofluorescence analysis showed that $p150^{Glued}$ localized to the disorganized spindle poles of metaphase-arrested, ciliobrevin D-treated cells (Fig. 3.5).

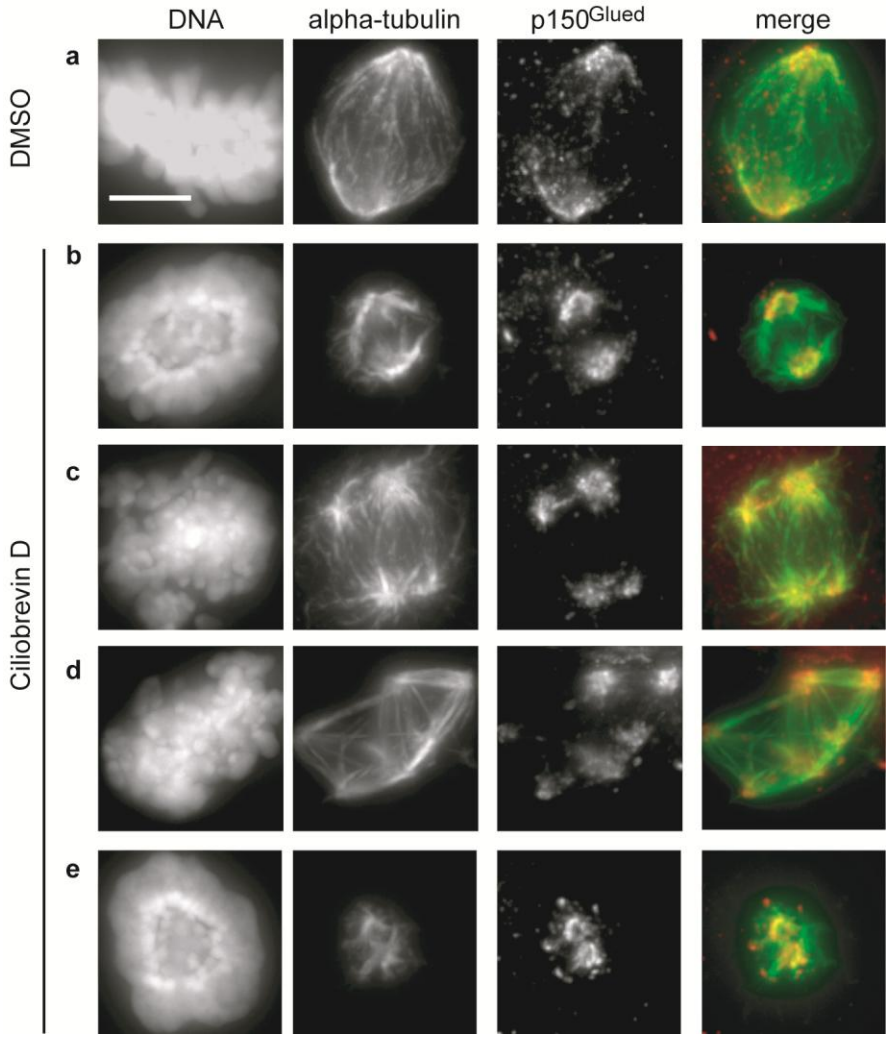

Figure 3.5 Ciliobrevin D does not affect the localization of p150^{Glued} at spindle poles. **(a-e)** NIH-3T3 cells were incubated with 10 µM proteosome inhibitor MG132 for 90 min and subsequently cultured in a medium with both MG132 (10 µM) and either or ciliobrevin D **(b-e)** at a 50 µM dose or an equivalent amount of DMSO **(a)**. Cells were then fixed and stained for DNA, α-tubulin, and p150^{Glued}. Individual channels and an overlay of CREST and α-tubulin are shown. Scale bar, 5 µm.

I then analyzed the targeting of $p150^{Glued}$ to kinetochores. Because kinetochore recruitment of $p150^{Glued}$ and dynein depends on microtubule-attachment status, I treated the cells with the microtubule poison nocodazole, to be able to disregard effects due to differences in attachment. To ensure that ciliobrevin treatment does not disrupt outer kinetochore structure, I also analyzed the localization of two outer kinetochore proteins under the same conditions. These proteins were ZW10 (the component of the RZZ complex that recruits dynein to kinetochores by interacting with the dynactin component p50; Starr et al., 1998), and the kinetochore-associated kinesin-like protein Centromere protein E (CENP-E; Yen et al., 1991). Quantitative analysis showed that $p150^{Glued}$, ZW10, and CENP-E were localized to outer kinetochores at comparable levels to control cells, indicating that recruitment of these proteins and kinetochore structure itself are not disrupted by the ciliobrevins (Fig. 3.6). These results suggest that dynein is properly recruited to kinetochores and spindle poles in ciliobrevin-treated cells and that the spindle phenotypes result from loss of dynein motor activity.

Figure 3.6 Quantitative analysis of ciliobrevin effects on protein localization at unattached kinetochores. (a-f) NIH-3T3 cells were treated with the designated compounds (at 50 μM) or an equivalent amount of DMSO for 45 min before addition of 1 μg/mL nocodazole (and either ciliobrevins or DMSO) for another 45 min. The cells were then fixed and stained with CREST, $p150^{Glued}$, and either ZW10 **(b, d)** or CENP-E **(c, e)**. Fluorescence intensities at individual kinetochores were quantified. Data shown here represent the intensity distributions of 2-4 independent experiments, with each experiment involving the analysis of 4-7 cells and 10-15 kinetochores per cell per condition (120-390 kinetochores per condition). **(a-c)** Histograms show the distribution of signal intensities of $p150^{Glued}$ **(a)**, ZW10 **(b)**, and CENP-E **(c)** in cells treated as above. **(d,e)** Representative images of cells treated and quantified as described above. Numbers associated with individual micrographs represent the average immunofluorescence intensity of the respective protein at the analyzed kinetochores in each image, relative to the overall average signal observed in DMSO-treated cells. Scale bar, 5 μm.

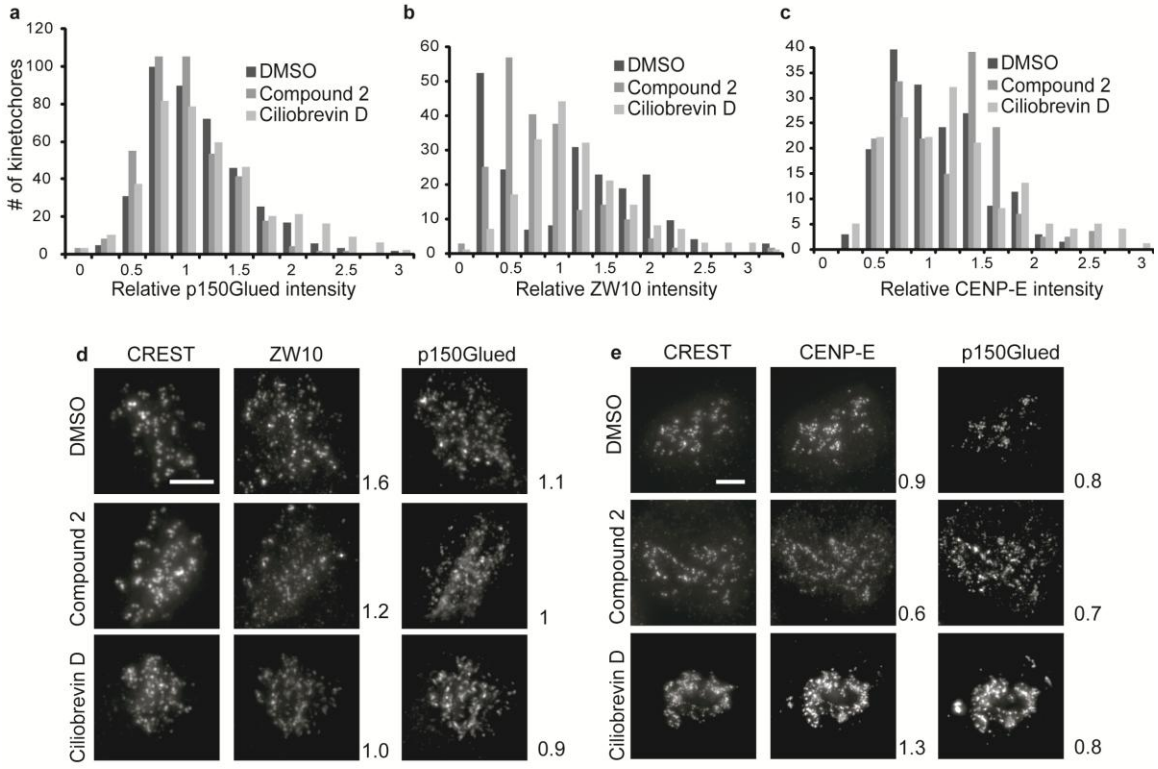
a
b
c
# of kinetochores
DMSO
Compound 2
Ciliobrevin D
Relative p150Glued intensity
Relative ZW10 intensity
Relative CENP-E intensity
d
e
CREST
ZW10
p150Glued
CENP-E
DMSO
Compound 2
Ciliobrevin D
1.6
1.1
1.2
1
1.0
0.9
0.9
0.8
0.6
0.7
1.3
0.8

Ciliobrevin's effects are reversible and its use reveals dynein's role in the maintenance of bipolarity

To further characterize the mitotic defects associated with ciliobrevin treatment, I established a GFP-tubulin-expressing NIH-3T3 stable cell line and used it for real-time confocal microscopy (Fig. 3.7 and 3.8). Severe defects were observed within minutes of ciliobrevin D treatment: spindles appeared collapsed, bipolarity was lost, spindle poles appeared disorganized and cells arrested in mitosis (Fig. 3.7b). Upon relief of inhibition, bipolar spindles rapidly re-emerged and chromosomes were segregated at anaphase (Fig. 3.7c-d). Interestingly, upon ciliobrevin D wash-out, a minority of cells (~5%) went through a transient multipolar stage, after which the supernumerary poles were coalesced and bipolarity was recovered, in accordance with dynein's roles in pole focusing (Fig. 3.7d). No pronounced defects in chromosome segregation were apparent in either class of cells.

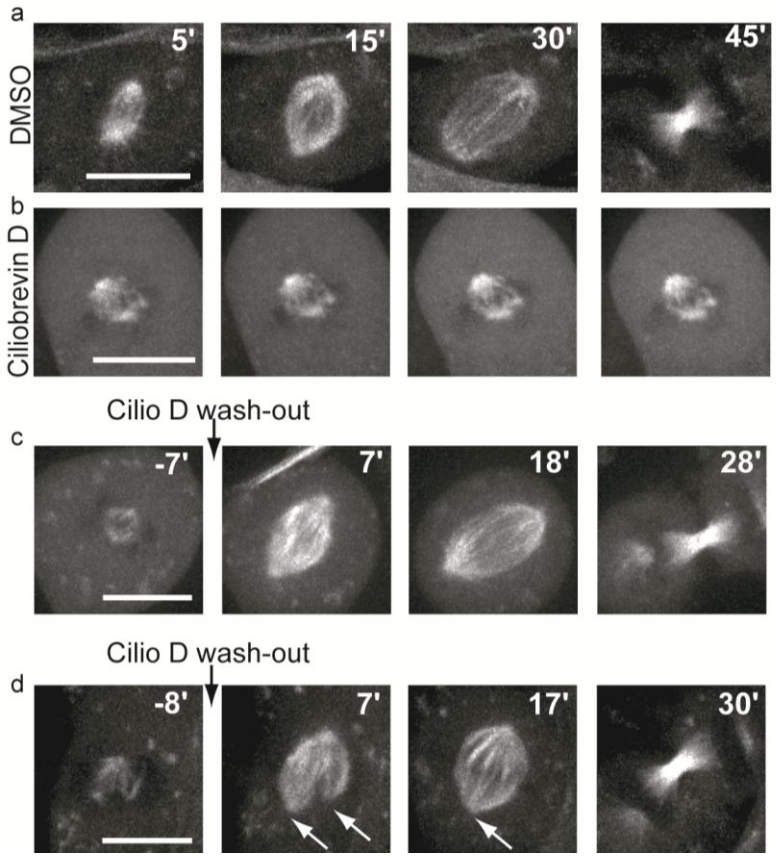

Figure 3.7 Ciliobrevin D's effects on mitotic spindles are fast and reversible. (a-d) The media of asynchronous populations of NIH-3T3 cells stably expressing GFP-tubulin were exchanged for medium containing Ciliobrevin D or DMSO. Prophase cells were identified and time-lapse images were acquired. **(a, b)** Representative images of cells after the addition of 50 µM ciliobrevin D **(b)** or an equivalent amount of DMSO **(a)**. **(c, d)** Representative images of the cells after the addition of 50 µM ciliobrevin D followed by removal of the compound ("wash-out"). Examples show the recovery of bipolar spindle morphology, which may involve pole re-focusing of supernumerary poles (**d**, arrows). Times (min) relative to compound addition **(a, b)**, or compound wash-out **(c, d)** are shown. Scale bar, 5 µm.

I next examined the effects of ciliobrevin exposure on pre-formed spindles of metaphase-arrested cells. Again, I observed several defects in spindle size and shape and pole fragmentation within minutes of ciliobrevin D addition (Fig. 3.8a-d). The live-cell recordings also suggested that ciliobrevin D treatment caused a four-fold reduction in overall microtubule levels in dividing cells (Fig. 3.8e). Although the inactive compound 2 also caused a two-fold reduction of tubulin fluorescence, spindle defects were not observed. Importantly, I found that microtubule levels in non-dividing cells were unaffected by inhibitor treatment (Fig. 3.8f-g), indicating that the ciliobrevins are not tubulin poisons and that these effects are mitosis-specific. I then examined the recovery of these disrupted spindles after ciliobrevin removal. Within minutes after wash-out, microtubule levels recovered and supernumerary poles in multipolar spindles coalesced to re-establish bipolarity (Fig. 3.8c-d), highlighting dynein's role in pole focusing. Together these data are consistent with ciliobrevin D inhibiting dynein's functions in pole organization and focusing. Because these spindle-disrupting effects are seen in cells that were already bipolar at the start of the experiment, these data reveal a hitherto under-appreciated requirement for dynein activity in the maintenance of spindle bipolarity (as opposed to its mere establishment).

Figure 3.8 Ciliobrevin D's effects on metaphase-arrested and interphase cells. (a-e) NIH-3T3 cells stably expressing GFP-tubulin were arrested in metaphase with MG132 (10 μM) and subsequently treated with DMSO **(a)** or 30 μM of either compound 2 **(b)** or ciliobrevin D **(c, d)**. The compounds were later washed out at the indicated time. Time-lapse images were acquired at the indicated times (min relative to the initial MG132 treatment). Representative examples of ciliobrevin D-treated cells show recovery of the spindle into a bipolar morphology after severe pole disruption **(c)** or severe microtubule depolymerization **(d)**. **(e)** Quantification of GFP-tubulin intensities of images corresponding to the indicated times, relative to the initial intensity for each condition. Average of 2-3 cells is shown. **(f, g)** Ciliobrevin D does not disrupt the interphase microtubule network. NIH-3T3 cells stably expressing GFP-tubulin that were in interphase were incubated in 30 μM ciliobrevin D or an equivalent amount of DMSO for 30 min before the compounds were washed out. Post-wash-out images were acquired after 15 min and compared to images acquired 15 min before wash-in. **(f)** Histogram depicting the ratio of microtubule intensities after and before washout of the relevant compound, as gauged by GFP intensity (*n*= 2 independent experiments, >10 cells per condition). Average ± s.e.m. shown **(g)** Representative images of the cells quantified above and their individual pre-washout/post-washout ratios. Scale bars, **(a-d)** 5 μm; **(g)** 10 μm.

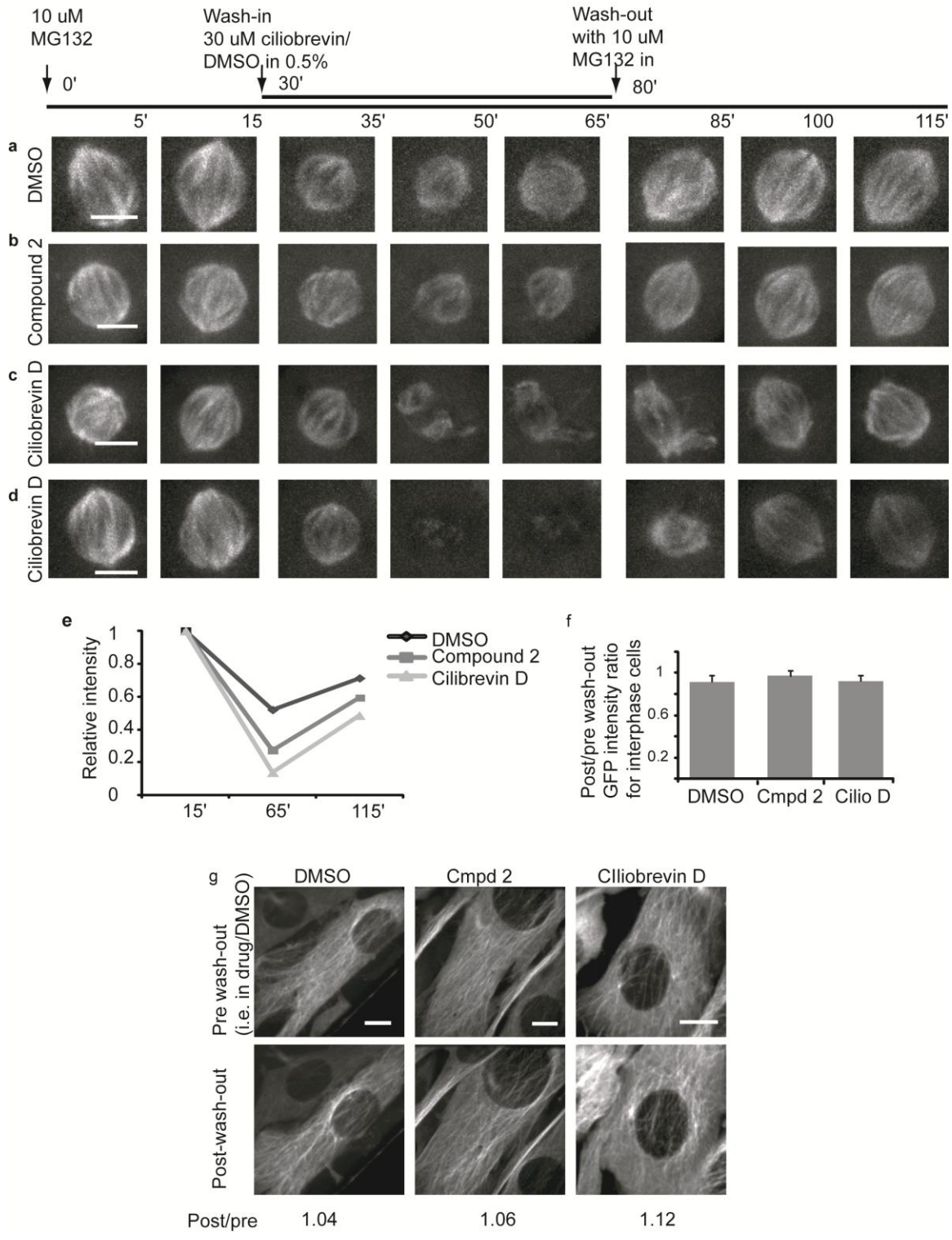
10 uM
MG132
0'
Wash-in
30 uM ciliobrevin/
DMSO in 0.5%
30'
Wash-out
with 10 uM
MG132 in
80'
5'
15
35'
50'
65'
85'
100
115'
a
DMSO
b
Compound 2
c
Ciliobrevin D
d
Ciliobrevin D
e
Relative intensity
1
0.8
0.6
0.4
0.2
0
15'
65'
115'
DMSO
Compound 2
Cilibrevin D
f
Post/pre wash-out
GFP intensity ratio
for interphase cells
1
0.6
0.2
DMSO
Cmpd 2
Cilio D
g
DMSO
Cmpd 2
CIliobrevin D
Pre wash-out
(i.e. in drug/DMSO)
Post-wash-out
Post/pre
1.04
1.06
1.12

Conclusions and discussion

In this Chapter, I examined the effects of ciliobrevin D on mitotic cells, in a collaborative effort to characterize this molecule as the first specific small-molecule inhibitor of the motor protein dynein. I showed that, as expected from previously published studies of dynein inhibition with cruder molecular biology tools, ciliobrevin D reversibly causes a severe disruption to pre-formed spindles, precludes *de novo* spindle assembly and disrupts proper kinetochore-microtubule interactions in human and murine cells. The use of ciliobrevin D on metaphase-arrested cells revealed that dynein is involved not only on spindle bipolarity formation, but also in its maintenance. The data shown here, together with the work of collaborators in the Kapoor, Gelfand, O'Donnell and Chen laboratories, validate ciliobrevin D as the first specific, reversible, ATP-competitive small-molecule antagonist of the AAA+ ATPase minus-end-directed motor protein dynein (Firestone et al. 2012).

My work also reveals the limitations of ciliobrevin D in mitotic research: because it inhibits both pole- and kinetochore-localized dynein, causing severe spindle disruption and thus activating the spindle assembly checkpoint, its use in checkpoint silencing studies is precluded. In order to be able to use a dynein inhibitor for such studies, the molecule would need to inhibit the kinetochore-localized dynein only (i.e. not the dynein molecules at the poles). Further chemical derivation and structure-activity-relationship studies could feasibly lead to the discovery of dynein isoform-selective ciliobrevins (i.e. to distinguish cytoplasmic dynein 1 from 2). However, given that both kinetochore- and pole-associated cytoplasmic dynein are both type 1, the generation of

a kinetochore-specific ciliobrevin will likely be extremely challenging, if at all possible. This is because, although we do not yet know what the binding site for ciliobrevin D on dynein's motor domain is, the fact that it is ATP-competitive suggests it is likely to bind at or near the active site—which is the same for all cytoplasmic dynein 1 molecules, regardless of their intracellular localization. Nevertheless, it is possible that the binding to different recruiting partners that leads to dynein's differential localization is regulated by post-translational modifications on dynein's polypeptides. If so, and if those modifications induced structural changes to the ciliobrevin binding site, it may be possible to discover kinetochore-specific dynein 1 ciliobrevin inhibitors. However, this remains, in my opinion, unlikely. A more feasible approach might be to screen for molecules that abrogate dynein's interaction with the kinetochore recruiting factor, i.e. molecules that disturb the p50–ZW10 interaction, in analogous fashion to previously used dominant-negative strategies. However, shortcomings would include the need to undertake an entirely new chemical screen and to overcome the challenges involved in using small molecules to impede protein-protein interaction (Arkin and Wells, 2004).

Notwithstanding this limitation for checkpoint silencing studies, the ciliobrevin compounds represent an important new, specific tool for biochemical, biophysical, structural, cellular and clinical studies of dynein and its associated processes. For instance, ciliobrevins may be used to dissect the recently described relationship between cilia and cell cycle progression at the G1/S transition (Li et al. 2011; Kim et al. 2011). Supporting this, anecdotal evidence from my own and my colleagues' studies with ciliobrevin D suggests the molecule inhibits mitotic entry (data not shown).

Furthermore, given that ciliobrevins are the first class of Hedgehog signaling inhibitors downstream of Smoothened, they are significant additional tools for Hedgehog research and may also have clinical applications (in particular, ciliobrevins 7 and 8—not described here—which affect cilia formation without inhibiting dynein activity, Firestone et al. 2012). Ciliobrevin D and derivatives may also be used in *in vitro* and crystallographic studies to dissect the heretofore elusive details of dynein's mechanochemical cycle. What is more, ciliobrevin D will likely be useful in a variety of cellular studies of interphase cells, such as research on Golgi architecture, endosome recycling, axonal transport, neurodegeneration, as well as mRNA localization during embryonic patterning. Lastly, ciliobrevins may also provide a privileged starting point for the development of specific antagonists of the variety of other AAA+ family members, which includes not only biologically interesting proteins, but also clinically relevant targets such as the peroxisome proteins Pex1 and Pex6, hereditary spastic paraplegia-inducing paraplegin and spastin, and the myc-mediator oncogenes TIP49a/b (Ogura and Wilkinson, 2001).

Chapter 4: Discussion and future directions

Summary

In the previous Chapters, I examined different mechanisms that contribute to mitotic regulation. In Chapter 2, I examined the effect of constitutive Mad1 localization to different parts of the chromosome. Using a fusion protein of Mad1 and the kinetochore protein Mis12, I showed that constitutive Mad1 localization at the kinetochore leads to constitutive checkpoint arrest even after all chromosomes have bioriented. This finding indicated that the localization of Mad1-Mad2 at the kinetochore is sufficient for the establishment of checkpoint arrest. I also showed that ectopic localization of Mad1-Mad2 to the chromosome "arm" by fusion of Mad1 to H2B, or to the centromere by fusion of Mad1 to CENP-E, was not able to evoke checkpoint arrest, lending some support to the notion that kinetochores are essential for checkpoint signaling. Being able to uncouple checkpoint signaling from chromosome biorientation using the Mis12-Mad1 fusion, I then showed that BubR1, Mps1 and Aurora B activities (but not those of Polo) are necessary for the maintenance of checkpoint arrest, independently of the status of chromosome biorientation. In Chapter 3, I examined the mitotic effects of ciliobrevin D, work that contributed to the validation of the molecule as the first specific

small-molecule inhibitor of the motor protein dynein. I showed that dynein inhibition by ciliobrevin D not only recapitulates previously reported mitotic roles of dynein, but also reveals a new function for this motor protein in the maintenance of spindle bipolarity. I also explained why the molecule is not useful for further examination of the roles of dynein in the metaphase-to-anaphase transition. In this Chapter, I discuss further implications of these results, as well as possible directions in which these results can be taken to extend our knowledge of mitosis.

Future directions

The role of kinetochores in checkpoint signaling

In Chapter 2, I showed that constitutive Mad1 localization at kinetochores is sufficient to induce checkpoint arrest, even if all chromosomes are bioriented. Following this, I wanted to examine whether constitutive localization of Mad1 on other parts of the chromosome would lead to the same result. Several lines of evidence suggest that checkpoint activity can originate in the cytoplasm, suggesting that kinetochores are not essential for checkpoint signaling (Windecker et al., 2009; Meraldi et al., 2004a). Therefore, I reasoned that ectopic localization experiments should allow examination of the role of kinetochores and determine whether they are necessary for checkpoint signaling.

Contrary to that seen with the Mis12-Mad1 fusion protein, fusion of Mad1 to neither H2B nor CENP-B led to checkpoint arrest. I took these data to support the notion

that kinetochores are essential for checkpoint signaling. However, several questions were left unanswered. Firstly, the fact that ectopic localization with those fusion partners and with those specific linkers used did not result in checkpoint arrest does not mean that all possible ectopic localization experiments would give the same result. In other words, the negative results may have been due to the wrong choice of partners or, more simply, to technical issues. Secondly, although I showed that H2B-Mad1 recruits Mad2 all along the chromosome, I did not examine whether that ectopically recruited C-Mad2 was able to recruit and activate cytoplasmic O-Mad2 with rates comparable to control values of Mad2 activation at the kinetochore. For instance, it is possible that technical issues such as the length of the linker precluded Mad1-bound-C-Mad2 from catalytically amplifying O-Mad2 molecules in the cytoplasm, even though it correctly bound Mad1 on the chromosome. This issue could be addressed with FRAP experiments to examine Mad2's dynamics, as has been done *in vitro* and for Mad2 at the kinetochore (Howell et al., 2000; Shah et al., 2004; Howell et al., 2004; Vink et al., 2006). Even with these control experiments, the notion that kinetochores are essential for checkpoint signaling would remain underdetermined, as a specific configuration may exist in which ectopic recruitment of Mad1-Mad2 may elicit checkpoint arrest. Different strategies for ectopic localization may therefore prove more useful.

Alternatively, reduced kinetics for Mad2 activation at the chromosome arm may indicate not a mere technical deficiency, but the fact that additional factors are needed in the vicinity of the core tetramer to make O-Mad2 amenable for activation. For instance, it has been shown that Mps1 activity is needed for the sustained recruitment

of O-Mad2 to the kinetochore, and it has been speculated that this may be required to antagonize cytoplasmic Mad2's interactions with its inhibitor p31 (Hewitt et al., 2010). This hypothesis could be tested by depleting p31/Comet in cells expressing H2B-Mad1 and observing whether checkpoint arrest can be established in that case. Additionally, an ectopic recruitment strategy that not only mislocalizes Mad1-Mad2, but also ectopically recruits other checkpoint pathway components close to the core tetramer may also shed light on these issues. Such a strategy is further discussed in following section and in the Appendix chapter.

Conditional recruitment of Mad1 to kinetochores or other chromosomal locations

The use of a Mis12 fusion to constitutively localize Mad1 at kinetochores was a successful method to show that kinetochore Mad1 localization is sufficient to induce checkpoint arrest independently of biorientation. A modification that would make this approach useful for the examination of a variety of mitotic questions would be to make Mad1's interaction with Mis12—and, hence, Mad1-Mad2's localization at kinetochores and checkpoint arrest— not constitutive but conditional.

A system that synchronized cells at metaphase without the need for chemical inhibitors with questionable off-target and secondary effects (e.g. the use of the proteosome inhibitor MG132), or for the inhibition of other key mitotic enzymes, would be a useful research tool for the study of post-anaphase processes. The conditional recruitment and release of Mad1 to and from kinetochores might allow us to reliably synchronize cells by arresting in them metaphase (owing to Mad1 kinetochore

localization) and releasing into anaphase upon the removal of Mad1. This approach makes the assumption that the release of the engineered Mad1-Mad2 from the bioriented kinetochores would be sufficient to induce checkpoint silencing, analogously to what happens in normal cells with dynein stripping— it must be noted, however, that the importance of this mechanism is debatable. This uncertainty notwithstanding, such a conditional system would not only be useful as a synchronization tool, but may also be useful in studies of the inter-relationships between the different checkpoint silencing mechanisms.

A conditional Mad1-recruitment system may be achieved by combining the idea of the Mis12-Mad1 fusion with the rapamycin-dependent dimerization of FRB and FKBP (Banaszynski et al., 2005). For instance, we could use a mCherry-Mis12-FRB and FKBP-GFP-Mad1 combination to recruit Mad1 to kinetochores in a conditional fashion. The components would need to be tested for localization, dimerization and release depending on rapamycin presence, kinetics, non-alteration of kinetochore-microtubule interactions, etc. A potential technical pitfall is that rapamycin wash-out is difficult to achieve in cells. An alternative strategy may be to use a chemical biological system that controls not protein localization, but stability. By fusing Mis12-Mad1 to the protein FKBP(L106P, hereafter FKBP*), we could control stability of the protein (and, hence, the establishment of and release from checkpoint arrest) with the small molecule Shield: FKBP* acts as a degradation tag on its own, but its proteolysis is prevented in the presence of this compound (Banaszynski et al., 2006). The FKBP*/Shield system has been successfully used to control protein expression in vertebrate and insect cells, as

well as in whole organisms, but it has not so far been used specifically in mitotic cells (Armstrong and Goldberg, 2007; Herm-Gotz et al., 2007; Banaszynski et al., 2008). Before using this approach, we would need to validate its use during mitosis. For further explanation and discussion of these strategies, as well as for preliminary results, please refer to the Appendix chapter.

The control of checkpoint arrest establishment and release independently of chromosome biorientation need not be limited to manipulations of Mad1. It has recently been shown that, the MCC being the most downstream effector of checkpoint signaling, expression of a fusion of Mad2 and BubR1 (or of Mad2 and BubR1 that are artificially dimerizable *via* leucine zippers) is sufficient to induce checkpoint arrest in budding yeast (Lau and Murray, 2012). Expressing FRB-FKBP-dimerizable or FKBP*/Shield-regulated versions of these proteins in human cells might be an alternative mechanism for cell synchronization and the examination of post-anaphase events. Given that these are the most downstream components of the systems, the kinetics of onset and release might be faster than those achieved by the regulation of Mad1 localization or stability. This strategy, of course, remains to be experimentally tested.

Finally, it may be worth revisiting the question of whether it is possible to establish checkpoint arrest from a non-kinetochore location. Achieving it would not only show that kinetochores are not essential for the checkpoint, but it would also allow us to tackle other fundamental questions about the SAC signaling pathway. For instance, it would inform us on what the minimal components of the checkpoint are, which may

lead to improved *in vitro* reconstitution assays and analyses. Moreover, if we knew how to reconstitute checkpoint arrest from defined ectopic location, we would be able to carry out quantitative studies of how the checkpoint stop-anaphase signal is amplified from a single locus (analogously to signaling from a single non-bioriented kinetochore). A system that might be amenable for this may be the lac–*ISceI*–tet cell line, which contains a single stable integration of an array of lac operators, followed by an array of tet operators (Soutoglou et al., 2007). This method would involve recruiting pairs of checkpoint proteins (e.g. Mad1 and a kinase) fused to lacI or TetR respectively and examining whether that recruitment could evoke checkpoint arrest (and release). This method is further explained in the Appendix chapter. Similarly to the H2B and CENP-B fusions described above, negative results will not necessarily indicate that the system is not useful and that kinetochores are necessary for checkpoint signaling.

The role of kinase activity in checkpoint maintenance and silencing

In Chapter 2, I showed that Aurora B or Mps inhibition *via* small molecules is sufficient to override the arrest caused by the expression of Mis12-Mad1. This indicates that Aurora B and Mps1 activities are needed for the maintenance of checkpoint arrest, independently of their roles in kinetochore assembly and checkpoint protein recruitment. How does kinase inhibition elicit entry into anaphase? Kinases are opposed by phosphatases. In the absence of sustained kinase activity, phosphatase activity tips the equilibrium towards dephosphorylation of substrates. More importantly, what are

the relevant Aurora and Mps1 substrates and sites? How are the kinase circuits inter-related? What are the relevant opposing phosphatase complexes?

Feasible kinase substrate candidates downstream of kinetochore recruitment are the members of the MCC, the APC/C-cdc20 complex and other silencing players, such as p31/Comet and dynein. In fact, a few phosphorylation events on MCC components have been identified in different organisms. For instance, phosphorylation of Mad2 by Mps1, of BubR1 by Aurora and of cdc20 by Bub1 have been shown to affect checkpoint arrest and release (Tang et al., 2004; King et al., 2007; Shepperd et al. 2012). Interestingly, both positive and negative effects on checkpoint arrest have been observed (Shepperd et al. 2012). These results should be re-valued and evaluated in more detail in the light of the updated models of direct kinase roles in checkpoint signaling.

Furthermore, my results that inhibition of either kinase is sufficient to override the checkpoint are in line with evidence that Aurora B and Mps1 act in a common pathway (Jelluma et al. 2010; Lan and Cleveland, 2010). Nevertheless, the fact this sufficient inhibition occurs after biorientation has been achieved and Mps1 has been released to the cytoplasm suggests that a more complex pathway may be in place. It is also very likely that the checkpoint silencing circuit will include different types of motifs and feedback loops. Therefore, it is paramount that the whole set of players and interactions be identified. Identification of kinase/phosphatase substrates could be done, for instance, using a combination of bioinformatics, chemical genetics, mass spectrometry and high-throughput RNAi screens, to be later validated in cell biological experiments

(e.g. Hegemann et al. 2011; Hengeveld et al. 2012; Oppermann et al. 2012). Our Mis12-Mad1 construct may be of use in such screens and validation assays.

It will also be interesting to examine how the kinase/phosphatase circuits interact with the other mechanisms of checkpoint silencing and what their relative contributions are in a variety of different model organisms. For instance, does PP1 dephosphorylation affect dynein stripping in higher eukaryotes? Could PP1-gamma be responsible for activating p31/Comet? The fact that Aurora B or Mps1 inhibition is sufficient to override checkpoint arrest in human cells suggests that they might be the most important components of the system. Furthermore, the fact that Mad1-Mad2 remain at the kinetochores of the segregating chromosomes supports the idea that dynein stripping might play a merely accessory role in checkpoint silencing (this work and also Canman et al., 2002). This is also in line with the fact that dynein is not necessary for mitosis of lower eukaryotes. A dynein small molecule inhibitor that acted only at kinetochores would have been a very useful tool to examine these questions in more detail. Unfortunately, as discussed in Chapter 3, ciliobrevin D is not useful for these types of experiments, as its inhibition of pole-localized dynein leads to the disruption of bipolar spindles and the maintenance of checkpoint arrest. The development of a small molecule that inhibited the interactions between dynein and ZW10 would be useful tool in this regard.

Finally, could a better understanding of checkpoint silencing lead to the development of better therapeutic strategies in cellular hyper-proliferative diseases such as cancer? Preventing checkpoint silencing not only delays proliferation, but also

increases the probabilities of death in mitosis (Janssen and Medema, 2011). As such, it could provide alternative strategies and uncover new combination therapies that might be effective.

Perspective

The field has come a long way since the initial identification of the first checkpoint components in 1991 (Hoyt et al., 1991; Li and Murray, 1991). Nevertheless, several unanswered question still remain. For instance, what is the precise architecture of the kinetochore, before and after attachment? Although significant structural advances have been made recently, we still do not fully grasp how the interactions between the kinetochore and checkpoint components change upon biorientation. Are kinetochores really essential for checkpoint activity *per se*, or is their role actually to couple biorientation with silencing? Similarly, how does the structural change upon biorientation translate into checkpoint silencing, especially in the cytoplasm? And what do the details of checkpoint silencing differ in different organisms? Is silencing complexity correlated with the rise of complexity in kinetochore structure, attachment modes, and centromere specification?

Another important advance has been the recognition that checkpoint kinases do indeed have a direct role in checkpoint signaling, and we are beginning to uncover how their phosphorylations prevent cdc20 activity. Nevertheless, as mentioned above, crucial details such as specific kinase substrates and their relevant sites, the possible

inter-plays of different kinase loops and the relevant phosphatase regulation are still unknown.

Moreover, unresolved issues still remain with the Mad2-template model. What is the definitive answer on the question of C-Mad2 auto-catalytic amplification in the cytoplasm? What is p31/Comet's physiological contribution as a "brake"? How are Mad1-C-Mad2 complexes in the cytoplasm regulated? How does SAC activity originate in the cytoplasm independently of kinetochores, and is this a physiologically important process, or is it just a minor component? Likewise, we need a much clearer understanding of the amplification parameters and kinetics in cells and a more careful examination of the notion that a single non-bioriented chromosome can establish as robust an arrest as the full set of unattached kinetochores in metaphase.

Contributions of this thesis

In this thesis, I have contributed to the study of some fundamental questions of the spindle assembly checkpoint mechanism. Is Mad1-Mad2 kinetochore localization sufficient for checkpoint arrest? Is kinase activity necessary for checkpoint signaling *per se*? Can we develop chemical tools for the study of checkpoint silencing? I have arrived at some answers, but, invariably, more questions remain. Are kinetochores necessary for checkpoint signaling? What are the kinase substrates relevant for checkpoint signal maintenance? What is the circuit for checkpoint silencing?

Clearly, much more cellular, biochemical, structural and biophysical research remains to be done in these and other areas to achieve a complete description of the

complex workings of the spindle assembly checkpoint. I hope the findings and tools described in this thesis will be of use for future investigation in these areas.

Appendix: Towards a system for conditional checkpoint signaling independently of chromosome biorientation

Summary

In the previous Chapters, I showed how constitutively kinetochore-localized Mad1 is sufficient to induce spindle assembly checkpoint signaling independently of chromosome biorientation. I discussed how it would be beneficial to have a conditional system for Mad1 recruitment to the kinetochore or elsewhere on the chromosome that would allow us not only to reliably synchronize and release cells at the metaphase-to-anaphase transition, but also to investigate, among others, questions regarding the need for kinetochores as signaling hubs, the minimal components sufficient for checkpoint signaling and the mechanism of checkpoint signaling amplification. In this Chapter, I describe preliminary efforts towards the development of such a system. Firstly, I describe attempts to use a rapamycin-dependent dimerizer system of the domains FRB and FKBP fused to Mis12 and Mad1, respectively. This approach proved unsuccessful due to inappropriate expression levels of the fusion proteins involved.

Secondly, I describe a related approach consisting on Shield-dependent rescue of an FKBP(L106P)-Mis12-Mad1 fusion protein (hereafter, FKBP*-Mis12-Mad1). I was able to validate the use of this approach in mitotic cells, and preliminary results indicate that Shield-rescued FKBP*-Mis12-Mad1 does indeed induce metaphase arrest. Lastly, I describe a system to conditionally recruit checkpoint components to ectopic locations on the chromosome arm, by interaction of lac and tet repressors to their respective DNA operators. This system, although promising, is still in the cloning stage. The full development of these of other systems for a rapid, reversible and tunable induction of checkpoint signaling independently of chromosome biorientation would be a significant tool for the dissection of long-standing mitotic questions.

Conditional checkpoint signaling independently of chromosome biorientation

Rapamycin-dependent FRB-FKBP-mediated Mis12-Mad1 dimerization

The localization of Mad1 at the kinetochore is sufficient to induce checkpoint arrest even when chromosomes are bioriented. I reasoned that if I could conditionally and reversibly recruit Mad1 to kinetochores by an artificial heterodimerization method, I may be able to conditionally establish and release a checkpoint-based metaphase arrest independently of the checkpoint's primary signal, i.e., I would have a reliable system for arresting and releasing cells at the experimenter's convenience, without the need for inhibition of kinases or other mitotic proteins that might be under study.

The first approach I took towards this was using a rapamycin-dependent FRB-FKBP dimerization system. Rapamycin is a 31-membered macrolide small molecule that has been of use in molecular biological studies due to its ability to simultaneously bind with high affinity to the FRB domain of mTOR and to the protein FKBP, thereby inducing their heterodimerization (Banaszynski et al., 2005). This feature has been exploited as a research tool to heterodimerize proteins by fusing them to FRB and FKBP and it has proven a successful strategy to control the spatio-temporal activation of a variety of proteins. Moreover, the system has been successfully used in the Kapoor laboratory to ectopically recruit the PP2A regulatory subunit R5B to the chromosome "arm", by using an H2B-FRB, FKBP-R5B system (Dr Lei Tan, Kapoor laboratory, personal communication).

Encouraged by this background, I decided to use the rapamycin- dependent FRB-FKBP dimerization to conditionally localize Mad1 at the kinetochore by inducing its dimerization with Mis12. To prevent the default localization of Mad1 to kinetochores, I decided to use a truncation of Mad1 (Mad1F10) that lacks amino acids 1-320, which encode Mad1's kinetochore-localizing sequences (Canman et al., 2002). I produced a FKBP-Mad1F10-GFP construct (Fig. A.1) and used it together with the previously developed Mis12-mCherry-FRB construct (a gift from Dr Lei Tan, Kapoor laboratory).

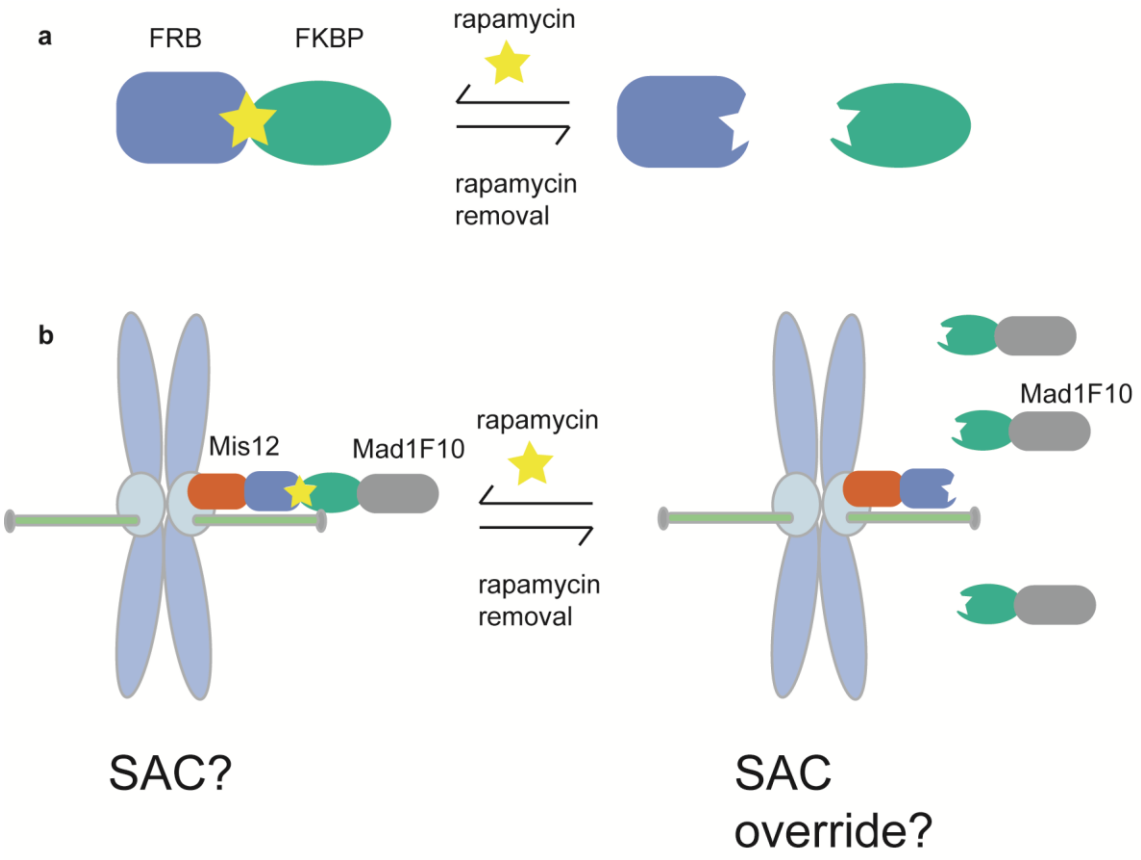

Figure A.1 Schematic representation of FRB-FKBP dimerization-mediated system for microtubule-independent, conditional checkpoint arrest. (a) FRB and FKBP dimerize in the presence of rapamycin and separate upon rapamycin removal. **(b)** Proposed system: in cells expressing Mis12-FRB and FKBP-Mad1F10, the addition of rapamycin would recruit Mad1F10 to kinetochores through the dimerization of FRB and FKBP, which would lead to checkpoint arrest. Upon rapamycin removal, dimerization would be abrogated, Mad1F10 would be released from kinetochores and the spindle assembly checkpoint would be overridden (if Mad1-Mad2 removal from bioriented kinetochores were sufficient for checkpoint silencing).

I generated and examined stable cell lines or transient transfections in all possible permutations of the components: I made a double stable cell line with both constructs, stable cell lines with a single component to which I transiently transfected the other one, or transiently transfected both elements under a variety of protocols. To examine the dimerization dynamics of FKBP-Mad1F10 and FRB-Mis12, I performed near simultaneous live-imaging for mCherry and GFP channels of metaphase-arrested cells after the addition of 20 nM rapamycin. Under none of the conditions examined did I see GFP signal at (Mad1F10 recruitment to) the kinetochores, even after incubation in 50 nM of rapamycin for over 6 hours (for comparison, PP2A R5B was 8-fold enriched after 15 min in 20 nM rapamycin, Dr Tan, personal communication). It is likely this is due to either low expression levels of Mis12-FRB or low level of recruitment at the kinetochores (also observed by Dr Tan). Moreover, GFP signal in the cytoplasm was heterogeneous and mostly localized to cytoplasmic aggregations. In addition to these setbacks, the fact that it would be difficult to wash rapamycin off to reverse the dimerization prompted me to stop optimizing this system and focus on an alternative strategy instead.

Shield1-dependent FKBP(L106P)-Mis12-Mad1 fusion protein level control

My second approach towards the development of a system for conditional checkpoint arrest and release independent of the checkpoint's primary signal was the FKBP*/Shield system developed by Dr Wandless and colleagues (Banaszynski et al., 2006). They developed a system for the control of protein levels by manipulating the degradation of

a novel degron consisting of a FKBP mutant (L106P) with the rapamycin-derived small molecule “Shield”. FKBP* remains semi-unfolded in the cytoplasm and is thus targeted for degradation by the proteosome. If fused to a protein of interest, FKBP* will act as a degradation tag for the fusion protein. In the presence of Shield, FKBP* can fold properly and it thus “shielded” from its degradation. Dr Wandless’ group showed that this system allows specific, rapid, reversible, tunable control of protein levels in interphase cells (Fig. A.2a). The strategy has been successfully used with a variety of proteins in cells and whole organisms (e.g. Banaszynski et al., 2008, Herm-Gotz et al., 2007, Armstrong and Goldberg, 2007).

The system seemed applicable to regulate Mad1 at kinetochores by manipulating protein levels of Mis12-Mad1 as opposed to manipulating Mad1 recruitment. Because all characterization of the FKBP*/Shield system had been done in interphase cells, I first needed to validate the approach in single mitotic cells. In the following sections, I describe my validation of the system in mitotic cells using FKBP*-GFP and I then describe experiments using mCherry-FKBP*-Mis12-Mad1.

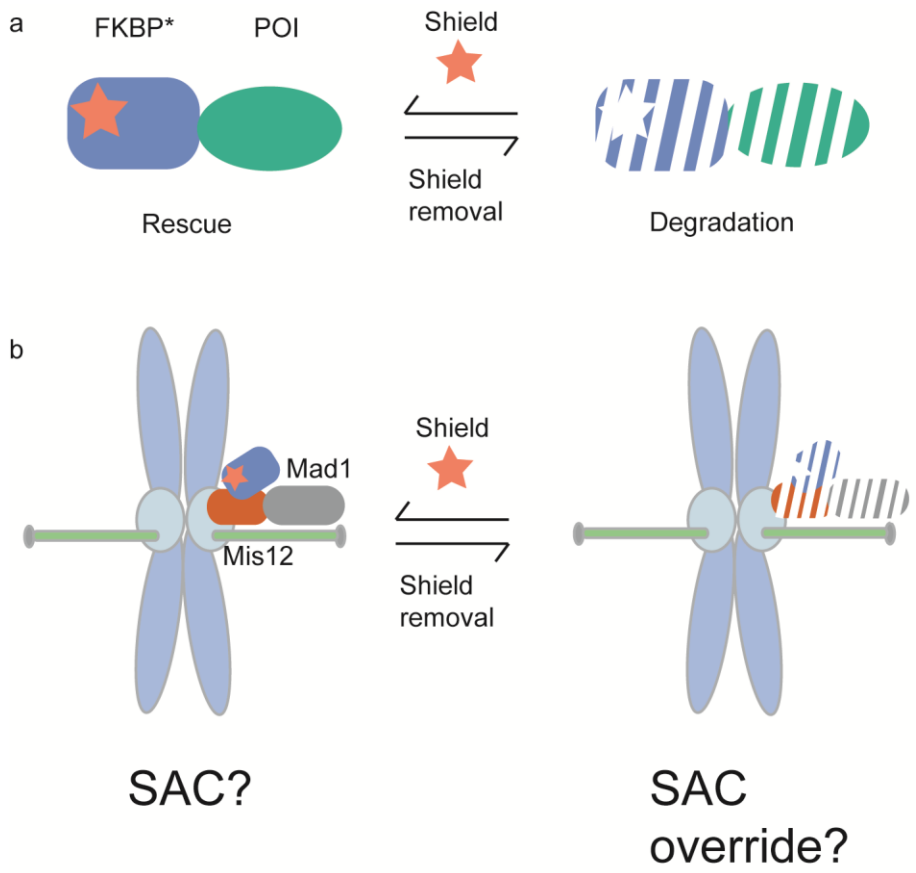

Figure A.2 Schematic representation of FKBP*/Shield-mediated system for microtubule-independent, conditional checkpoint arrest. (a) FKBP* is a degron that targets fused proteins of interest (POI) for degradation. The small molecule Shield allows the correct folding of FKBP* and prevents its degradation, thus rescuing expression levels of the POI. **(b)** Proposed system: in cells expressing FKBP*-Mis12-Mad1, the addition of Shield would rescue the expression of the fusion protein, which would be recruited to kinetochores and, analogously to mCherry-Mis12-Mad1, lead to checkpoint arrest. Upon Shield removal, FKBP*-Mis12-Mad1 would be degraded and the spindle assembly checkpoint would be overridden (if Mad1-Mad2 removal from bioriented kinetochores were sufficient for checkpoint silencing).

Validation with FKBP*-GFP

To examine whether the FKBP*/Shield system can be used in mitotic cells and, if so, whether it exhibits the same kinetics as in interphase cells, I fused FKBP* to GFP and made stable FKBP*-GFP RPE-1 and HeLa cell lines. I arrested the cells in mitosis using the microtubule depolymerizing drug nocodazole and followed the changes in GFP protein levels by quantifying the fluorescence signals of the cells upon Shield wash-in (to measure GFP "rescue") or Shield wash-out (to measure GFP degradation).

Shield-dependent rescue and FKBP* degradation were observable at a single-cell level in interphase and mitotic (nocodazole-arrested) cells. The kinetics of GFP rescue in mitotic cells in the presence of 1 µM Shield reached a ~2-fold enrichment (relative to starting levels) by 5 h (Fig. A.3 b, e). Published experiments show that FKBP* is rescued to ~10% of its maximal level by 4 h interphase cells (Banaszynski et al., 2006). Because I imaged cells for five to eight hours, I was not able to record the maximum rescue levels. Nevertheless, taking the published data as reference, I would expect a ~20-fold enrichment of FKBP* fusion protein levels by 24 h in the presence of Shield. Higher final concentrations of Shield should also improve the extent of protein level rescue, but this variable was not explored. The kinetics of FKBP*-mediated degradation of GFP were similar to the rates seen for interphase NIH-3T3 cells for both interphase and mitotic cells (Banaszynski et al., 2006): after 16 h-22 h exposure to 1 µM Shield, half-maximal degradation was achieved in ~1 h in mitotic cells with quasi-first-order kinetics (Fig A.3 c, d, f).

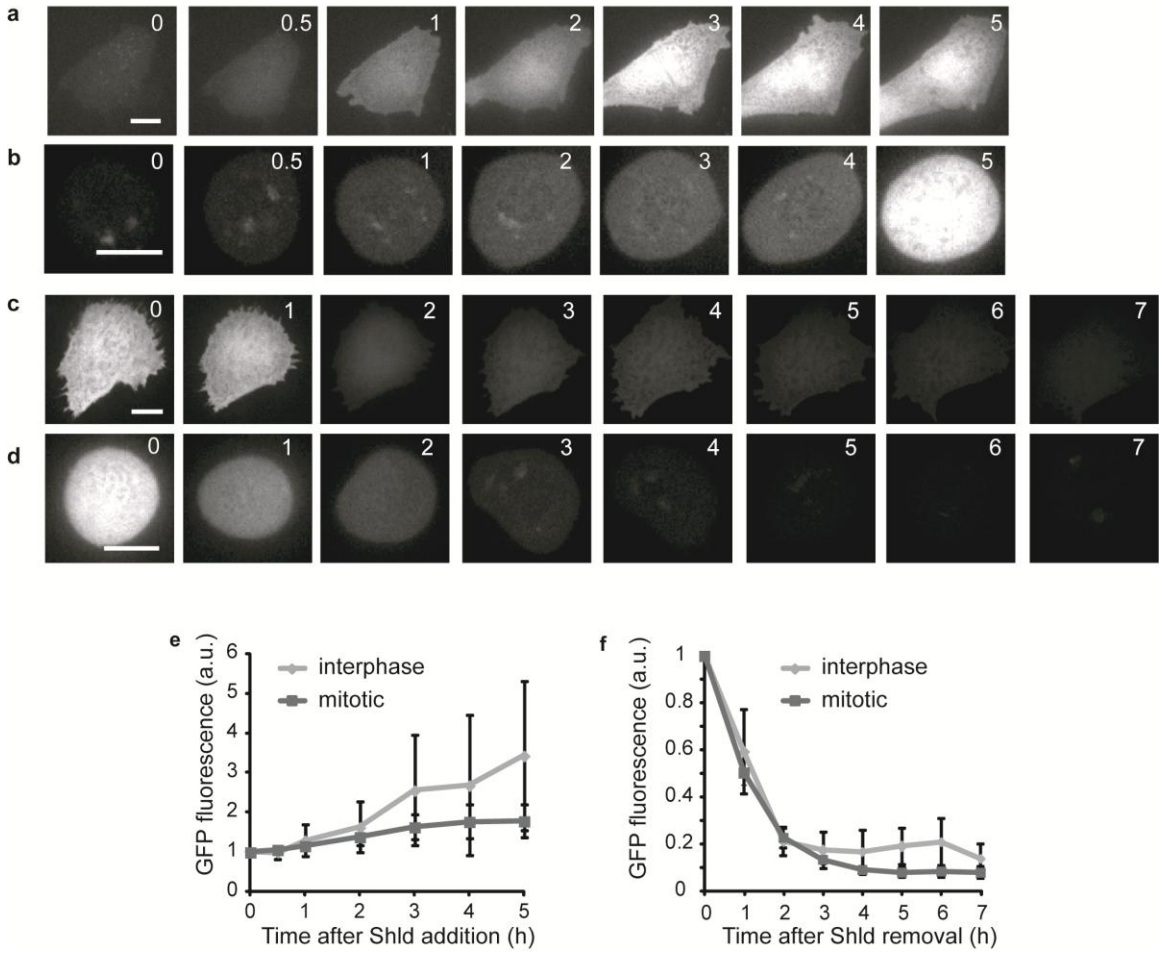

Figure A.3 Shield-dependent regulation of GFP expression levels in RPE-1 cells. (a-f) A stable retroviral RPE-1 cell line containing FKBP*-GFP was subjected to addition of 1 µM Shield **(a, b, e)** or its removal after overnight incubation **(c,d,f)**. Interphase **(a, c)** and mitotic **(b, d)** cells were identified imaged in approximately hourly intervals (shown in top right corner of each image). **(e,f)** GFP fluorescence levels were quantified for each condition (3-8 cells per condition). Average ± s.d. shown. Scale bar, 10 µm.

From these preliminary experiments I conclude that the FKBP*/Shield system can be used to control protein levels in mitotic cells and that the changes in GFP levels in mitosis are similar to those seen in interphase cells. In the next section, I describe how I have started using this system to conditionally arrest and release cells in and out of mitosis, independently of the checkpoint's primary signal.

Experimentation with FKBP*-Mis12-Mad1

To regulate the levels of Mad1 present at the kinetochores, I decided to make the fusion protein mCherry-FKBP*-Mis12-Mad1. Preliminary experiments using transient transfection showed that the fusion is rescued by Shield (1 µM), that the stabilized fusion protein localizes at kinetochores and that it induces metaphase arrest in agreement with data described in Chapter 2 for mCh-Mis12-Mad1 (Fig. A.4 and 2.3). In fact, the mitotic index increase seen with a 24-hour rescue of mCherry-FKBP*-Mis12-Mad1 (46%, 1 µM Shield, > 250 cells, 2 coverslips, 1 experiment) was higher than that previously seen with 24-hour expression of mCherry-Mis12-Mad1 (27.6% ± 2%, *n*= 3 independent experiments, > 400 cells counted per condition per time; Fig. A.4 and 2.3). Although these percentages may not be directly comparable, the strong metaphase arrest seen with Shield rescue was certainly encouraging.

The mCherry-FKBP*-Mis12-Mad1 fusion protein was detectable by immunofluorescence but not by live imaging (presumably because expression level was below fluorescence detection limit, as seen with other Mis12 constructs, Dr Tan, personal communication). Hence, I decided to make a stable cell line, such that I could

incubate the cells in medium with Shield for longer times. A HeLa mCherry-FKBP*-Mis12-Mad1 stable cell line has been made and is ready for testing.

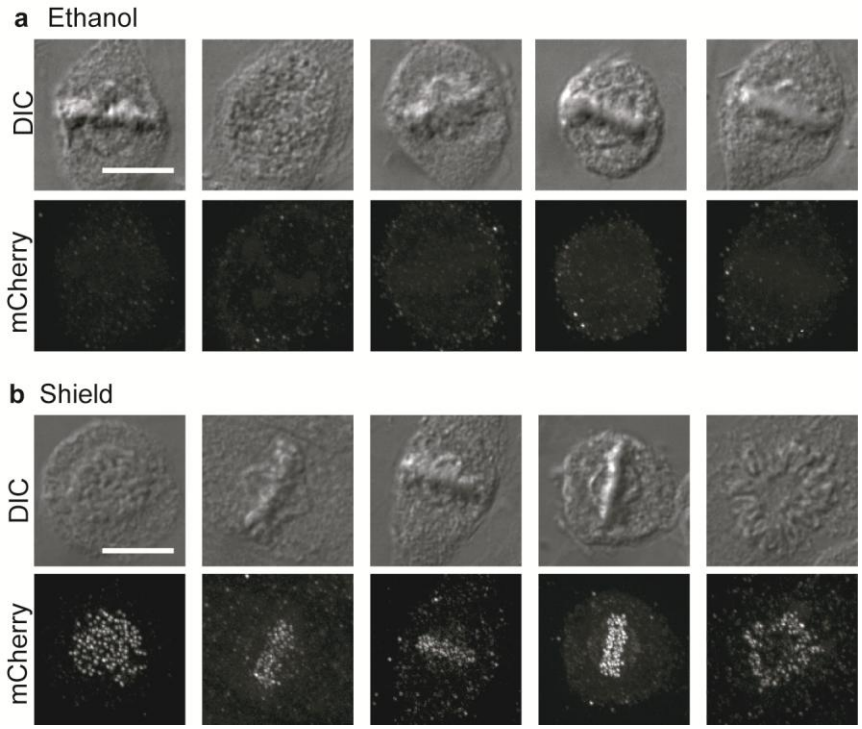

Figure A.4 Shield-dependent expression and kinetochore localization of mCherry-FKBP*-Mis12-Mad1 in HeLa cells. (a, b) Twenty-four hours after transient transfection with mCherry-FKBP*-Mis12-Mad1, HeLa cells were incubated in 1 µM Shield **(b)** or an equivalent amount of ethanol **(a)**. Twenty-four hours later, they were imaged live. No mCherry signal was detectable for either population (not shown). Following these live imaging experiments (i.e. after a ~ 28-hour incubation in Shield or ethanol), additional equivalent coverslips were fixed and processed for immunofluorescence. Staining for mCherry is shown, together with DIC image of these fixed cells. Scale bar, 10 µm.

Lac-Tet repressor/operator system

The third approach to study checkpoint signaling independently of its primary signal that I will describe is a system for conditionally recruiting Mad1 and other checkpoint components to ectopic chromosomal locations, i.e. at a specific point on the chromosome, away from the kinetochore. This system would allow us to investigate long-standing questions on checkpoint signaling. For instance, can we reconstitute checkpoint activity away from the kinetochore? If so, what are the minimal requirements for checkpoint signaling? The system would also allow us to examine checkpoint signal amplification and re-evaluate the long-standing belief that a single non-bioriented chromosome is sufficient for checkpoint arrest in a more precise and controlled manner.

The system that we envisioned for achieving this is a dual lac operator/repressor- tet element/repressor system, based on reagents previously developed by Dr Misteli (NIH; Soutoglou et al., 2007). These and similar systems have been successfully used to recruit DNA damage proteins to an experimentally controlled DNA double strand break, as well as for visualizing gene expression in real time and following chromosome segregation patterns (Chubb et al., 2002, Janicki et al., 2004, Bakhoum et al., 2009, Thompson and Compton, 2010). Dr Misteli's system consists of a NIH-3T3-derived cell line that contains a stable insertion of an array of lac operators (lacO), followed by a *ISce*I restriction site, followed by an array of tetracycline responsive elements (TRE) at a defined site on one chromosome (hereafter, the lac–*ISce*I–tet cell line).

We hypothesized that, if we made a derivation of the lac–*ISceI*–tet cell line that also stably expressed fusion proteins of the lac-repressor (lacI) and tet-repressor (TetR) with checkpoint proteins, we would be able to conditionally recruit checkpoint proteins to the ectopic location to examine the questions on checkpoint signaling outlined above (Fig. A.5).

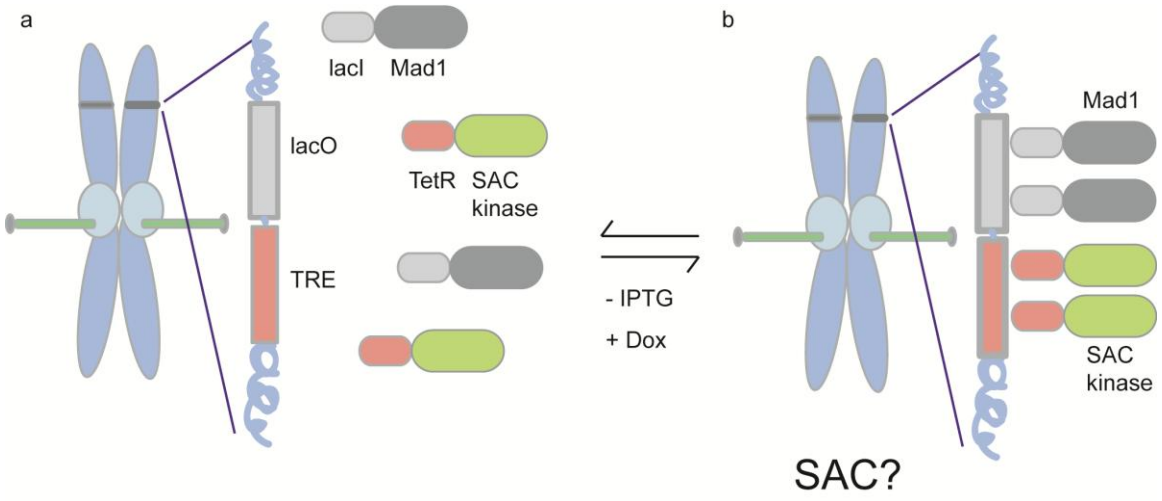

Figure A.5 Schematic representation of lac and tet operator/repressor recruitment-mediated system for microtubule-independent, conditional checkpoint arrest from an ectopic location. (a) The cells used in the proposed system contain a stable, non-centromeric, chromosomal insertion of an array of lac operators followed by an array of tet responsive elements. The cells would also express fusion proteins of combinations of checkpoint proteins (Mad1 and Mps1 depicted) fused to the lac and tet repressors, respectively. (b) Upon the removal of IPTG and addition of doxycycline, the repressor-fused checkpoint proteins would be recruited to the corresponding array, which may lead to checkpoint arrest.

We reasoned that we might be able to reconstitute checkpoint activity by combining the ectopic recruitment of two different classes of checkpoint proteins: a structural, detection protein (e.g. Mad1) and an amplification protein (e.g. a checkpoint kinase). We decided to start with a combination of a TetR-Mad1 and Mps1-lacI. Experiments to validate the approach are under way.

Materials and methods

Cell lines, and plasmid and siRNA transfection

HeLa and NIH-3T3 cells were grown in Dulbecco's modified Eagle's medium (DMEM; Invitrogen) and RPE-1 cells, in DMEM-F12 1:1 mixture (Invitrogen), supplemented with 10% fetal bovine serum (HeLa and RPE-1; Sigma) or 10% bovine calf serum (NIH-3T3; Sigma), 2 mM L-Glutamine (Invitrogen), 1X non-essential amino acid solution (Invitrogen) and penicillin–streptomycin (100 U ml^{-1} and 100 µg ml^{-1} respectively; Invitrogen), at 37 °C in a humidified atmosphere with 5% CO2. Cells were plated on poly-D-Lysine-coated (Sigma) glass coverslips (Fisher Scientific) in 6-well or 12-well dishes. All stable cell lines were generated by retroviral infection with pMSCV-based plasmids with the appropriate open reading frame (ORF) fused to the relevant fusion partner by overlap PCR and cloned into GFP- or mCherry-tagged vectors by Gateway technology, followed by selection with puromycin (Sigma), following suppliers' and standard protocols. The linker used between the Mis12, H2B or CENP-B(1-158) and Mad1 (or AA) ORFs was: 5'- GGCGGTTCACGCGGCCGCTCAAGCTTGGGAGGCGGTAGT-3'.

All plasmid transfections were done with FuGENE HD (Roche Diagnostics), following manufacturer's instructions, 24 hours (unless otherwise specified) before processing for immunofluorescence, live imaging or lysis for western blots. siRNA transfections were performed by reverse transfection with Lipofectamine RNAiMax

(Invitrogen) following manufacturer's instructions, 24 hours before plasmid transfection. siRNA duplexes against Mad2 (5'-AAGAGUCGGGACCACAGUUUA-3'), BubR1 (5'-AACGGGCATTTGAATATGAAA-3') and GFP (5'-GGCAAGCUGACCCUGAAGUUC-3') were purchased from Dharmacon Research.

Antibodies

Antibodies used for immunofluorescence were: polyclonal antibodies against mCherry (1: 500; custom-generated and validated by L. Tan, Kapoor laboratory, by immunization of rabbits with recombinant GST-tagged full-length mCherry at Cocalico Biologicals and subsequent serum affinity purification using a HiTrap NHS activated column, GE Healthcare Life Sciences; antibody directly conjugated to Dy-light 549 from Thermo Scientific was used for CENP-E co-localization experiments), CENP-E (HX-1; 1: 2000; a gift from T. Yen, Fox Chase Cancer Center, Philadelphia, PA), ZW10 (1: 1000; abcam), anti-gamma-tubulin (1:500 dilution, Sigma-Aldrich, T6557); monoclonal antibodies against -tubulin (DM1A, FITC-conjugated; 1: 6000 Sigma-Aldrich, F2168), Mad1 (9B10; 1: 500; Santa Cruz Biotechnology), $p150^{Glued}$ (1: 1000; BD Transduction Laboratories), Bub1 (1: 1000; abcam) and ROD (43-K; 1: 100; Santa Cruz); human CREST anti-serum (1: 20000; a gift from W. Brinkley, Baylor College of Medicine, Houston, TX). Secondary antibodies conjugated to fluoroscein isothyocyante (FITC), Dylight-549, DyLight 649- or Cy5 were from Jackson ImmunoResearch (1:400). The same mCherry (1: 1000) and anti-Mad1 (1: 500) antibodies were used for western blots, following standard procedures. Secondary

antibodies were IRDye 800CW from Li-Cor Biosciences. Blots were detected using the Odyssey Infrared Imaging System (Li-Cor).

Immunofluorescence microscopy

For all immunofluorescence experiments, cells were pre-extracted with 100 mM K-Pipes at pH 6.9, 4 M Glycerol, 1 mM EGTA, 5 mM MgCl2 and 0.5% Triton X-100 at 37 °C for 90 s and then fixed with 3.7% formaldehyde in 100 mM PIPES at pH 6.9, 10 mM EGTA, 1 mM MgCl2and 0.2% Triton X-100 at room temperature (or on ice, for cold-treatment experiments) for 10 min. Cells were blocked with 2% bovine serum albumin and 0.1% Triton-X in TBS for 15 min. Antibodies were diluted in the same medium. DNA was stained with Hoechst 33342 (Sigma).

Images were acquired as Z-stacks with 0.2 µm spacing using a 100×, 1.35 NA objective on a DeltaVision Image Restoration Microscope (Applied Precision Instruments and Olympus) and processed by iterative constrained deconvolution (SoftWoRx, Applied Precision Instruments). Images shown are maximal intensity projections of the Z-stacks that were cropped and processed using ImageJ (NIH). Magnified optical sections (insets) show individual kinetochores more clearly. Image analysis was performed using SoftWoRx or ImageJ (NIH) software.

For chromosome spreads, cells were arrested in nocodazole (1 µg ml-1) for 60 min, harvested by trypsinization, incubated in 0.0075 M KCl for 30 min and spun in a cytospin at 1000 r.p.m. for 1 min before processing for immunofluorescence as above.

Small-molecule inhibition treatments

For microtubule depolymerization, cells were incubated in 1 µg ml-1 nocodazole at 37 °C for 45 min before fixation. For cold treatment, cells were incubated with 10 µM MG132 for 2 h and then incubated in ice-cold L-15 medium (Invitrogen) on ice for 10 min before fixation. For inhibition of Aurora B activity, before fixation, cells were incubated in 50 nM hesperadin for 90 min, 2 µM ZM447439 for 60 min, or equivalent amounts of DMSO for the respective intervals, at 37 °C. For inhibition of Mps1 activity, cells were incubated in 10 µM Mps1-IN-1 (a kind gift from N. Gray, Harvard Medical School, Boston, MA) or 500 nM reversine (Cayman Chemicals) for 2 hours. For Plk-1 inhibition, cells were incubated in 80 nM BI2536 for 90 min before fixation. For all instances were cells were counted, DNA (stained with Hoechst stain) and spindle morphology were used to determine cell cycle stage.

For analysis of the effects on ciliobrevin compounds on the spindle, cells were incubated in medium containing 10 µM MG132 for 90 min. The medium was then exchanged with DMEM containing 0.5% (v/v) calf serum, 10 µM MG132, and either 50 µM of the indicated benzoyl dihydroquinazolinones or an equivalent amount of the DMSO vehicle, and the cells were cultured for an additional 60 min at 37 °C. For cold-treatment experiments, the cells were incubated on ice, and the medium was exchanged with ice-cold DMEM containing 0.5% (v/v) calf serum, 10 µM MG132, and either 50 µM of the indicated compounds or an equivalent amount of the DMSO vehicle.

To examine the localization of p150^{Glued}, ZW10, and CENP-E, NIH-3T3 cells were incubated for 45 min with DMEM containing 0.5% fetal bovine serum and either 50 µM ciliobrevin D, 50 µM analog 2, or an equivalent amount of DMSO. The cells were then incubated in medium that also contained 1 µg/mL nocodazole (and the respective compounds/DMSO) for another 45 min. The cells were fixed as above.

p150^{Glued} localization in cells with intact microtubules was also examined by culturing NIH-3T3 cells in DMEM containing 10% fetal bovine serum and 10 µM MG132 for 90 min. The medium was then exchanged with DMEM containing 0.5% (v/v) fetal bovine serum, 10 µM MG132, and 50 µM ciliobrevin D or an equivalent amount of DMSO. The cells were then fixed and processed for immunostaining as above. The anti-p150^{Glued} and CREST antibodies were incubated overnight at 4 °C; all other antibodies were incubated for 1 hour at room temperature.

Live imaging

Cells were grown on 22 mm × 22 mm glass coverslips (Fisher Scientific) coated with poly-D-lysine (Sigma) and imaged one day or two days after transfection (with mCherry-Mis12-Mad1 or mCh-H2B-Mad1, respectively), by mounting in Rose chambers and using L-15 medium without phenol-red (Invitrogen), at 35–37 °C. Images were acquired using a Nikon TE2000 confocal microscope equipped using a Plan Apochromat 100X/1.4 NA oil-immersion objective and a PerkinElmer Wallac UltraView confocal head, an argon ion laser (Solamere) and Metamorph software (Universal Imaging). GFP and mCherry fluorescences were obtained with 488-nm and 568-nm excitation filters, respectively.

Confocal stacks were acquired with 0.5 µm spacing. Images were analyzed and processed with either Metamorph or ImageJ software. Images shown are maximal projections of the Z-stacks.

For Aurora B inhibition experiments, hesperadin or DMSO were washed into the chamber by exchanging the L-15 medium (10% fetal bovine serum) with the compounds at the aforementioned concentrations. For live-imaging studies of ciliobrevin effects wash-in experiments of mitotic cells were conducted by adding L-15 medium containing 0.5% fetal bovine serum and either 50 µM ciliobrevin D or an equivalent amount of DMSO. In washout experiments, the compound or solvent vehicle was removed by exchanging the medium twice with L-15 containing 10% FBS. To study the effects of ciliobrevins on MG132-arrested cells, the GFP-tubulin-expressing cells were incubated in L-15 medium containing 10% fetal bovine serum and 10 µM MG132. Thirty minutes later, the medium was exchanged to L-15 with 0.5% fetal bovine serum, 10 µM MG132, and either 30 uM of the indicated compounds or an equivalent amount of DMSO. Fifty minutes after the wash-in, the compounds were washed out by exchanging the medium twice with L-15 containing 10% fetal bovine serum and 10 µM MG132.

Fluorescence-signal quantification

To quantify interphase microtubule intensities, the GFP-tubulin-expressing NIH-3T3 cells were incubated with L-15 medium containing 0.5% fetal bovine serum and either 30 µM ciliobrevin D or an equivalent amount of DMSO for 15 min. Interphase cells were identified by DIC microscopy, and an 8- to 12-plane Z-stack (0.2 µm step size)

encompassing the network of cytoplasmic microtubules was acquired for the GFP channel. For ciliobrevin D experiments, a mitotic cell was imaged before the interphase cells, to ensure microtubule depolymerization had occurred. Ciliobrevin D or DMSO was washed out by exchanging the medium twice with L-15 containing 10% fetal bovine serum 35-50 min after the initial addition of compound or solvent vehicle. The cells were then re-visited and imaged as before, approximately 15 min after the wash-out (at which time the microtubule density of the imaged mitotic cells had recovered). To quantify microtubule intensity in individual cells before and after ciliobrevin/DMSO wash-out, planes of the Z-stack that showed maximal microtubule intensity were summed, and GFP intensity was measured for a region of interest in the cell cytoplasmic and in a nearby background area of the same size. The background-corrected intensity was calculated as (GFP-tubulin fluorescence – background fluorescence)/background fluorescence, and the corresponding ratio of post- and pre-wash-out intensities was calculated for each cell.

To quantify intensity of mCherry, $p150^{Glued}$, ZW10 or CENP-E signal at individual kinetochores, CREST signal from deconvolved Z-stacks was used to identify individual kinetochores. A region of interest (ROI) was drawn at the corresponding position for the mCherry channel, at the identified planes, and the integrated density of the sum of the ROIs was calculated. To account for background fluorescence, the corrected fluorescence was calculated as in ref.15: briefly, by measuring the fluorescence of a slightly larger box and scaling the “inner” fluorescence to the ratio of the areas. The same treatment was done for the corresponding CREST staining, and the corrected

mCherry fluorescence was normalized to the corrected CREST fluorescence. An analogous method was used to measure the mCherry or GFP fluorescence of whole cells or spindles, after the summation of fluorescence of individual planes of a Z-stack acquired by live imaging.

Appendix methods

Rapamycin-dependent, FRB-FKBP-mediated Mis12-Mad1 dimerization

The pMSCV Mis12-mCherry-FRB construct was a gift from Dr Lei Tan (Kapoor laboratory). The pMSCV FKBP-Mad1F10-GFP construct was produced by PCR overlap cloning, followed by Gateway cloning, using standard or manufacturer's procedures. HeLa stable cell lines of either construct or both constructs together were produced by retroviral infection, followed by selection with puromycin (and subsequently hygromycin, for the double cell line). For the single cell lines, the remaining construct was transiently transfected using Fugene HD (Roche Diagnostics). Subsequent treatments were carried out 24 or 48 hours after transfection (both options were examined fully in different experiments). To examine dimerization of FKBP-Mad1F10-GFP and Mis12-mCherry-FRB, cells were arrested in metaphase with 10 µM MG132 for 30 min and metaphase cells were localized and imaged live with GFP and mCherry channels to obtain respective Z-stacks. The medium was then exchanged to one containing 10 µM MG132 and 20 nM rapamycin and the cells were re-visited and imaged at 30 min intervals for over 5 hours.

Shield1-dependent FKBP*-Mis12-Mad1 fusion protein level control

The pMSCV FKBP*-GFP and mCherry-FKBP*-Mis12-Mad1 constructs were produced by PCR overlap cloning, followed by Gateway cloning, using standard or manufacturer's procedures. The original FKBP* plasmid was a gift from Dr Matthew Pratt (USC). HeLa and RPE-1 stable cell lines of the GFP construct were produced by retroviral infection, followed by selection with puromycin. For mCherry-FKBP*-Mis12-Mad1, HeLa cells were transiently transfected using Fugene HD; subsequent treatments were done 24 hours after transfection. To examine the kinetics of Shield-dependent rescue of FKBP*-GFP or mCherry-FKBP*-Mis12-Mad1, cells were arrested in mitosis by incubation with 1ug/ml nocodazole for 30-45 min, and mitotic and interphase cells were localized and imaged live with DIC and GFP channels. The medium was then exchanged to one containing 1ug/ml nocodazole and 1 µM Shield (Clontech; or an equivalent amount of ethanol, as control) and the cells were re-visited and imaged at hourly intervals for 5 hours. To examine the kinetics of FKBP*-GFP degradation upon Shield removal, cells were incubated in 1 µM Shield for 16 or 22 hours, they were then incubated in a medium containing 1 µM Shield and 1ug/ml nocodazole for 1 hour, at which point mitotic and interphase cells were localized and imaged live with DIC and GFP channels. After this initial imaging, the medium was exchanged to one containing only 1 µM Shield and the cells were re-visited and imaged at hourly intervals for 7 hours. Fluorescence intensity of GFP rescue or degradation was measured by calculating the intensity of GFP in the whole cell and then corrected for background as described above.

Bibliography

Abrieu, A., Magnaghi-Jaulin, L., Kahana, J.A., Peter, M., Castro, A., Vigneron, S., Lorca, T., Cleveland, D.W., and Labbe, J.C. (2001). Mps1 is a kinetochore-associated kinase essential for the vertebrate mitotic checkpoint. Cell *106*, 83-93.

Arasaki, K., Tani, K., Yoshimori, T., Stephens, D.J., and Tagaya, M. (2007). Nordihydroguaiaretic acid affects multiple dynein-dynactin functions in interphase and mitotic cells. Mol Pharmacol *71*, 454-460.

Arkin, M.R., and Wells, J.A. (2004). Small-molecule inhibitors of protein-protein interactions: progressing towards the dream. Nat Rev Drug Discov *3*, 301-317.

Armstrong, C.M., and Goldberg, D.E. (2007). An FKBP destabilization domain modulates protein levels in Plasmodium falciparum. Nat Methods *4*, 1007-1009.

Bader, J.R., and Vaughan, K.T. (2010). Dynein at the kinetochore: Timing, Interactions and Functions. Semin Cell Dev Biol *21*, 269-275.

Bakhoum, S.F., Thompson, S.L., Manning, A.L., and Compton, D.A. (2009). Genome stability is ensured by temporal control of kinetochore-microtubule dynamics. Nat Cell Biol *11*, 27-35.

Banaszynski, L.A., Chen, L.C., Maynard-Smith, L.A., Ooi, A.G., and Wandless, T.J. (2006). A rapid, reversible, and tunable method to regulate protein function in living cells using synthetic small molecules. Cell *126*, 995-1004.

Banaszynski, L.A., Liu, C.W., and Wandless, T.J. (2005). Characterization of the FKBP.rapamycin.FRB ternary complex. J Am Chem Soc *127*, 4715-4721.

Banaszynski, L.A., Sellmyer, M.A., Contag, C.H., Wandless, T.J., and Thorne, S.H. (2008). Chemical control of protein stability and function in living mice. Nat Med *14*, 1123-1127.

Barford, D. (2012). Structural insights into anaphase-promoting complex function and mechanism. Philos Trans R Soc Lond B Biol Sci *366*, 3605-3624.

Barnhart, E.L., Dorer, R.K., Murray, A.W., and Schuyler, S.C. (2011). Reduced Mad2 expression keeps relaxed kinetochores from arresting budding yeast in mitosis. Mol Biol Cell *22*, 2448-2457.

Blacque, O.E., Cevik, S., and Kaplan, O.I. (2008). Intraflagellar transport: from molecular characterisation to mechanism. Front Biosci *13*, 2633-2652.

Bouchard, P., Penningroth, S.M., Cheung, A., Gagnon, C., and Bardin, C.W. (1981). erythro-9-[3-(2-Hydroxynonyl)]adenine is an inhibitor of sperm motility that blocks dynein ATPase and protein carboxylmethylase activities. Proc Natl Acad Sci U S A *78*, 1033-1036.

Bullock, S.L., Nicol, A., Gross, S.P., and Zicha, D. (2006). Guidance of bidirectional motor complexes by mRNA cargoes through control of dynein number and activity. Curr Biol *16*, 1447-1452.

Burke, D.J., and Stukenberg, P.T. (2008). Linking kinetochore-microtubule binding to the spindle checkpoint. Developmental Cell *14*, 474-479.

Canman, J.C., Sharma, N., Straight, A., Shannon, K.B., Fang, G., and Salmon, E.D. (2002). Anaphase onset does not require the microtubule-dependent depletion of kinetochore and centromere-binding proteins. J Cell Sci *115*, 3787-3795.

Carter, A.P., Cho, C., Jin, L., and Vale, R.D. (2011). Crystal structure of the dynein motor domain. Science *331*, 1159-1165.

Chao, W.C., Kulkarni, K., Zhang, Z., Kong, E.H., and Barford, D. (2012). Structure of the mitotic checkpoint complex. Nature *484*, 208-213.

Cheeseman, I.M., and Desai, A. (2008). Molecular architecture of the kinetochore-microtubule interface. Nat Rev Mol Cell Biol *9*, 33-46.

Cheeseman, I.M., Niessen, S., Anderson, S., Hyndman, F., Yates, J.R., 3rd, Oegema, K., and Desai, A. (2004). A conserved protein network controls assembly of the outer kinetochore and its ability to sustain tension. Genes Dev *18*, 2255-2268.

Chen, R.H., Waters, J.C., Salmon, E.D., and Murray, A.W. (1996). Association of spindle assembly checkpoint component XMAD2 with unattached kinetochores. Science *274*, 242-246.

Chen, R.H., Shevchenko, A., Mann, M., and Murray, A.W. (1998). Spindle checkpoint protein Xmad1 recruits Xmad2 to unattached kinetochores. J Cell Biol *143*, 283-295.

Chen, R.H., Brady, D.M., Smith, D., Murray, A.W., and Hardwick, K.G. (1999). The spindle checkpoint of budding yeast depends on a tight complex between the Mad1 and Mad2 proteins. Mol Biol Cell *10*, 2607-2618.

Chou, T.F., Brown, S.J., Minond, D., Nordin, B.E., Li, K., Jones, A.C., Chase, P., Porubsky, P.R., Stoltz, B.M., Schoenen, F.J*., et al.* (2011). Reversible inhibitor of p97, DBeQ, impairs both ubiquitin-dependent and autophagic protein clearance pathways. Proc Natl Acad Sci U S A *108*, 4834-4839.

Chubb, J.R., Boyle, S., Perry, P., and Bickmore, W.A. (2002). Chromatin motion is constrained by association with nuclear compartments in human cells. Curr Biol *12*, 439-445.

Chung, E., and Chen, R.H. (2002). Spindle checkpoint requires Mad1-bound and Mad1-free Mad2. Mol Biol Cell *13*, 1501-1511.

De Antoni, A., Pearson, C.G., Cimini, D., Canman, J.C., Sala, V., Nezi, L., Mapelli, M., Sironi, L., Faretta, M., Salmon, E.D*., et al.* (2005). The Mad1/Mad2 complex as a template for Mad2 activation in the spindle assembly checkpoint. Curr Biol *15*, 214-225.

DeLuca, J.G., Howell, B.J., Canman, J.C., Hickey, J.M., Fang, G., and Salmon, E.D. (2003). Nuf2 and Hec1 are required for retention of the checkpoint proteins Mad1 and Mad2 to kinetochores. Curr Biol *13*, 2103-2109.

DeLuca, J.G., and Musacchio, A. (2012). Structural organization of the kinetochore-microtubule interface. Curr Opin Cell Biol *24*, 48-56.

DeWitt, M.A., Chang, A.Y., Combs, P.A., and Yildiz, A. (2012). Cytoplasmic dynein moves through uncoordinated stepping of the AAA+ ring domains. Science *335*, 221-225.

Ditchfield, C., Johnson, V.L., Tighe, A., Ellston, R., Haworth, C., Johnson, T., Mortlock, A., Keen, N., and Taylor, S.S. (2003). Aurora B couples chromosome alignment with anaphase by targeting BubR1, Mad2, and Cenp-E to kinetochores. J Cell Biol *161*, 267-280.

Dujardin, D.L., and Vallee, R.B. (2002). Dynein at the cortex. Curr Opin Cell Biol *14*, 44-49.

Emanuele, M.J., Lan, W., Jwa, M., Miller, S.A., Chan, C.S., and Stukenberg, P.T. (2008). Aurora B kinase and protein phosphatase 1 have opposing roles in modulating kinetochore assembly. J Cell Biol *181*, 241-254.

Erzberger, J.P., and Berger, J.M. (2006). Evolutionary relationships and structural mechanisms of AAA+ proteins. Annu Rev Biophys Biomol Struct *35*, 93-114.

Fang, G. (2002). Checkpoint protein BubR1 acts synergistically with Mad2 to inhibit anaphase-promoting complex. Mol Biol Cell *13*, 755-766.

Faulkner, N.E., Dujardin, D.L., Tai, C.Y., Vaughan, K.T., O'Connell, C.B., Wang, Y., and Vallee, R.B. (2000). A role for the lissencephaly gene LIS1 in mitosis and cytoplasmic dynein function. Nat Cell Biol *2*, 784-791.

Firestone, A.J., Weinger, J.S., Maldonado, M., Barlan, K., Langston, L.D., O'Donnell, M., Gelfand, V.I., Kapoor, T.M., and Chen, J.K. (2012). Small-molecule inhibitors of the AAA+ ATPase motor cytoplasmic dynein. Nature *484*, 125-129.

Gaetz, J., and Kapoor, T.M. (2004). Dynein/dynactin regulate metaphase spindle length by targeting depolymerizing activities to spindle poles. J Cell Biol *166*, 465-471.

Goetz, S.C., and Anderson, K.V. (2010). The primary cilium: a signaling centre during vertebrate development. Nat Rev Genet *11*, 331-344.

Gorbsky, G.J., Sammak, P.J., and Borisy, G.G. (1987). Chromosomes move poleward in anaphase along stationary microtubules that coordinately disassemble from their kinetochore ends. J Cell Biol *104*, 9-18.

Griffis, E.R., Stuurman, N., and Vale, R.D. (2007). Spindly, a novel protein essential for silencing the spindle assembly checkpoint, recruits dynein to the kinetochore. J Cell Biol *177*, 1005-1015.

Grill, S.W., and Hyman, A.A. (2005). Spindle positioning by cortical pulling forces. Dev Cell *8*, 461-465.

Hardwick, K.G., Johnston, R.C., Smith, D.L., and Murray, A.W. (2000). MAD3 encodes a novel component of the spindle checkpoint which interacts with Bub3p, Cdc20p, and Mad2p. J Cell Biol *148*, 871-882.

Hardwick, K.G., and Murray, A.W. (1995). Mad1p, a phosphoprotein component of the spindle assembly checkpoint in budding yeast. J Cell Biol *131*, 709-720.

Hardwick, K.G., Weiss, E., Luca, F.C., Winey, M., and Murray, A.W. (1996). Activation of the budding yeast spindle assembly checkpoint without mitotic spindle disruption. Science *273*, 953-956.

Hartwell, L.H., and Weinert, T.A. (1989). Checkpoints: controls that ensure the order of cell cycle events. Science *246*, 629-634.

Hauf, S., Cole, R.W., LaTerra, S., Zimmer, C., Schnapp, G., Walter, R., Heckel, A., van Meel, J., Rieder, C.L., and Peters, J.M. (2003). The small molecule Hesperadin reveals a role for Aurora B in correcting kinetochore-microtubule attachment and in maintaining the spindle assembly checkpoint. J Cell Biol *161*, 281-294.

Hegemann, B., Hutchins, J.R., Hudecz, O., Novatchkova, M., Rameseder, J., Sykora, M.M., Liu, S., Mazanek, M., Lenart, P., Heriche, J.K., et al. (2011). Systematic phosphorylation analysis of human mitotic protein complexes. Sci Signal 4, rs12.

Hengeveld, R.C., Hertz, N.T., Vromans, M.J., Zhang, C., Burlingame, A.L., Shokat, K.M., and Lens, S.M. (2012). Development of a chemical genetic approach for human aurora B kinase identifies novel substrates of the chromosomal passenger complex. Mol Cell Proteomics 11, 47-59.

Herm-Gotz, A., Agop-Nersesian, C., Munter, S., Grimley, J.S., Wandless, T.J., Frischknecht, F., and Meissner, M. (2007). Rapid control of protein level in the apicomplexan Toxoplasma gondii. Nat Methods *4*, 1003-1005.

Hoffman, D.B., Pearson, C.G., Yen, T.J., Howell, B.J., and Salmon, E.D. (2001). Microtubule-dependent changes in assembly of microtubule motor proteins and mitotic spindle checkpoint proteins at PtK1 kinetochores. Mol Biol Cell *12*, 1995-2009.

Holland, A.J., and Cleveland, D.W. (2012). Losing balance: the origin and impact of aneuploidy in cancer. EMBO Rep *13*, 501-514.

Holzbaur, E.L., Hammarback, J.A., Paschal, B.M., Kravit, N.G., Pfister, K.K., and Vallee, R.B. (1991). Homology of a 150K cytoplasmic dynein-associated polypeptide with the Drosophila gene Glued. Nature *351*, 579-583.

Hook, P., and Vallee, R.B. (2006). The dynein family at a glance. J Cell Sci *119*, 4369-4371.

Howell, B.J., Hoffman, D.B., Fang, G., Murray, A.W., and Salmon, E.D. (2000). Visualization of Mad2 dynamics at kinetochores, along spindle fibers, and at spindle poles in living cells. J Cell Biol *150*, 1233-1250.

Howell, B.J., McEwen, B.F., Canman, J.C., Hoffman, D.B., Farrar, E.M., Rieder, C.L., and Salmon, E.D. (2001). Cytoplasmic dynein/dynactin drives kinetochore protein transport to the spindle poles and has a role in mitotic spindle checkpoint inactivation. J Cell Biol *155*, 1159-1172.

Howell, B.J., Moree, B., Farrar, E.M., Stewart, S., Fang, G., and Salmon, E.D. (2004). Spindle checkpoint protein dynamics at kinetochores in living cells. Curr Biol *14*, 953-964.

Hoyt, M.A., Totis, L., and Roberts, B.T. (1991). S. cerevisiae genes required for cell cycle arrest in response to loss of microtubule function. Cell *66*, 507-517.

Huangfu, D., and Anderson, K.V. (2005). Cilia and Hedgehog responsiveness in the mouse. Proc Natl Acad Sci U S A *102*, 11325-11330.

Hughes, S.M., Vaughan, K.T., Herskovits, J.S., and Vallee, R.B. (1995). Molecular analysis of a cytoplasmic dynein light intermediate chain reveals homology to a family of ATPases. J Cell Sci *108 (Pt 1)*, 17-24.

Hunt, S.D., and Stephens, D.J. The role of motor proteins in endosomal sorting. Biochem Soc Trans *39*, 1179-1184.

Hunt, T., Nasmyth, K., and Novak, B. The cell cycle. Philos Trans R Soc Lond B Biol Sci *366*, 3494-3497.

Hyman, J. M., Firestone, A. J., Heine, V. M., Zhao, Y., Ocasio, C. A., Han, K., Sun, M., Rack, P. G., Sinha, S., Wu, *et. al.* (2009). Small-molecule inhibitors reveal multiple strategies for Hedgehog pathway blockade. Proc Natl Acad Sci U S A *106*, 14132-7.

Inoue, M., Arasaki, K., Ueda, A., Aoki, T., and Tagaya, M. (2008). N-terminal region of ZW10 serves not only as a determinant for localization but also as a link with dynein function. Genes Cells *13*, 905-914.

Iouk, T., Kerscher, O., Scott, R.J., Basrai, M.A., and Wozniak, R.W. (2002). The yeast nuclear pore complex functionally interacts with components of the spindle assembly checkpoint. J Cell Biol *159*, 807-819.

Janicki, S.M., Tsukamoto, T., Salghetti, S.E., Tansey, W.P., Sachidanandam, R., Prasanth, K.V., Ried, T., Shav-Tal, Y., Bertrand, E., Singer, R.H.*, et al.* (2004). From silencing to gene expression: real-time analysis in single cells. Cell *116*, 683-698.

Janke, C., Ortiz, J., Lechner J., Shevchenko A., Shevchenko A., Magiera A.M., Schramm C. and Schiebel E. (2001). The budding yeast proteins Spc24p and Spc25p interact with Ndc80p and Nuf2p at the kinetochore and are important for kinetochore clustering and checkpoint control. EMBO J *20*, 777 – 791.

Janssen, A., Medema, R.H. (2011). Mitosis as an anti-cancer target. Oncogene *30*, 2799-2809.

Jelluma, N., Dansen, T.B., Sliedrecht, T., Kwiatkowski, N.P., and Kops, G.J. (2010). Release of Mps1 from kinetochores is crucial for timely anaphase onset. J Cell Biol *191*, 281-290.

Jiang, J., and Hui, C.C. (2008). Hedgehog signaling in development and cancer. Dev Cell *15*, 801-812.

Kallio, M.J., McCleland, M.L., Stukenberg, P.T., and Gorbsky, G.J. (2002). Inhibition of aurora B kinase blocks chromosome segregation, overrides the spindle checkpoint, and perturbs microtubule dynamics in mitosis. Curr Biol *12*, 900-905.

Kang, J., Yang, M., Li, B., Qi, W., Zhang, C., Shokat, K.M., Tomchick, D.R., Machius, M., and Yu, H. (2008). Structure and substrate recruitment of the human spindle checkpoint kinase Bub1. Mol Cell *32*, 394-405.

Kang, J., and Yu, H. (2009). Kinase signaling in the spindle checkpoint. J Biol Chem *284*, 15359-15363.

Kardon, J.R., and Vale, R.D. (2009). Regulators of the cytoplasmic dynein motor. Nat Rev Mol Cell Biol *10*, 854-865.

Karess, R. (2005). Rod-ZW10-Zwilch: a key player in the spindle checkpoint. Trends Cell Biol *15*, 386-392.

Kim, J., Kato, M., and Beachy, P.A. (2009). Gli2 trafficking links Hedgehog-dependent activation of Smoothened in the primary cilium to transcriptional activation in the nucleus. Proc Natl Acad Sci U S A *106*, 21666-21671.

Kim, S., Zaghloul, N.A., Bubenshchikova, E., Oh, E.C., Rankin, S., Katsanis, N., Obara, T., and Tsiokas, L. (2011). Nde1-mediated inhibition of ciliogenesis affects cell cycle re-entry. Nat Cell Biol *13*, 351-360.

King, E.M., Rachidi, N., Morrice, N., Hardwick, K.G., and Stark, M.J. (2007). Ipl1p-dependent phosphorylation of Mad3p is required for the spindle checkpoint response to lack of tension at kinetochores. Genes Dev *21*, 1163-1168.

King, S.J., Brown, C.L., Maier, K.C., Quintyne, N.J., and Schroer, T.A. (2003). Analysis of the dynein-dynactin interaction *in vitro* and *in vivo*. Mol Biol Cell *14*, 5089-5097.

King, S.M. (2012). Integrated control of axonemal dynein AAA(+) motors. J Struct Biol.

Kiyomitsu, T., and Cheeseman, I.M. (2012). Chromosome- and spindle-pole-derived signals generate an intrinsic code for spindle position and orientation. Nat Cell Biol *14*, 311-317.

Kline, S.L., Cheeseman, I.M., Hori, T., Fukagawa, T., & Desai, A. (2006). The human Mis 12 complex is required for kinetochore assembly and proper chromosome segregation. J Cell Biol *173*, 9-17.

Kon, T., Nishiura, M., Ohkura, R., Toyoshima, Y.Y., and Sutoh, K. (2004). Distinct functions of nucleotide-binding/hydrolysis sites in the four AAA modules of cytoplasmic dynein. Biochemistry *43*, 11266-11274.

Kon, T., Oyama, T., Shimo-Kon, R., Imamula, K., Shima, T., Sutoh, K., and Kurisu, G. (2012). The 2.8 A crystal structure of the dynein motor domain. Nature *484*, 345-350.

Koshland, D.E., Mitchison, T.J., and Kirschner, M.W. (1988). Polewards chromosome movement driven by microtubule depolymerization *in vitro*. Nature *331*, 499-504.

Kulukian, A., Han, J.S., and Cleveland, D.W. (2009). Unattached kinetochores catalyze production of an anaphase inhibitor that requires a Mad2 template to prime Cdc20 for BubR1 binding. Dev Cell *16*, 105-117.

Kwiatkowski, N., Jelluma, N., Filippakopoulos, P., Soundararajan, M., Manak, M.S., Kwon, M., Choi, H.G., Sim, T., Deveraux, Q.L., Rottmann, S*., et al.* (2010). Small-molecule kinase inhibitors provide insight into Mps1 cell cycle function. Nat Chem Biol *6*, 359-368.

Lad, L., Lichtsteiner, S., Hartman, J.J., Wood, K.W., and Sakowicz, R. (2009). Kinetic analysis of Mad2-Cdc20 formation: conformational changes in Mad2 are catalyzed by a C-Mad2-ligand complex. Biochemistry *48*, 9503-9515.

Lan, W., and Cleveland, D.W. (2010). A chemical tool box defines mitotic and interphase roles for Mps1 kinase. J Cell Biol *190*, 21-24.

Lau, D.T., and Murray, A.W. (2012). Mad2 and Mad3 cooperate to arrest budding yeast in mitosis. Curr Biol *22*, 180-190.

Lee, S.H., Sterling, H., Burlingame, A., and McCormick, F. (2008). Tpr directly binds to Mad1 and Mad2 and is important for the Mad1-Mad2-mediated mitotic spindle checkpoint. Genes Dev *22*, 2926-2931.

Li, A., Saito, M., Chuang, J.Z., Tseng, Y.Y., Dedesma, C., Tomizawa, K., Kaitsuka, T., and Sung, C.H. (2011). Ciliary transition zone activation of phosphorylated Tctex-1 controls ciliary resorption, S-phase entry and fate of neural progenitors. Nat Cell Biol *13*, 402-411.

Li, R., and Murray, A.W. (1991). Feedback control of mitosis in budding yeast. Cell *66*, 519-531.

Li, Y., and Benezra, R. (1996). Identification of a human mitotic checkpoint gene: hsMAD2. Science *274*, 246-248.

Liu, D., Vader, G., Vromans, M.J., Lampson, M.A., and Lens, S.M. (2009). Sensing chromosome bi-orientation by spatial separation of aurora B kinase from kinetochore substrates. Science *323*, 1350-1353.

Liu, D., Vleugel, M., Backer, C.B., Hori, T., Fukagawa, T., Cheeseman, I.M., and Lampson, M.A. (2010). Regulated targeting of protein phosphatase 1 to the outer kinetochore by KNL1 opposes Aurora B kinase. J Cell Biol *188*, 809-820.

Luo, X., Tang, Z., Xia, G., Wassmann, K., Matsumoto, T., Rizo, J., and Yu, H. (2004). The Mad2 spindle checkpoint protein has two distinct natively folded states. Nat Struct Mol Biol *11*, 338-345.

Luo, X., and Yu, H. (2008). Protein metamorphosis: the two-state behavior of Mad2. Structure *16*, 1616-1625.

Maciejowski, J., George, K.A., Terret, M.E., Zhang, C., Shokat, K.M., and Jallepalli, P.V. (2010). Mps1 directs the assembly of Cdc20 inhibitory complexes during interphase and mitosis to control M phase timing and spindle checkpoint signaling. J Cell Biol 190, 89-100.

Maldonado, M., and Kapoor, T.M. (2011). Constitutive Mad1 targeting to kinetochores uncouples checkpoint signaling from chromosome biorientation. Nat Cell Biol *13*, 475-482.

Mansfeld, J., Collin, P., Collins, M.O., Choudhary, J.S., and Pines, J. (2011). APC15 drives the turnover of MCC-CDC20 to make the spindle assembly checkpoint responsive to kinetochore attachment. Nat Cell Biol *13*, 1234-1243.

Mao, Y., Desai, A., and Cleveland, D.W. (2005). Microtubule capture by CENP-E silences BubR1-dependent mitotic checkpoint signaling. J Cell Biol *170*, 873-880.

Mapelli, M., Massimiliano, L., Santaguida, S., and Musacchio, A. (2007). The Mad2 conformational dimer: structure and implications for the spindle assembly checkpoint. Cell *131*, 730-743.

Martin-Lluesma, S., Stucke, V.M., and Nigg, E.A. (2002). Role of Hec1 in spindle checkpoint signaling and kinetochore recruitment of Mad1/Mad2. Science *297*, 2267-2270.

Meadows, J.C., Shepperd, L.A., Vanoosthuyse, V., Lancaster, T.C., Sochaj, A.M., Buttrick, G.J., Hardwick, K.G., and Millar, J.B. (2011). Spindle checkpoint silencing requires association of PP1 to both Spc7 and kinesin-8 motors. Dev Cell *20*, 739-750.

Meraldi, P., Draviam, V.M., and Sorger, P.K. (2004a). Timing and checkpoints in the regulation of mitotic progression. Dev Cell *7*, 45-60.

Meraldi, P., Honda, R., and Nigg, E.A. (2004b). Aurora kinases link chromosome segregation and cell division to cancer susceptibility. Curr Opin Genet Dev *14*, 29-36.

Merdes, A., Heald, R., Samejima, K., Earnshaw, W.C., and Cleveland, D.W. (2000). Formation of spindle poles by dynein/dynactin-dependent transport of NuMA. J Cell Biol *149*, 851-862.

Merdes, A., Ramyar, K., Vechio, J.D., and Cleveland, D.W. (1996). A complex of NuMA and cytoplasmic dynein is essential for mitotic spindle assembly. Cell *87*, 447-458.

Mitchison, T., Evans, L., Schulze, E., and Kirschner, M. (1986). Sites of microtubule assembly and disassembly in the mitotic spindle. Cell *45*, 515-527.

Moore, J.K., Stuchell-Brereton, M.D., and Cooper, J.A. (2009). Function of dynein in budding yeast: mitotic spindle positioning in a polarized cell. Cell Motil Cytoskeleton *66*, 546-555.

Morgan, D.O. (2008a). SnapShot: cell-cycle regulators I. Cell *135*, 764-764 e761.

Morgan, D.O. (2008b). SnapShot: Cell-cycle regulators II. Cell *135*, 974-974 e971.

Murray, A.W. (2011). A brief history of error. Nat Cell Biol *13*, 1178-1182.

Musacchio, A. (2011). Spindle assembly checkpoint: the third decade. Philos Trans R Soc Lond B Biol Sci *366*, 3595-3604.

Musacchio, A., and Salmon, E.D. (2007). The spindle-assembly checkpoint in space and time. Nat Rev Mol Cell Biol *8*, 379-393.

Nilsson, J., Yekezare, M., Minshull, J., and Pines, J. (2008). The APC/C maintains the spindle assembly checkpoint by targeting Cdc20 for destruction. Nat Cell Biol *10*, 1411-1420.

Ogura, T., and Wilkinson, A.J. (2001). AAA+ superfamily ATPases: common structure--diverse function. Genes Cells *6*, 575-597.

Oppermann, F.S., Grundner-Culemann, K., Kumar, C., Gruss, O.J., Jallepalli, P.V., and Daub, H. (2012). Combination of chemical genetics and phosphoproteomics for kinase signaling analysis enables confident identification of cellular downstream targets. Mol Cell Proteomics 11, O111 012351.Palframan, W.J., Meehl, J.B.,

Jaspersen, S.L., Winey, M., and Murray, A.W. (2006). Anaphase inactivation of the spindle checkpoint. Science *313*, 680-684.

Pazour, G.J., Wilkerson, C.G., and Witman, G.B. (1998). A dynein light chain is essential for the retrograde particle movement of intraflagellar transport (IFT). J Cell Biol *141*, 979-992.

Petersen, J., and Hagan, I.M. (2003). S. pombe aurora kinase/survivin is required for chromosome condensation and the spindle checkpoint attachment response. Curr Biol *13*, 590-597.

Petronczki, M., Lenart, P., and Peters, J.M. (2008). Polo on the Rise-from Mitotic Entry to Cytokinesis with Plk1. Dev Cell *14*, 646-659.

Pfau, S.J., and Amon, A. (2012). Chromosomal instability and aneuploidy in cancer: from yeast to man. EMBO Rep *13*, 515-527.

Pinsky, B.A., and Biggins, S. (2005). The spindle checkpoint: tension versus attachment. Trends Cell Biol *15*, 486-493.

Pinsky, B.A., Kung, C., Shokat, K.M., and Biggins, S. (2006). The Ipl1-Aurora protein kinase activates the spindle checkpoint by creating unattached kinetochores. Nat Cell Biol *8*, 78-83.

Pinsky, B.A., Nelson, C.R., and Biggins, S. (2009). Protein phosphatase 1 regulates exit from the spindle checkpoint in budding yeast. Curr Biol *19*, 1182-1187.

Qiu, W., Derr, N.D., Goodman, B.S., Villa, E., Wu, D., Shih, W., and Reck-Peterson, S.L. (2012). Dynein achieves processive motion using both stochastic and coordinated stepping. Nat Struct Mol Biol *19*, 193-200.

Reddy, S.K., Rape, M., Margansky, W.A., and Kirschner, M.W. (2007). Ubiquitination by the anaphase-promoting complex drives spindle checkpoint inactivation. Nature *446*, 921-925.

Rieder, C.L., Cole, R.W., Khodjakov, A., and Sluder, G. (1995). The checkpoint delaying anaphase in response to chromosome monoorientation is mediated by an inhibitory signal produced by unattached kinetochores. J Cell Biol *130*, 941-948.

Rieder, C.L., Schultz, A., Cole, R., and Sluder, G. (1994). Anaphase onset in vertebrate somatic cells is controlled by a checkpoint that monitors sister kinetochore attachment to the spindle. J Cell Biol *127*, 1301-1310.

Rosenberg, J.S., Cross, F.R., and Funabiki, H. (2011). KNL1/Spc105 recruits PP1 to silence the spindle assembly checkpoint. Curr Biol *21*, 942-947.

Santaguida, S., and Musacchio, A. (2009). The life and miracles of kinetochores. EMBO J *28*, 2511-2531.

Santaguida, S., Tighe, A., D'Alise, A.M., Taylor, S.S., and Musacchio, A. (2010). Dissecting the role of MPS1 in chromosome biorientation and the spindle checkpoint through the small molecule inhibitor reversine. J Cell Biol *190*, 73-87.

Santaguida, S., Vernieri, C., Villa, F., Ciliberto, A., and Musacchio, A. (2011). Evidence that Aurora B is implicated in spindle checkpoint signaling independently of error correction. EMBO J *30*, 1508-1519.

Saurin, A.T., van der Waal, M.S., Medema, R.H., Lens, S.M., and Kops, G.J. (2011). Aurora B potentiates Mps1 activation to ensure rapid checkpoint establishment at the onset of mitosis. Nat Commun *2*, 316.

Schmidt, H., Gleave, E.S., and Carter, A.P. (2012). Insights into dynein motor domain function from a 3.3-A crystal structure. Nat Struct Mol Biol *19*, 492-497.

Schroer, T.A. (2004). Dynactin. Annu Rev Cell Dev Biol *20*, 759-779.

Shah, J.V., Botvinick, E., Bonday, Z., Furnari, F., Berns, M., and Cleveland, D.W. (2004). Dynamics of centromere and kinetochore proteins; implications for checkpoint signaling and silencing. Curr Biol *14*, 942-952.

Shepperd, L.A., Meadows, J.C., Sochaj, A.M., Lancaster, T.C., Zou, J., Buttrick, G.J., Rappsilber, J., Hardwick, K.G., and Millar, J.B. (2012). Phosphodependent Recruitment of Bub1 and Bub3 to Spc7/KNL1 by Mph1 Kinase Maintains the Spindle Checkpoint. Curr Biol *22*, 891-899.

Simonetta, M., Manzoni, R., Mosca, R., Mapelli, M., Massimiliano, L., Vink, M., Novak, B., Musacchio, A., and Ciliberto, A. (2009). The influence of catalysis on mad2 activation dynamics. PLoS Biol *7*, e10.

Sironi L., Melixetian M., Faretta M., Prosperini E., Helin K., Musacchio A. (2001). Mad2 binding to Mad1 and Cdc20, rather than oligomerization, is required for spindle checkpoint. Embo J *20*, 6371-6382.

Sironi, L., Mapelli, M., Knapp, S., De Antoni, A., Jeang, K.T., and Musacchio, A. (2002). Crystal structure of the tetrameric Mad1-Mad2 core complex: implications of a 'safety belt' binding mechanism for the spindle checkpoint. EMBO J *21*, 2496-2506.

Soutoglou, E., Dorn, J.F., Sengupta, K., Jasin, M., Nussenzweig, A., Ried, T., Danuser, G., and Misteli, T. (2007). Positional stability of single double-strand breaks in mammalian cells. Nat Cell Biol *9*, 675-682.

Starr, D.A., Williams, B.C., Hays, T.S., and Goldberg, M.L. (1998). ZW10 helps recruit dynactin and dynein to the kinetochore. J Cell Biol *142*, 763-774.

Stehman, S.A., Chen, Y., McKenney, R.J., and Vallee, R.B. (2007). NudE and NudEL are required for mitotic progression and are involved in dynein recruitment to kinetochores. J Cell Biol *178*, 583-594.

Sudakin, V., Chan, G.K., and Yen, T.J. (2001). Checkpoint inhibition of the APC/C in HeLa cells is mediated by a complex of BUBR1, BUB3, CDC20, and MAD2. J Cell Biol *154*, 925-936.

Tang, Z., Bharadwaj, R., Li, B., and Yu, H. (2001). Mad2-Independent inhibition of APCCdc20 by the mitotic checkpoint protein BubR1. Dev Cell *1*, 227-237.

Tang, Z., Shu, H., Oncel, D., Chen, S., and Yu, H. (2004). Phosphorylation of Cdc20 by Bub1 provides a catalytic mechanism for APC/C inhibition by the spindle checkpoint. Mol Cell *16*, 387-397.

Thompson, S.L., and Compton, D.A. (2010). Proliferation of aneuploid human cells is limited by a p53-dependent mechanism. J Cell Biol *188*, 369-381.

Vaisberg, E.A., Koonce, M.P., and McIntosh, J.R. (1993). Cytoplasmic dynein plays a role in mammalian mitotic spindle formation. J Cell Biol *123*, 849-858.

Vallee, R.B., McKenney, R.J., and Ori-McKenney, K.M. (2012). Multiple modes of cytoplasmic dynein regulation. Nat Cell Biol *14*, 224-230.

Vanoosthuyse, V., and Hardwick, K.G. (2009). A novel protein phosphatase 1-dependent spindle checkpoint silencing mechanism. Curr Biol *19*, 1176-1181.

Varetti, G., Guida, C., Santaguida, S., Chiroli, E., and Musacchio, A. (2011). Homeostatic control of mitotic arrest. Mol Cell *44*, 710-720.

Varma, D., Monzo, P., Stehman, S.A., and Vallee, R.B. (2008). Direct role of dynein motor in stable kinetochore-microtubule attachment, orientation, and alignment. J Cell Biol *182*, 1045-1054.

Vink, M., Simonetta, M., Transidico, P., Ferrari, K., Mapelli, M., De Antoni, A., Massimiliano, L., Ciliberto, A., Faretta, M., Salmon, E.D*., et al.* (2006). *In vitro* FRAP

identifies the minimal requirements for Mad2 kinetochore dynamics. Curr Biol *16*, 755-766.

Wadsworth, P., Lee, W.L., Murata, T., and Baskin, T.I. (2011). Variations on theme: spindle assembly in diverse cells. Protoplasma *248*, 439-446.

Wan, X., O'Quinn, R.P., Pierce, H.L., Joglekar, A.P., Gall, W.E., DeLuca, J.G., Carroll, C.W., Liu, S.T., Yen, T.J., McEwen, B.F*., et al.* (2009). Protein architecture of the human kinetochore microtubule attachment site. Cell *137*, 672-684.

Waters, J.C., Chen, R.H., Murray, A.W., and Salmon, E.D. (1998). Localization of Mad2 to kinetochores depends on microtubule attachment, not tension. J Cell Biol *141*, 1181-1191.

Weinert, T.A., Hartwell, L.H. (1988). The *RAD9* gene controls the cell cycle response to DNA damage in *Saccharomyces cerevisiae*. Science *241*, 317-322.

Windecker, H., Langegger, M., Heinrich, S., and Hauf, S. (2009). Bub1 and Bub3 promote the conversion from monopolar to bipolar chromosome attachment independently of shugoshin. EMBO Rep *10*, 1022-1028.

Xia, G., Luo, X., Habu, T., Rizo, J., Matsumoto, T., and Yu, H. (2004). Conformation-specific binding of p31(comet) antagonizes the function of Mad2 in the spindle checkpoint. EMBO J *23*, 3133-3143.

Yang, M., Li, B., Liu, C.J., Tomchick, D.R., Machius, M., Rizo, J., Yu, H., and Luo, X. (2008). Insights into mad2 regulation in the spindle checkpoint revealed by the crystal structure of the symmetric mad2 dimer. PLoS Biol *6*, e50.

Yang, M., Li, B., Tomchick, D.R., Machius, M., Rizo, J., Yu, H., and Luo, X. (2007). p31comet blocks Mad2 activation through structural mimicry. Cell *131*, 744-755.

Yen, T.J., Compton, D.A., Wise, D., Zinkowski, R.P., Brinkley, B.R., Earnshaw, W.C., and Cleveland, D.W. (1991). CENP-E, a novel human centromere-associated protein required for progression from metaphase to anaphase. EMBO J *10*, 1245-1254.

Young, A., Dictenberg, J.B., Purohit, A., Tuft, R., and Doxsey, S.J. (2000). Cytoplasmic dynein-mediated assembly of pericentrin and gamma tubulin onto centrosomes. Mol Biol Cell *11*, 2047-2056.

Zich, J., Sochaj, A.M., Syred, H.M., Milne, L., Cook, A.G., Ohkura, H., Rappsilber, J., and Hardwick, K.G. (2012). Kinase activity of fission yeast Mph1 is required for Mad2 and Mad3 to stably bind the anaphase promoting complex. Curr Biol *22*, 296-301.